

University of Naples Federico II
Department of Pharmacy



FRANCO ITALIENNE | ITALO FRANÇAISE

In co-advisor with
University of Tours

PhD in Pharmaceutical Science- XXXIV cycle

*Peptide-based dynamic nanovectors
for anticancer and antimicrobial drugs*

Italian Tutor:

Prof. *Stefania Galdiero*

Stefania Galdiero

French Tutor:

Prof. *Igor Chourpa*

Igor Chourpa

Candidate:

Valentina Del Genio

Valentina Del Genio

Coordinator: Prof. Maria Valeria D'Auria



UNIVERSITY OF TOURS

DOCTORAL SCHOOL: SSBCV

RESEARCH TEAM: NMNS

(Nano-Medicament et Nano-Sonde)

THESIS of

Valentina DEL GENIO

14 July 2022

to obtain the title of: **DOCTOR**

Discipline : Pharmaceutical Science

PEPTIDE-BASED DYNAMIC NANOVECTORS FOR ANTICANCER AND ANTIMICROBIAL DRUGS

Members of the Doctoral Committee

Reviewers:

Prof. BRYSZEWSKA Maria
Prof. DE LA MATA Francisco Javier

University of Lodz (Polland)
University of Alcalá de Henares (Spain)

Examinators:

Prof. GALDIERO Stefania (director)

University of Naples Federico II (Italy)

Stefania Galdiro
Prof. CHOURPA Igor (director)

University of Tours (France)

Prof. FALANGA Annarita (co-director)

University of Naples Federico II (Italy)

Annarita Falanga
Dr. HERVE-AUBERT Katel (co-director)

University of Tours (France)

Prof. ISERNIA Carla

University of Campania Luigi Vanvitelli (Italy)

Prof. PASSIRANI Catherine

University of Angers (France)

LIST OF PUBLICATIONS

1. **Del Genio V**, Falanga A, Allard-Vannier E, Hervé-Aubert K, Leone M, Bellavita R, Uzbekov R, Chourpa I, Galdiero S. *Design and validation of nanofibers made of self-assembled peptides to become multifunctional stimuli-sensitive nanovectors of anticancer drug doxorubicin in Triple Negative Breast Cancer*. Small, 2022 submitted
2. **Del Genio V**, Bellavita R, Falanga A, Hervé-Aubert K, Chourpa I, Galdiero S. *Peptide-based nanovectors to overcome limitations of anti-cancer and antimicrobial therapies*. Pharmaceutics, 2022 in revision.
3. Falanga A, **Del Genio V**, Kaufman E A, Zannella C, Franci G, Weck M, Galdiero S. *Engineering of Janus-Like Dendrimers with Peptides Derived from Glycoproteins of Herpes Simplex Virus Type 1: Toward a Versatile and Novel Antiviral Platform* International Journal of Molecular Sciences. 2021;22(12), 6488.
4. Falanga A, **Del Genio V**, Galdiero S. *Peptides and Dendrimers: How to Combat Viral and Bacterial Infections* Pharmaceutics. 2021;13(1):101.
5. Lombardi L, Falanga A, **Del Genio V**, Palomba L, Galdiero M, Franci G, Galdiero S. *A boost to the antiviral activity: Cholesterol tagged peptides derived from glycoprotein B of Herpes Simplex virus type I*. International Journal of Biological Macromolecules, 2020;162:882-893.
6. Falanga A, Siciliano A, Vitiello M, Franci G, **Del Genio V**, Galdiero S, Guida M, Carraturo F, Fahmi A, Galdiero E. *Ecotoxicity Evaluation of Pristine and Indolicidin-coated Silver Nanoparticles in Aquatic and Terrestrial Ecosystem*. International Journal of Nanomedicine, 2020;15:8097-8108.
7. Falanga A, Lombardi L, Galdiero E, **Del Genio V**, Galdiero S. *The world of cell penetrating: the future of medical applications* Future Medicinal Chemistry, 2020;12(15):1431-1446.
8. Lombardi L, Falanga A, **Del Genio V**, Galdiero S. *A New Hope: Self-Assembling Peptides with Antimicrobial Activity* Pharmaceutics, 2019;11(4):166.

INDEX

<u>Summary</u>	<u>5</u>
<u>Introduction</u>	<u>8</u>
1.1 Nanomedicine	8
1.2 Drugdelivery	9
1.3 Biological barriers and cell membrane crossing	10
1.4 Nanoparticles for drug delivery	11
1.5 Peptides and drug development	13
1.6 Cell penetrating peptide (CPPs)	14
1.7 Nanosystem in cancer application	17
1.7.1 Cell targeting peptides (CTP)	18
1.7.2 On-demand strategies for cancer	19
1.8 Nanosystem in antimicrobial application	20
1.9 Objectives	23
<u>Nanosystem for cancer applications</u>	<u>25</u>
<u>Chapter 1. Drug delivery systems for cancer therapy</u>	<u>25</u>
<u>Nanosystem for antimicrobial applications</u>	<u>26</u>
<u>Chapter 2 Drug delivery systems for antiviral therapy</u>	<u>26</u>
<u>2.1 Introduction</u>	<u>28</u>
<u>2.2 Peptide engineering strategy</u>	<u>30</u>
2.2.1 Design	30
2.2.2 Peptide synthesis	31

2.2.3 Chemical conjugation	31
2.2.4 Antiviral analysis	32
2.2.5 Structural studies	34
2.2.6 Membrane fluidity and DLC analysis	35
2.2.7 Binding and surface plasmon resonance analysis	36
2.2.8 Conclusion and future perspectives	39
2.3 Dendrimer Strategy	40
2.3.1. Design	40
2.3.2. Peptide Synthesis	40
2.3.3. Dendrimer functionalization	40
2.3.4. Structural study	42
2.3.5. Cytotoxicity studies	43
2.3.6. Antiviral assays	43
2.3.7. Conclusion and future perspectives	46
Chapter 3 Drug delivery systems for antibacterial applications	47
3.1 Introduction	47
3.2 Result and discussion	50
3.2.1 Peptide synthesis	50
3.2.2 AgNPs preparation and indolicidin functionalitazion	50
3.2.3 Toxicity Tests on D. Magna	51
3.2.4 Toxicity Tests on R. subcapitata	54
3.2.5 Effect of Nanoparticles on Seed Germination	55
3.3 Conclusion and future perspectives	55
Chapter 4 Experimental Studies	57
4.1 Chemistry	57
4.2 Conformational analysis	60
4.3 Biology	63

5 List of abbreviations.	66
6 References	70

Summary

Biomedical research devotes a huge effort to develop novel nanovectors for sustainable and controlled delivery of drugs, to augment their therapeutic effectiveness and to achieve personalized medicine. This PhD thesis is focused on the development of peptide-based nanovectors that can be used in various situations, namely to deliver anticancer drugs or antimicrobial drugs. The introduction presents the concept of nanotechnology, a science that stimulates important innovations in the medical and healthcare treatments. Through the control of materials at the nanoscale level, it is possible to produce nanovectors able to protect drugs from degradation, to modulate pharmacokinetics, to enhance intracellular penetration and intracellular distribution while reducing undesired secondary effects. The introduction describes drug delivery strategies aimed at improving the specificity of current therapeutic approaches, in particular through the use of peptides. Then there are two main sections devoted respectively to the anti-cancer and anti-microbial nanovectors. Section 1 is focused on the design, synthesis and characterization of new generation of self-assembling nanovectors based on peptides and designed for stimuli-responsive release of drugs. Peptide self-assembly is governed by noncovalent interactions that can be modulated by varying the amino acid sequences and manipulating the environmental parameters. Decorated on their surface with a cell-penetrating peptide gH625, the nanovectors shown and enhanced uptake in cancer cells. The superparamagnetic iron oxide nanoparticles (SPION) were additionally included in the formulation, to (i) favour accumulation in target tissues with help of external magnetic field and (ii) follow their biodistribution by MRI. Section 2 describes the use of peptides for the development of drug delivery tools useful for antimicrobial applications. In particular, we obtained several analogues of an antiviral peptide developed in our laboratory against *Herpes Simplex Virus type 1*. The obtained peptide analogues were characterized by the presence of a PEG-Cholesterol moiety which favours the interaction with the membrane bilayer of the target cell and enhances the anti-microbial activity. These results were further exploited to develop a carrier based on the use of a Janus dendrimer functionalized with two different antiviral sequences. Finally, we also designed nanovectors made of silver nanoparticles which combine the action of both silver ions and of an antimicrobial peptide indolicidin and demonstrate an enhanced antibacterial activity and a lower cyto- and endo-toxicity.

Sommaire

La recherche biomédicale consacre un effort considérable pour développer de nouveaux nanovecteurs pour une délivrance contrôlée de médicaments, afin d'augmenter leur efficacité thérapeutique et parvenir à une médecine personnalisée. Cette thèse de doctorat porte sur le développement de nanovecteurs à base de peptides pouvant être utilisés dans diverses situations, notamment pour délivrer des médicaments anticancéreux ou des médicaments antimicrobiens. L'introduction présente le concept de nanotechnologie, une science qui stimule d'importantes innovations dans les traitements médicaux et sanitaires. Grâce au contrôle des matériaux à l'échelle nanométrique, il est possible de produire des nanovecteurs capables de protéger les médicaments de la dégradation, de moduler leur pharmacocinétique, d'améliorer leur pénétration intracellulaire et la distribution intracellulaire tout en réduisant les effets secondaires indésirables. L'introduction décrit des stratégies de délivrance de médicaments visant à améliorer la spécificité des approches thérapeutiques actuelles, notamment par l'utilisation de peptides. Ensuite, deux sections principales sont consacrées respectivement aux nanovecteurs anticancéreux et antimicrobiens. La section 1 est axée sur la conception, la synthèse et la caractérisation d'une nouvelle génération de nanovecteurs anticancéreux auto-assemblés basés sur des peptides et conçus pour la libération de médicaments en réponse aux stimuli. L'auto-assemblage des peptides est régi par des interactions non covalentes qui peuvent être modulées en faisant varier les séquences d'acides aminés et en manipulant les paramètres environnementaux. Décorés en leur surface avec un peptide gH625 pénétrant dans les cellules, les nanovecteurs ont montré et amélioré l'absorption dans les cellules cancéreuses. Les nanoparticules d'oxyde de fer superparamagnétique (SPION) ont également été incluses dans la formulation, afin de (i) favoriser l'accumulation dans les tissus cibles à l'aide d'un champ magnétique externe et (ii) suivre leur biodistribution par IRM. La section 2 décrit l'utilisation de peptides pour le développement d'outils d'administration de médicaments utiles pour les applications antimicrobiennes. En particulier, nous avons obtenu plusieurs analogues d'un peptide antiviral développé dans notre laboratoire contre le virus *Herpes Simplex Virus de type 1*. Les analogues peptidiques obtenus ont été caractérisés par la présence d'un fragment PEG-Cholestérol qui favorise l'interaction avec la bicouche membranaire de la cellule cible et améliore l'activité anti-microbienne. Ces résultats ont ensuite été exploités pour développer un nanovecteur basé sur l'utilisation d'un dendrimère Janus fonctionnalisé avec deux séquences antivirales différentes. Enfin, nous avons également conçu des nanovecteurs constitués de nanoparticules d'argent qui combinent l'action des ions d'argent et d'un peptide antimicrobien indolicidine et démontrent une activité antibactérienne accrue et une cyto- et endo-toxicité plus faible.

Sommario

La ricerca biomedica dedica un grande interesse allo sviluppo di nuovi nanovettori per la somministrazione sostenibile e controllata di farmaci, per aumentare la loro efficacia terapeutica al fine di effettuare una medicina personalizzata. Questa tesi di dottorato è focalizzata sullo sviluppo di nanovettori a base di peptidi che possano essere utilizzati in varie situazioni, in particolare per il trasporto di farmaci antitumorali o farmaci antimicrobici. L'introduzione presenta il concetto di nanotecnologia, una scienza che oggi stimola importanti innovazioni nelle cure mediche e sanitarie. Attraverso il controllo dei materiali di nano dimensioni, è possibile produrre nanovettori in grado di proteggere i farmaci dalla degradazione, di modularne la farmacocinetica, di potenziarne la penetrazione e la distribuzione intracellulare riducendo gli effetti collaterali indesiderati. Inoltre, nell'introduzione sono descritte le strategie di *drug delivery* volte a migliorare la specificità degli attuali approcci terapeutici, in particolare attraverso l'uso di peptidi. Ci sono poi due sezioni principali dedicate rispettivamente ai nanovettori anticancro e antimicrobici. La Sezione 1 è incentrata sulla progettazione, sintesi e caratterizzazione di nanovettori nuova generazione basati su peptidi autoassemblanti e progettati per il rilascio controllato di farmaci. L'autoassemblaggio dei peptidi è governato da interazioni non covalenti che possono essere modulate variando le sequenze amminoacidiche e manipolando i parametri ambientali. I nanovettori sono stati decorati sulla loro superficie con il peptide gH625 che aumenta la penetrazione cellulare e migliora l'assorbimento nelle cellule tumorali. Nella formulazione sono state incluse nanoparticelle di ossido di ferro superparamagnetiche (SPION) al fine di (i) favorire l'accumulo nei tessuti bersaglio con l'aiuto di un campo magnetico esterno e (ii) seguire la loro biodistribuzione mediante la risonanza magnetica. La Sezione 2 descrive l'uso dei peptidi per lo sviluppo di nanosistemi utili per applicazioni antimicrobiche. In particolare, sono stati ottenuti diversi analoghi di un peptide antivirale sviluppato nel nostro laboratorio contro il virus *Herpes Simplex Virus di tipo 1*. Gli analoghi peptidici ottenuti sono stati coniugati al PEG-colesterolo al fine di favorire l'interazione con il doppio strato di membrana della cellula bersaglio e potenziare l'attività antivirale. Questi risultati sono stati ulteriormente sfruttati per sviluppare un vettore basato sull'uso di un dendrimero *Janus* funzionalizzato con due diverse sequenze antivirali. Infine, sono stati progettati nanovettori per il trasporto di peptidi antibatterici, costituiti da nanoparticelle d'argento che combinano l'azione dell'argento a quella del peptide indolicidina evidenziando una maggiore attività antibatterica e una minore citotossicità ed ecotossicità.

Introduction

1.1 Nanomedicine

Nanotechnology is concerned with nanostructures that are smaller than 100 nanometers in at least one dimension and that can be modified at the atomic or molecular level. It is an interdisciplinary research field that includes chemistry, biology, engineering, and medicine, and has determined effective outcomes in different subfields and in daily life. Interestingly, nanotechnology has induced a significant innovation in medical and healthcare treatments and therapies through the control of nanoscale materials and the development of nanosystems capable of acting at a molecular level. Nanosized materials, which compared to bulk materials present unique physicochemical properties, can be exploited for many biomedical applications with a key challenge represented by personalized medicine to overcome the drawbacks of current therapies, enhance medical visualization and diagnosis of diseases, and develop biosensors. (Figure 1)

Nanotechnology has the power to play a critical role in a variety of customized drug applications such as drug delivery, tissue engineering, gene therapy, molecular imaging, etc. The drug delivery field is a main outcome of these recent achievements,^{1, 2} and represents a crucial challenge.³

Compared with conventional medicines, the utilization of nanomaterials represents an advancement due to the possibility of accessing targeting tissues, deep molecular targets, of producing lower side effects and controlled drug release. Nano-sized drug carriers provide a wide range of practical applications for a targeted drug delivery process, such as: delivering poorly soluble, unstable, or systemically toxic drugs with extended blood half-lives and reduced side effects. The drug accumulation can be increased decorating the surface of nanocarriers with targeting agents. Furthermore, in recent years, metal nanoparticles have been used for diagnosis and therapeutics purposes. The extension in use and applications of metal nanoparticles can be explained by their distinctive small size, as well as their enormous surface-area-to-volume ratio, high responsiveness to living tissues, stability at elevated temperatures, and cellular transportation.⁴

One of the most successful carrier approved by US Food and Drug Administration (FDA) is liposomes, which can be referred to as some of their commercialized types, including Doxil (doxorubicin encapsulated in liposomes), AmBisome (liposomal amphotericin B), and Liposomal morphine.⁵ Recently a new version of paclitaxel was approved, which is loaded in albumin nanoparticles (Abraxane™) with fewer side effects and improved efficacy due to the higher dose of the drug that can be administered and delivered.⁶

The advances in polymer science, chemistry, engineering, biology and physics have an impact on the development of the diverse types of carriers with unique characteristics and performance in medical sciences.

Despite significant advances in drug delivery system development, some deficiencies still exist, such as low drug loading capacity, low thermal chemical stability and unwanted release of the drug from nanocarriers. Thus, considerable efforts are dedicated to the

development of ideal drug delivery systems, which should have a controlled and stable release.

1.2 Drug delivery

For a successful drug delivery system, the design is important, with particular attention to the choice of materials, to obtain a nanopatform of dimensions in the range of 1-100 nm, and characterized by composition, structure and load of the drug optimal for the specific treatment of the selected disease. For each material, it is essential that those factors are considered to render the nanovector (NV) most suitable to its application.

Drug delivery by NVs presents several advantages, such as:

- the delivery of a therapeutic agent directly to the target to increase its efficacy while reducing the side effects;^{7, 8}
- the possibility to customize the drug release, solubility, half-life, bioavailability and immunogenicity of the drug.⁹

The use of nanocarriers such as liposomes, micelles, and nanoparticles of different origin^{10, 11} has been shown to improve the solubility of drugs and prevent their degradation by enzymes, pH, and other factors during blood circulation (Table 1). In addition, tunable size, shape and structure of NVs allow to reach relevant drug loading capacity. Moreover, being comparable in size to human cell organelles, they can interact with various ligands, both hydrophilic and hydrophobic, and target cells and intracellular compartments.

Three main factors must be considered when choosing the type of NV to use: size, *in vitro* and *in vivo* stability, and surface charge. The selection of the size of the NV directly affects their performance and depends on the application of the nanosystem. Clearly, this is a key factor to consider when optimizing their biodistribution and pharmacokinetics. The stability of the NV is also important to reach and advance in the clinical trial stages. Furthermore, *in vivo* nanocarriers interact with different blood constituents including proteins and cells, which can cause high dilution in the blood, while enzymes, which may not be accounted for *in vitro* studies, could affect the functionality or stability of nanocarriers. The last point is the surface charge of the NV, which should be considered because the plasma membranes of cells are negatively charged. Thus, cells easily take in positively charged (cationic) NVs by adsorption-mediated endocytosis in comparison to negatively charged and neutral nanocarriers.

Certainly, the delivery of a therapeutic agents directly to the target is a critical challenge, important to increase its efficacy while reducing the side effects.

Unfortunately, the development of drug resistant cells has further complicated the scenario bringing to ineffectiveness of current therapies and the uncontrolled use or the overuse of drugs have determined the insurgence of resistance issues. For this reason, the development of innovative drug delivery tools is aimed at the obtainement of effective treatments both for bacterial/viral and oncological pathologies. Thus, the design of novel delivery strategies is based on the understanding of the pathology to target.

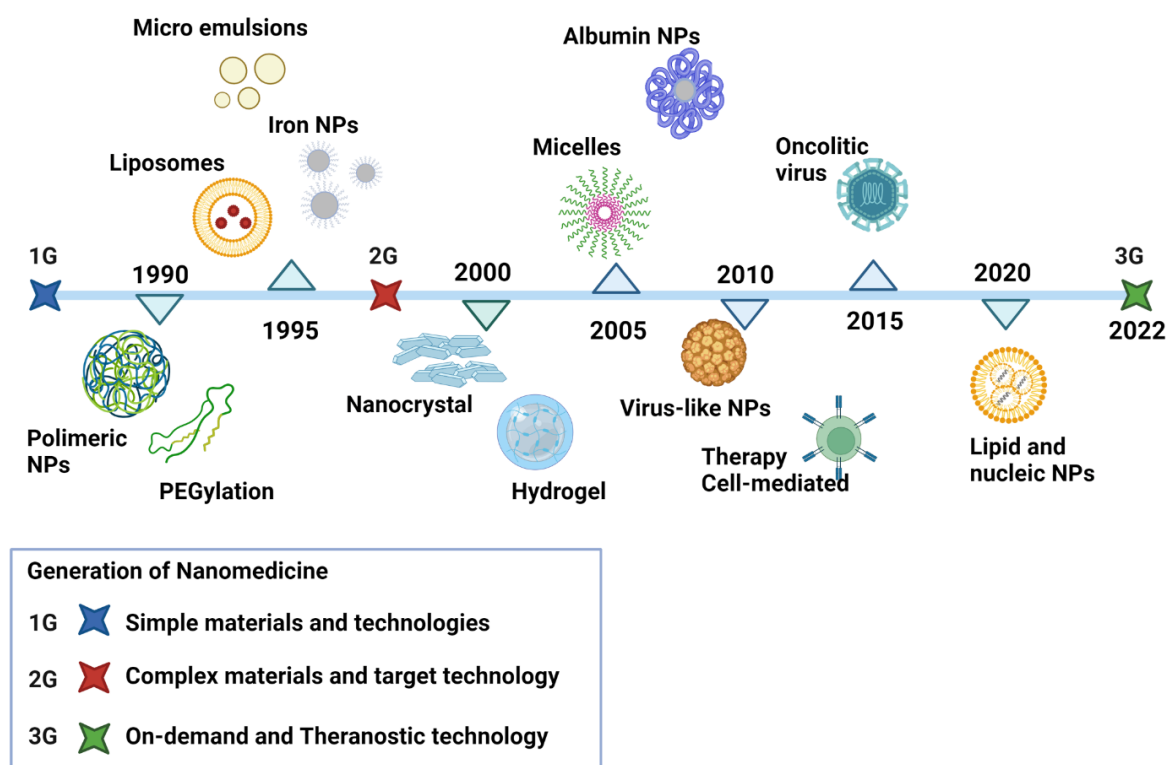


Figure 1. Timeline of development in the field of nanomedicines.

1.3 Biological barriers and cell membrane crossing

To design novel drug delivery systems, it is key to take into consideration the different biological barriers starting from tissues to cells, and organelles to ensure an ideal therapeutic index of drugs.¹² The NV role is to prolong blood circulation and penetration through barriers, increase tissue accumulation and enhance cellular uptake while inhibiting the drug efflux. Eventually, it should control intracellular drug distribution until the action site is reached.

The presence of endothelial barriers represents the main difficulty which prevents drug extravasation from the bloodstream.¹³ In cancer, the so-called enhanced permeability and retention (EPR) effect and the existence of nanoscale gaps between vascular endothelial cells allows substances to leak into tumors favouring the preferential accumulation of the NVs in the tumor site. However, low interstitial fluid pressure (IFP) and highly cross-linked extracellular matrix (ECM) formed by the strong metabolism of tumor cells resulting in a large amount of collagen and polysaccharides produced in the tumor site dramatically prevent the further penetration and diffusion in tumors; the drugs fail to spread throughout the entire tumor and just accumulate at the edge of it. To reduce their clearance by RES (reticuloendothelial system), the NVs may be coated with a shell of polyethylene glycol (PEG). The PEGylation is a very common strategy to avoid adsorption of opsonin proteins on the nanosystem surface (formation of the protein corona)¹⁴⁻¹⁶ and to prolong their blood circulation *in vivo*, and improve delivery to the target tissues.¹⁷

Furthermore, the blood-brain barrier (BBB) allows the passage of less than 2% of molecules, including ions, nutrients, specific peptides and proteins, and leukocytes.^{18, 19} It is composed of tight junctions between vascular endothelial cells, a capillary basement membrane and a

glial membrane formed by astrocytes and pericytes. The junctions in the brain blood improve the function of the BBB to prevent most substances from entering the brain parenchyma for protection of the central nervous system (CNS). Controlling drug translocation across the BBB is helpful to improve the distribution of such drugs.

The pharmacokinetics of the drug can be analysed through parameters such as size (Graham's law),^{20, 21} concentration gradient (Fick's law),²² ionization (Henderson-Hasselbalch equation)²³ and lipid solubility which can all be exploited to increase passive diffusion. The passage across the cell membrane can be summarized in two different processes: passive and active transport. In passive transport,^{24, 25} a substance can cross the membrane without requirement of an external input of chemical energy, this phenomenon is also known as simple diffusion, facilitated diffusion and osmosis. In simple diffusion, very small molecules and hydrophobic substances cross the membrane freely, without the aid of protein systems. The speed of this process depends on the concentration gradient: the greater the difference in concentration between inside and outside, the faster the process. In facilitated diffusion, the molecules cross the membrane aided by transport proteins, which facilitate and speed up their passage. Osmosis is the diffusion of water molecules from a region where the concentration of a solute is lower to a region where the concentration of the solute is higher.²⁶ It is a particular type of facilitated diffusion and occurs in cases where the passage of a solute according to gradient (from a zone with a higher concentration to one with a lower concentration) is prevented.

Active transport is also an important strategy exploited in several drug delivery tools.²⁷ For instance, the existence of different types of malignancies and the variety of tumor cell characteristics render the need of active targeting strategies important. Active transport strategies are based on the ability to target a receptor that is distinctly overexpressed in tumor cells, and which is easily accessible. The diversity of active transport strategies opens the door for a future of personalized therapy where the active targeting system is specifically tailored to result in the maximum specific damage for a patient's tumor. As said, tumor cells frequently overexpress certain receptors on their membranes. This creates a higher affinity of tumor cells towards the molecules that specifically bind these receptors. For active transport, these molecules are attached to the surface of the NV as a targeting ligand, and thanks to their increased affinity towards the receptors, they enhance internalization/uptake, efficacy and specificity through receptor-mediated endocytosis. The targeting ligands can be antibodies, peptides, nucleic acids, or other small molecules.²⁸

1.4 Nanoparticles for drug delivery

Nanoparticles can be classified in:

- polymeric
- non-polymeric
- lipidic.

Polymer-based nanoparticles include dendrimers, micelles, nanogels, protein nanoparticles, chitosan, dextran, albumin, heparin, gelatin, and collagen chitosan-coated PLGA nanoparticles.^{29, 30} Non-polymeric nanoparticles include carbon nanotubes, nanodiamonds, metallic nanoparticles, quantum dots, and silica-based nanoparticle.^{31, 32} Lipid-based nanoparticles can be divided into liposomes and solid lipid nanoparticles.³³⁻³⁵

Below are reported the most widely used kind of carriers.

Micelles are self-assembling colloidal nanocarriers, which range from 10 to 100 nm and can deliver water-insoluble drugs. They are made of amphiphiles that consist of a hydrophilic tail and a hydrophobic head and once placed in water, spontaneously assemble to form a spherical monolayer made of an external hydrophilic shell and a hydrophobic core. Polymeric micelles are widely used for drug delivery, and consist of two or more block polymers and their size ranges from 10 to 200 nm.^{10, 11} They possess a rather low critical micellar concentration (CMC) value, which renders them very stable at low concentration, which is key for prolonged blood circulation and increased EPR effect. The hydrophilic block of polymeric micelles is usually made up of polyethylene glycol (PEG), which is both biocompatible and with no cytotoxicity; while the variation in the different types and functions of polymeric micelles is determined by the nature of the hydrophobic block, which has to encapsulate the hydrophobic drug. Among the most used hydrophobic blocks there is: poly(propyleneoxide) (PPO) and aliphatic polyesters polymers such as poly(D,L-lactide) (PLA) and poly(ϵ -caprolactone) (PCL).²⁸

Liposomes are made of phospholipids possessing a hydrophilic head and a hydrophobic tail, which results in a spherical-shaped vesicle, characterized by a structure like the cell membrane: the hydrophobic tails of the lipids come together to form its hydrophobic region, thus distinguishing its aqueous internal compartment (hydrophilic region) from the bulk aqueous phase. Liposomes range from 50 to 200 nm and are stable, biocompatible, biodegradable, non-toxic, and non-immunogenic and can readily encapsulate hydrophilic molecules in their aqueous core, while hydrophobic ones can be encapsulated within the phospholipid. Thus, liposomes have the unique ability to deliver both hydrophobic and hydrophilic drugs, in contrast to micelles, which are used to encapsulate hydrophobic drugs.^{36, 37} Furthermore, liposomes are known to have relatively high drug loading efficacy, up to 0.25 mg drug/mg lipid.

Mesoporous silica nanoparticles (MSMs), are inorganic nanoparticles ranging from 2 to 50 nm and have high drug loading efficiency due to their high porous properties; furthermore the high density of silanol groups at their surface might favor subsequent functionalization processes.³⁸ Their unique properties make them very useful as drug delivery nanocarriers. MSMs have been employed as starting materials for the manufacture of 3D scaffolds for bone tissue engineering.

Dendrimers are 3D, hyper-branched, and globular nanoparticles (sizes range of 1–15 nm), with distinctive features, such as low polydispersity index, high-water solubility, biocompatibility, polyvalency. Their branched architecture is essential for their applications, and the plethora of ligands which can be bound on their external shell may have a major impact in their activity. Dendrimers can function as drugs themselves, or they can be carriers of a range of different drug molecules.^{39, 40}

Chitosan nanoparticles (CS) have a variety of beneficial properties *in vivo* such as amphipathicity, biocompatibility, biodegradability and biosafety.^{41, 42} CS are soluble in acidic solutions,⁴³ thereby they are responsive to the slightly acidic microenvironment found in tumors.

Poly (lactic-co-glycolic acid) (PLGA) are nanoparticles which present several advantages such as tunable biodegradation, straightforward surface modification, and easy procedures

of encapsulation.^{44, 45} The hydrolysis rate of the PLGA is sensitive to the ratio of lactic to glycolic acids, which is clearly correlated to the release of the drug. Moreover, surface modification is exploited to endow the nanoparticle of stealthiness and targeting capability. Because of its ease of use, wide availability, and simple and effective utility, it is one of the most widely exploited polymers in drug delivery.

1.5 Peptides and drug development

Peptides display a predictable metabolism, have a low incidence of side effects and their metabolites are rarely toxic. Peptides are suitable for interfering in protein/protein interactions⁴⁶ and for binding receptors in cells,⁴⁷ which often is rather challenging with traditional small molecule strategies. Furthermore, the developments of solid phase peptide synthesis represent a good opportunity for using synthetic peptides in medicinal applications. Rational design can be exploited to improve peptide properties, such as longer half-life, higher bioavailability, increased potency and efficiency sometimes simply modifying the peptide backbone, amino acid side chains and secondary structures.

Among modifications that can be introduced to improve peptide applications, lipidation is widely used to transform peptides into peptide therapeutics.⁴⁸ It was first exploited in the mid 1990s during the search for stable insulin with prolonged half-life.⁴⁹ Several other modifications have been developed to improve the properties of the peptides.⁵⁰ and to contrast their enzymatic degradation, such as the insertion of D-amino acids,⁵¹ C α -carbon methylation, cyclization of the backbone⁵² or secondary structure constraints,⁵³ β 3 amino acids⁵⁴ and N α -methylations, incorporation of non-canonical amino acids and conjugation of peptides with PEG, polysialic acid (PSA) and hydroxyethyl starch (HES).⁵⁵ Incorporation of D-amino acids may have a substantial effect on the half-life of peptides.⁵⁶ Furthermore, the incorporation of C α -alkylated amino acids into peptides reduces the flexibility of a peptide backbone and can act as an inducer and/or stabilizer of the helix, thus affecting the tertiary structure of the entire peptide. (Figure 2)

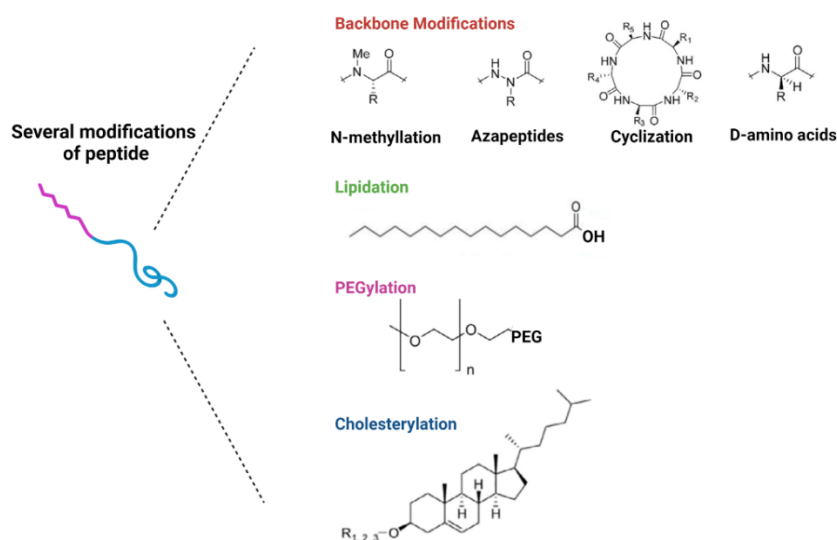


Figure 2. Most common peptide modification strategies.

Much research is dedicated to the use of peptides for the development of targeted NVs. Peptides can be synthesized easily and coupled to nanovectors to improve their bioavailability, recognition of specific target cells by interacting with molecules/receptors overexpressed on their surface (cell targeting peptides - CTP) and internalization into cells (cell penetrating peptides - CPP). Although peptides show high promise in the targeting and intracellular delivery of next-generation nanotherapeutics,⁵⁷ their proteolytic susceptibility is one of the major limitations of their activity in biological environments.⁵⁸ Numerous strategies have been devised to chemically enhance the resistance of peptides to proteolysis and it is possible to use these peptide modifications for the development of nanocarriers. Furthermore, conjugation of nanocarriers or other cargoes to peptides for targeting and cell penetration may already provide some degree of shielding, enhancing protease resistance can greatly increase targeting and transport efficiency. The peptide conjugation also increases the biocompatibility of many nanoparticles.

1.6 Cell penetrating peptides (CPPs)

One opportunity to improve control of diseases and reduce resistance issues is the use of cell-penetrating peptides (CPPs).⁵⁵ For instance, the poor tumor penetration stands as one of the most prominent issues, in fact nanomedicines generally locate nearby the tumor vessels and are unable to access the deep tumor tissue resulting in drug resistance and limited therapeutic efficacy. This serious obstacle in the treatment of many pathologies calls for more effective drug delivery systems.

CPPs are a group of short peptides, usually made of up to 40 amino acids with a positive net charge and a high content of hydrophobic residues, possessing a significant capacity to cross membranes, which have been used to transfer many biologically active cargoes into the cells. CPPs are also able to enter cells, transporting cargoes of several dimensions. Since their discovery, researchers have used CPPs as cutting-edge tools for the intracellular delivery of a whole range of drugs and diagnostics by exploiting their potential ability to internalize when both noncovalently and covalently coupled to cargo molecules.^{59, 60, 61}

CPPs can be classified according to their hydrophilicity and hydrophobicity, which are closely correlated to their different interaction with the membrane bilayer.⁶¹ The prototype is represented by the TAT peptide derived from the transactivator of transcription (TAT) of human immunodeficiency virus. TAT is a short stretch of 12 amino acids (GRKKRRQRRRPQ) that is able to pass through the cell membrane and deliver almost any cargo inside cells.^{62, 63}

CPPs have been classified in cationic, amphipathic, membranotropic and hydrophobic. Cationic CPPs (Tat,⁶² penetratin,⁶⁴ R9⁶⁵ and HR9⁶⁶) are rich in arginine, lysine and histidine residues.⁶⁷ Arginine is preferred because the guanidine head-group can form hydrogen bonds with phosphate, sulphate and carboxylate moieties that make the cell membrane negatively charged, and therefore favor the internalization process under physiological conditions. Arginine containing peptides are more active; whereas lysine containing peptides lacking a guanidine head group are less effective at penetrating the membrane.⁶⁵ Furthermore, since single interactions are weak, it has been determined that sequences of eight arginine residues have the highest membrane penetrating ability.⁶⁵

Amphipathic CPPs are usually chimeric peptides that contain both positively and negatively charged amino acids.³⁰ They are often divided into primary and secondary amphipathic peptides; primary amphipathic CPPs are typified by the fusion of a cationic and a hydrophobic sequence, whereas secondary amphipathic peptides are characterized by two faces – one hydrophobic and the other cationic, anionic or polar. Examples of amphipathic CPPs include trasportan,⁶⁸ pVEC,^{69, 70} MAP⁷⁰ and p28.⁶³

Membranotropic sequences were previously included into the group of amphipathic peptides because they have simultaneous hydrophobic and amphipathic features; examples are Pep-1,⁷¹ Cady,⁷² and gH625.^{73, 74} They are characterized by the presence of both large aromatic amino acids and small residues such as Ala/Gly^{75, 76} that facilitate membrane interaction and peptide insertion into the bilayer. Their amphipathicity is critical in interacting with the membrane bilayer and in the internalization process. These peptides can effectively foster lipid-membrane reorganization by destabilizing locally and temporarily the membrane bilayer.

Table 1. Cell-penetrating peptides selection to include cationic, amphipathic, membranotropic and hydrophobic peptides.

Name	Sequence	Origin	Nature	Structure
Tat	GRKKRRQRRRPPQ	HIV-1 transcriptional activator	Cationic	Random/ Random
Penetratin	RQIKIWFQNRRMKWKK	Antennapedia Drosophila melanogaster	Cationic Amphipathic	Random/ β-sheet
R9	RRRRRRRRR	Synthetic	Cationic	Random/ Random
pVEC,	LLIILRRRIRKQAHASK	Murine vascular endothelial cadherine	Membranotropic Amphipathic	β-sheet
MAP	KLALKLALKALKAALKLA	Synthetic	Cationic Amphipathic	Random/ α-helix
P28	LSTAADMQGVVTDGMASGLDKDYLP DD	Azurine sequence	Amphipathic	α-helix/ β-sheet/ random
Pep-1	KETWWETWWTEWSQPKKKRKV	Synthetic	Membranotropic Amphipathic	α-helical
CADY	GLWRALWRLLRSLWRLWRA	PPTG1 peptide	Membranotropic Amphipathic	Random/ α-helix
gH625	HGLASTLTRWAHYNALIRAF	Glycoprotein H of Herpes simplex virus Type 1	Membranotropic Viral	Random/ α-helix
C105Y	CSIPPEVKFNKPFVYLI	C-terminal tail of α 1 anti-trypsin	Hydrophobic	α-helix
BIP	VPMLKE	Synthetic	Hydrophobic
Pep-7	SDLWEMMMVSLACQY	Synthetic	Hydrophobic	α-helix
MPG	GALFLGFLGAAGSTMGAWSQPKKKRK V	HIV gp 41 and NLS of SV40T-antigen	Membranotropic Viral	Random/ β-sheet
Trasportan	GWTLNS/AGYLLGKINKALAALAKKIL	Galanin-mastoparan	Membranotropic Amphipathic	α-helix

Hydrophobic CPPs are those containing only nonpolar residues or motifs.⁷⁷ Very few hydrophobic CPPs have been discovered, for example, C105Y,⁷⁸ BIP⁷⁹ and Pep-7.⁸⁰

Hydrophobicity is a key parameter of CPPs and optimal hydrophobicity can lead to significantly improved uptake. Nonetheless, when hydrophobicity is too high and hydrophobic interactions between the CPP and the membrane are excessive, it is possible that the peptide may get stuck into the membrane bilayer and no internalization occurs (Table 1).

Multiple pathways exploited include direct penetration of the plasma membrane involving membrane interaction and direct penetration into the cytosol and endocytic uptake. Endocytosis is an energy-dependent pathway that includes macropinocytosis, clathrin- and caveolea-mediated endocytosis and clathrin- and caveolea-independent endocytosis. For a detailed analysis of these mechanisms of uptake, see recent reviews.^{81, 82}

Initially, much of the data supported direct translocation of most CPPs, but those results were subsequently found to be due to experimental artifacts.^{83, 84} Although the uptake mechanism is still being debated, endocytosis seems to be the main internalization mechanism. Unfortunately, endocytosis implies trapping of the cargo in endosomes and subsequent degradation in lysosomes, consequently leading to its limited delivery to the intracellular target or targeting back to the plasma membrane for recycling and subsequent ejection from the cell.

The properties of CPPs determine the mechanism to entry into cells that still remains unknown. These peptides could cross the plasmatic membrane and possibly deliver various kinds of molecules into the cell as proposed for TAT, poly-Arg,⁸⁵ Transportan,⁸⁶ MPG⁸⁷ or Pep-1,⁷¹ through an energy-independent pathway, with a direct translocation through the plasma membrane. Several studies indicated that CPPs mainly follow a cellular endocytosis-mediated uptake,⁸⁸ in particularly those with a high content in cationic residues, are first simply adsorbed at the cell surface bearing numerous anionic moieties, such as heparan sulfate, sialic or phospholipidic acid;⁸⁹ then CPP mediated transport proceeds through different endocytosis routes: caveolae,⁹⁰ macropinocytosis, clathrin-dependent pathway,⁹¹ cholesterol dependent clathrin-mediated pathways⁹² or the trans-Golgi network.⁹³ (Figure 3) The endocytic pathway ending in lysosomes, where common enzymatic degradation processes take place, decrease the intracellular bioavailability of the transported cargo. To overcome this problem, it is possible to use membranotropic peptides that are capable to partition into membranes and to cross cell membranes and enter cells. Those peptides are characterized by a propensity for membrane binding and a high interfacial hydrophobicity or amphipathicity. Fusion peptides derived from enveloped virus glycoproteins have recently been discovered as a novel class of CPPs; they are typically 20-30 residues long and potentially fold into amphipathic helices and are rich in glycines and alanines, which provide them with a high degree of conformational flexibility; the delicate balance between α helical and β structures is essential for membrane interaction together with the presence of aromatic residues which may help in overcoming the energy cost of peptide bond partitioning into membranes. In particular, the tryptophan is widely present in membranotropic CPP favouring membrane interactions as it is usually located at the interface between aqueous solution and lipidic domains (Table 1). Membranotropic peptides traverse efficiently biological membranes, promote lipid-membrane reorganizing processes, such as fusion or pore formation⁹⁴ may be able to circumvent the endosomal entrapment either favouring the escape from the endosome or by translocating a cargo through the plasma membrane directly

into the cytosol. Initially there is an interaction at the membrane interface with the external leaflet, which is thought to generate elastic stresses and to drive bilayer fusion, helping to overcome the hydration repulsion forces between approaching bilayers by orienting the poorly solvated face toward the external medium.⁹⁵ The increase of the polar head region will determine a curvature stress onto the overall lipid bilayer; creating bulges that protrude from the membrane and facilitate the formation of lipid contacts between fusing bilayers.⁹⁶ Hydrophobic peptides, promote reorganization of lipid membrane,^{75, 97} and are able to circumvent the endosomal entrapment either favouring the escape from the endosome or by translocating a cargo through the plasma membrane directly into the cytosol.

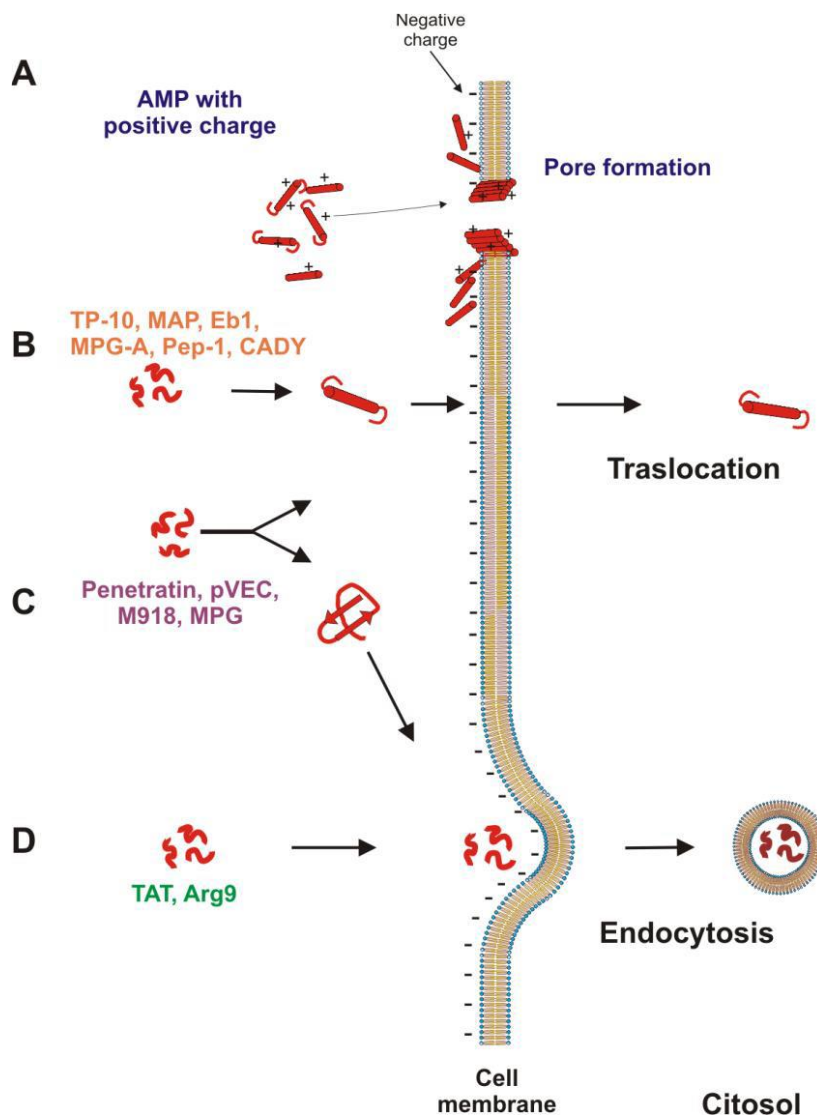


Figure 3. Proposed mechanisms of cellular internalization pathways of different CPPs.

1.7 Nanosystems in cancer applications

Cancer treatments have undergone tremendous changes in recent years and the understanding of the underlying biological processes have increased; the technological advances in treatment need innovative methods, such as targeted therapy. Today cancer can

be treated by surgery, chemotherapy, ionizing radiation therapy, hormonal therapy, targeted therapy. Surgical procedure is commonly practiced for non-hematological cancers, this method is based on removal of the cancer tissue from the body. The surgical procedure can give a complete or partial recover from the cancer, and effects depending on the type of cancer and the health condition of the individual. Unfortunately, often cancer cells cannot be completely removed by the surgical procedure, and even a presence of a single cancer cell that is invisible can regrow into a new tumor and spread to other parts of the body.

Chemotherapy uses anticancer drugs, to kill or destroy the cancer cells. The drugs used can interfere with the growth of tumors and even destroy the cancer cells. Chemotherapy is considered an effective method of cancer treatment; however, it can cause severe side effects on cells or tissues and this is a strong limitation. Radiation therapy also can damage normal cells and induce the side effects due to the use of ionizing radiations. The biologic therapy is based on helping the immune system to fight cancer, it uses a monoclonal antibody that blocks specific protein action by binding to cancer cells and trains the immune system to recognize and attack the cancer cells. This method of treatment is safe and does not have any major side effects. The hormone therapy treatment is based on the change of the hormone amounts in the body to treat certain types of cancer that depend on these chemicals to grow and spread. In this case, the side effects depend on the type of cancer, age, sex and the type of drug used in the treatment. Targeted treatments use specific agents for the deregulated proteins of cancer cells, that are generally inhibitors of enzymatic domains on the mutated, overexpressed, or otherwise critical proteins within the cancer cells.

Analysis of tumor microenvironment (TME) is important to develop innovative NVs. Several studies have shown that monoclonal antibodies (mAbs) could improve tumor targeting and anticancer effects.^{98,99} This therapy is limited because of high molecular weights, low tissue penetration and poor cellular uptake.^{100, 101}

NVs functionalized with peptides present important advantages, such as ability to traverse membranes, thereby enhancing the uptake, but is crucial to develop systems that have multiple functionalities and target specificity. The challenge is the development of nanosystem, able to accommodate several ligands and functionalities, such as drugs, diagnostic tools, CPPs and targeting peptides.¹⁰² The better understanding of the mechanisms that mediate cargo entry may guide the design of nanoplatfoms with desired properties improving cytosolic delivery efficiency and tissue selectivity allowing the achievement of better results for cargo delivery and to overcome the limitations of current therapies.

1.7.1 Cell targeting peptides (CTP)

Active drug targeting is critical for cancer treatments, where initially only passive targeting, exploiting the EPR effect, has been used. For cancer therapy, NVs with diameters of 10–100 nm, achieve EPR and deliver drugs effectively, while particles with sizes less than 1–2 nm can leak from the normal vasculature and damage normal cells and particles larger than 100 nm can be cleared from circulation by phagocytes. A wide range of studies highlights that passive targeting of NVs acts through the EPR effect, while active targeting relies on the interaction between ligands and receptors. The receptors found on cancer cells include transferrin receptors, folate receptors, glycoproteins, and epidermal growth factor receptors.

CTP are made of 3–15 amino acids that specifically identify and adhere to tumor cells/tumor vasculature, and thus may target tumor and tumor micro-environment. There are some common sequence motifs, such as RGD motif (Arg-Gly-Asp) which binds to α integrins, or NGR motif (Asn-Gly-Arg), which binds to a receptor aminopeptidase on the surface of endothelial cells (see the TumorHoPe database for an exhaustive list). This first-generation of CTPs have found high receptor availability due to the up-regulation of their target sites in metastasis-related angiogenesis. The RGD motif was incorporated into larger peptide structures such as knottins, whose highly constrained structure also confers high proteolytical stability. Cochran and collaborators obtained the engineered knottin EETI 2.5F, with high selectivity for integrin receptors, which provided outstanding imaging contrast for mouse cerebellar medulloblastoma.¹⁰³ This same peptide conjugated to gemcitabine proved to be a potent inhibitor of brain, breast, ovarian, and pancreatic cancer cell lines *in vitro*.¹⁰⁴ An important target at the tumor level is epidermal growth factor receptor (EGFR) that is overexpressed in a variety of tumors and many strategies were improved by introduction of GE11 peptide with a main sequence of YHWYGYTPQNVI that have high affinity for EGFR.¹⁰⁵ Cyclization has been applied to longer peptides such as the heptapeptide A7R (AT-196 WLPPR), which binds two glioma markers, VEGFR2 and NRP-1.¹⁰⁶ Lu *et al.* showed that the cyclic version of L-A7R could enhance the anti-glioblastoma effect *in vivo* by conjugating it to doxorubicin-loaded liposomes.¹⁰⁷ Cyclic peptides have also proven to be superior BBB shuttles that selectively enhance the delivery of cargoes into the brain.¹⁰⁸ A prominent example is that of apamin (CNCKAPETALCARRCQQH), a naturally occurring bicyclic peptide in bee venom that can circumvent the BBB and deliver several cargoes.¹⁰⁹

1.7.2 On-demand strategies for cancer

The development of activable NVs is a challenging approach used for target-specific delivery, particularly to cancer tissue. Various features typical of cancer cells can be exploited, in fact different strategies have been used for delivering cargoes that should be in specific sites.

In cancer cells there is an increase of anaerobic glycolysis, is accompanied by a high production of lactate and protons and low pH which assists in tumor growth, metastasis, and drug resistance. Thus, pH-responsive peptides can be coupled to NVs.¹¹⁰ The low pH insertion peptides (pHLIPs),¹¹¹ are able to change state according to the pH of their environment; at lower pH, their acidic amino acid residues bind protons losing their negative charge, thereby enabling deeper penetration into the membrane, which subsequently promotes their cell internalization.

Hypoxia is used for targeting cancer tissues with TAT fused to a fragment of the oxygen-dependent degradation domain of hypoxia-inducible factor-1 α protein, showed that such fusion constructs are stable in hypoxic environments and can penetrate cancer cells, while degradation occurs in the local microenvironment of normal cells, thus rendering the latter unaffected.¹¹²

Moreover, oxidative environment, could be used for the development of redox-nanocarriers, in fact the glutathione level inside the cancer cell is higher than that of normal tissue. Bioactive compounds conjugated to nanomaterials through disulfide bonds could be cleaved by GSH, or di-selenide bonds (Se-Se) also sensitive to redox potential.

Several enzymes are upregulated in cancer cell and can be used to induce a modification and drug release from different NVs. Membranes of tumor cells are extracellularly coated with different enzymes that are not expressed by healthy tissue. One family of such enzymes are matrix metalloproteases, which are endopeptidases capable of degrading protein structures in the extracellular matrix and are important for tumor invasion and metastasis.

Tsien *et al*¹¹³ blocked positively charged polyarginine CPPs through intramolecular shielding with a negatively charged peptide domain. The CPP and shielding domain are connected by a suitable peptide linker that can be cleaved by metalloproteases. In this way, the cell-penetrating ability of the CPP is reactivated by protons in the tumor cell microenvironment and the CPP can deliver the anticancer cargo exclusively into tumor cells, while the construct is unable to penetrate normal cells. This approach, in which the drug is not active in the bloodstream but becomes activated at the target site, may also be classified as a prodrug mechanism. Many nanosystems pH responsive or thermo-responsive have been developed for the targeted delivery on anticancer drug such as the doxorubicin.¹¹⁴ Several research groups have taken advantage of the combination of chitosan (CS) and PNVCL for cancer theranostics. Niu *et al.* developed a chitosan-based cascade-responsive Doxo delivery system to overcome some hard-to-treat cancers based on thermo-sensitive poly(N-vinylcaprolactam) (PNVCL)-chitosan (CS) nanoparticles, which were further modified with a CPP and loaded with Doxo. The base copolymer was optimized to undergo a phase change at the elevated temperatures of the tumor microenvironment. The acid-responsive properties of CS provide a second trigger for drug release, and the inclusion of CPP ensured the formulations accumulate in cancer tissue, demonstrated a significant reduction in tumor volume and prolonging of life span, with no obvious systemic toxicity. To prevent the premature release of the encapsulated species and endows the material with redox-responsive ICG release properties a prodrug was produced composed of mesoporous organosilica nanoparticles (HMONs) loaded with perfluoropentane (PFP) and the photothermal agent indocyanine green (ICG) and a disulfide-containing paclitaxel (PTX).

1.8 Nanosystem in antimicrobial applications

Several studies involving anti-bacterial drug delivery, based on functional materials, have been developed^{40, 115, 116} in clinical use, enabling loading, stability, and release of the drug. The antimicrobial activity of these (NVs) may act with a synergic activity both delivering other drugs and having their own antimicrobial activity. Currently, a serious increase in bacterial resistance and sepsis caused by drug-resistant bacteria infections has rendered infectious diseases even more difficult to treat. In fact, it is still an unresolved issue how to target the infection site and effectively treat and control sepsis and how to kill intracellular microbes. A high antibiotic concentration is needed to eliminate intracellular bacteria, resulting in possible adverse effects and toxicity. Moreover, biofilm can serve as a shelter for pathogenic microorganisms, which adapt to environmental pressure by adjusting their metabolism and developing strong drug resistance and resist from the attack of antibiotics and of the host system.

Drug delivery in the antimicrobial field is important to improve the drug pharmacokinetics and pharmacodynamics and NVs advantages include:

- improved antibiotic solubility,

- controlled and sustained release of the loaded antibiotic,
- prolonged systemic circulation,
- improved efficacy against intracellular infections since they can enter the host cells via endocytosis or other mechanisms as already reported for the NVs for cancer therapy.

The mechanism of microbial killing of NVs is different from that of conventional antibiotics; in fact, thanks to their physicochemical properties they can enter the bacterial cell membrane bilayers and reach the cytoplasm, simultaneously disrupting the function and integrity of the membrane. Zhang *et al*¹¹⁷ developed bioresponsive nanoparticles for drug targeted delivery of antibiotics and anti-inflammatory drugs to achieve effective sepsis control and treatment. Hou *et al*¹¹⁸ to overcome drug-resistance designed and constructed a mRNA encoding an antimicrobial peptide, an enzyme-sensitive linker peptide, and a lysosomal signal protein. While the S-thanatins (Ts) is an antibacterial peptide with specific targeting ability, which was coupled onto the surface of a liposome to act both as the targeting moiety and antibacterial component.¹¹⁹

Various classes of dendrimers (Figure 4) are able to inhibit microbial pathogens.¹²⁰ Cationic polyamidoamine (PAMAM) dendrimers, before being considered as active antimicrobials, were investigated as drug carriers to solubilize and deliver conventional antibiotics.^{121, 122} Dendrimer antimicrobial activity is strongly correlated to the effects of multivalency, deriving from the tree-like structure and clearly to the abundance of the active moieties. Cationic and/or amphiphilic dendrimers show antimicrobial activity associated with the disruption of the pathogen membrane and similar to other antimicrobial materials, the multivalency in terms of positive charges plays a key role in their antimicrobial activity, and high-generation cationic dendrimers proved to be biocides with high activity.¹²³ Peptide dendrimers based on di-, tetra- and octavalent lysine cores bound with tetra-(RLYR) or octapeptides (RLYRKVYG) elicited a strong antibacterial activity against both Gram-positives and Gram-negatives, with a major increase observed against Gram-negative bacteria.¹²⁴⁻¹²⁶

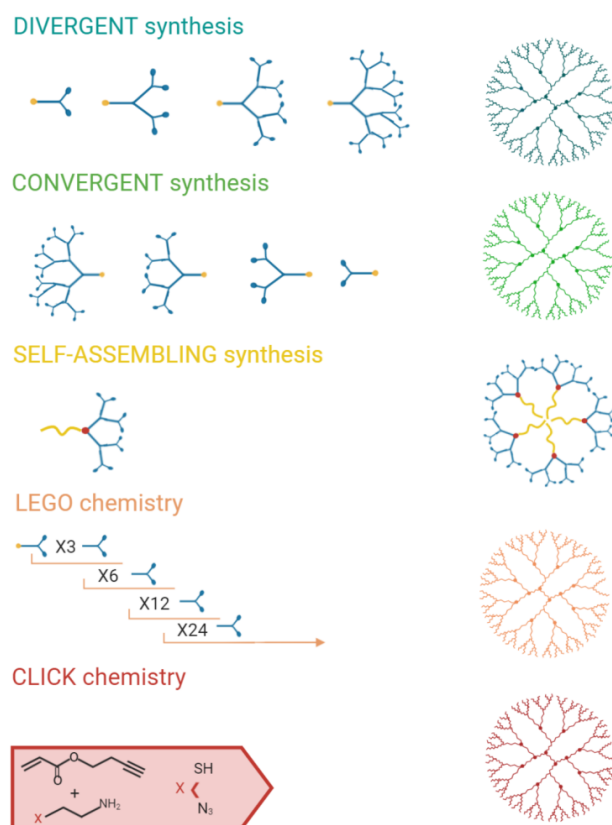


Figure 4. Synthetic strategies that can be exploited for different dendrimer development. Figure taken from *Pharmaceutics*, 2021;13(1):101.

Nanovectors have been successfully used for the delivery of antibiotics to prevent or treat bacterial colonization in biofilms (Figure 5),^{127, 128} Most antibacterial agents have difficulty in penetrating through the EPS matrix produced by a biofilm.¹²⁹ The entrapment of antibiotics in nanocarriers provides drug protection during the delivery process, thereby enhancing and prolonging the antimicrobial efficacy.

The interactions between biofilm and NVs are regarded as having three stages: NV transfer in the biofilm vicinity, attachment to the biofilm surface, and migration into the biofilm.¹³⁰ The interactions between biofilm and NVs are mainly determined by the electrostatic force. Both the surface charge of the NV and that of the biofilm matrix regulate the interaction. The negatively-charged matrix easily interacts with cationic nanoparticles through electrostatic attraction.¹³¹ Once the nanoparticles are deposited in the biofilm, they distribute and diffuse into the biofilm through the EPS matrix. After the nanoparticle distribution in the matrix, antimicrobial nanosystems can further kill pathogens via protein function inhibition, DNA damage, translation disturbance, and/or transcription dysregulation.¹³²

A nanosystem based on second-generation peptide dendrimer (2D-24) was able to penetrate the biofilm matrix and proved to have a promising synergistic effect when administered in combinations with ciprofloxacin, tobramycin, or carbenicillin, while cationic carbosilane dendritic system functionalized with an antibiotic and a peptide was developed to inhibit the formation of *S. aureus* biofilms, showing both antibiofilm damaging and antibiofilm inhibitory activities.¹³³ Antimicrobial peptide (AMP) sequence on the periphery of the

nanosystems increases their effective local concentration compared to soluble peptides and is the driving force for improved antibacterial activity. A novel versatile platform was developed in my thesis laboratory to immobilize one AMP (with the same strategy applicable to immobilize several AMPs) on a peptide-based biomaterial. The antimicrobial peptide WMR, previously identified as a modification of the native sequence of the marine antimicrobial peptide myxinidin, was used.¹³⁴⁻¹³⁶ The fiber structure was obtained through a self-assembling peptide module and a hydrophobic chain, while the external surface of the fiber was decorated with WMR. The self-assembled nanostructures showed increased stability and half-life. The multivalent presentation of WMR on self-assembled nanostructures improved anti-biofilm activity against the Gram-negative bacterium *P. aeruginosa* and the fungus *Candida albicans*. Interestingly, fibers were able both to inhibit the biofilm formation and to eradicate pre-formed biofilms with both processes being key for biomedical applications. This is a sound strategy to design smart materials, which may also contain a conventional antibiotic and be stimuli responsive (pH-driven), releasing the loaded antibiotic and antimicrobial peptide following a change in pH.

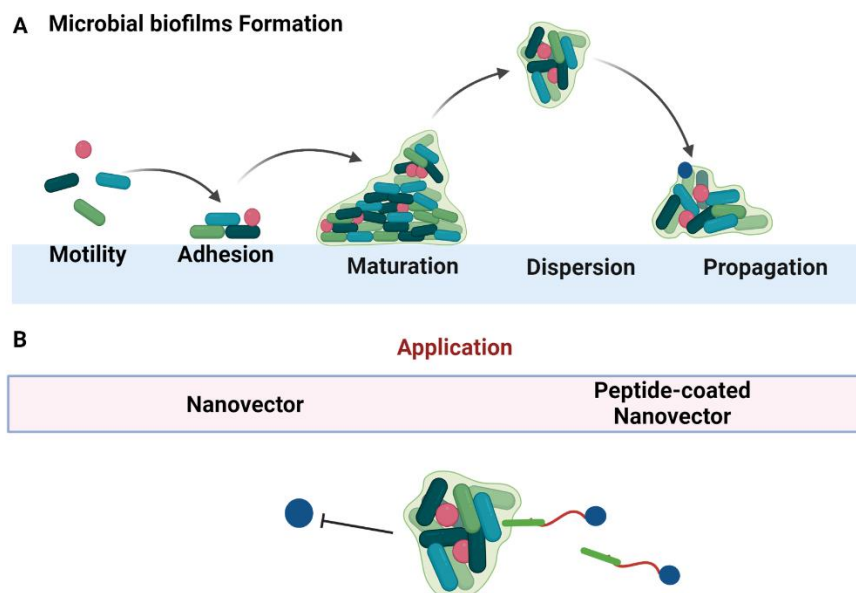


Figure 5. Steps for the formation of the antimicrobial biofilm (panel A) and nanovector inhibited by biofilm compared with nanovector functionalized to interact with the biofilm (panel B).

1.9 Objectives

Nanotechnology is an area of science devoted to the design, construction, and utilization of functional structures on the nanometer scale. The properties of nano-materials often differ from those of the corresponding bulk materials. Based on their multiple advantages, nanomedicine aims to improve bioavailability, dose response and specificity of therapeutic agents.¹³⁷ Indeed, although the nanomedicines have provided new opportunities for threatening and diagnosing cancer, their practical application has been limited by problems of toxicity, instability, and lack of selectivity for the disease site. In fact, NVs can be intrinsically toxic and/or immunogenic, display limited loading capacity, release the drug prematurely or incompletely, are poorly degradable thereby representing a long-term toxicity issue.¹³⁸⁻¹⁴⁰

These limitations inspire the development of new materials in order to achieve controlled, and targeted drug release and limited nanosystem toxicity.

The aim of this PhD project is the development of NVs for drug delivery systems. In particular, much attention is devoted to anticancer and antimicrobial nanosystems exploiting peptides.

The first aim of the PhD project has been the development of a dynamic anticancer nanovector (NV) based on peptides for cancer applications. The innovative approach is the formulation of a self assembled peptide NV based on weak interactions and functionalized on the surface with a peptide to enhance internalization (CPP), and a matrix metalloproteinase-9 (MMP-9) responsive sequence, which proved to enhance respectively the penetration and the tumor-triggered cleavage to release doxorubicin in Triple Negative Breast Cancer cells where MMP-9 levels are elevated. Moreover, loaded with superparamagnetic iron oxide nanoparticles (SPIONs) to favor targeted delivery through external magnetic field.

The second aim is the development of NVs to obtain: i) a more effective antiviral platform and ii) to contrast the serious increase in bacterial resistance and sepsis caused by drug-resistant bacteria infections. Infectious diseases are more difficult to treat and still represent an unsolved problem. The use of NVs as antimicrobial drug delivery tools ensures that the drug can be adsorbed, encapsulated or bound with an on-demand delivery mechanism. They also allow to improve the pharmacokinetics and pharmacodynamics of the drug and include several advantages such as improved antibiotic solubility, controlled and sustained release of loaded antibiotic, prolonged systemic circulation, and improved efficacy against intracellular infections. Exploiting their physico-chemical properties the NVs can enter the double layer of the bacterial cell membrane and reach the cytoplasm, simultaneously disrupting the function and integrity of the membrane. In this way it is possible to obtain a mechanism of microbial killing, completely different from conventional strategies.

Section 1

Nanosystem for cancer applications

25

Chapter 1. Drug delivery systems for cancer therapy

Section 2

Nanosystems for antimicrobial applications

The data reported in this section are published in:

Lombardi L, Falanga A, **Del Genio V**, Palomba L, Galdiero M, Franci G, Galdiero S *A boost to the antiviral activity: Cholesterol tagged peptides derived from glycoprotein B of Herpes Simplex virus type I*. International Journal Biological Macromolecules, 2020;162:882-893.

Falanga A, **Del Genio V**, Kaufman E A, Zannella C, Franci G, Weck M, Galdiero S. *Engineering of Janus-Like Dendrimers with Peptides Derived from Glycoproteins of Herpes Simplex Virus Type 1: Toward a Versatile and Novel Antiviral Platform* International Journal of Molecular Sciences 2021; 22(12), 6488.

Falanga A, Siciliano A, Vitiello M, Franci G, **Del Genio V**, Galdiero S, Guida M, Carraturo F, Fahmi A, Galdiero E. *Ecotoxicity Evaluation of Pristine and Indolicidin-coated Silver Nanoparticles in Aquatic and Terrestrial Ecosystem*. International Journal of Nanomedicine, 2020; 15:8097-8108.

27

Falanga A, **Del Genio V**, Galdiero S. *Peptides and Dendrimers: How to Combat Viral and Bacterial Infections* Pharmaceutics. 2021; 13(1):101.

Lombardi L, Falanga A, **Del Genio V**, Galdiero S. *A New Hope: Self-Assembling Peptides with Antimicrobial Activity* Pharmaceutics, 2019; 11(4):166.

Contributions in synthesis: Solid Phase Peptide synthesis, purification by HPLC and characterization, liposome preparation, functionalization of Dendrimers and Nanoparticles.

Contributions in characterization: Critical aggregation concentration (CAC) determination, Circular Dichroism, DLS and ζ -Potential measurement; membrane fluidity study, surface plasmon resonance, IR Spectroscopy.

Chapter 2

Drug delivery systems for antiviral applications

2.1 Introduction

The application of nanotechnology in the diagnosis, vaccine production, treatment and prevention of diseases is continuously receiving excellent research attention. Outbreaks and pandemic transmission of viruses, such as coronaviruses and influenza viruses, set off a global health emergency across the world. The recent COVID-19 pandemic has demonstrated its catastrophic impact worldwide on human health and on socioeconomic growth.¹⁴¹ Regarding vaccines, irrespective of the mechanism of action, their effectiveness and stability depend on the delivery medium. Drug delivery carriers have been successfully applied in the development of vaccines and the advanced research results have made possible to get from bench to bed so rapidly, demonstrating the key role played by drug delivery tools in medicine. In fact, based on these delivery platforms, the use of FDA approved nanoparticles has offered excellent results in vaccine delivery and the delivery of antiviral drugs.

A major challenge against infections triggered by many viruses is the lack of effective methods for prevention and treatment. Enveloped viruses are characterized by the presence of a lipid bilayer, which is acquired during assembly and is decorated by one or more glycoproteins. Envelope glycoproteins make up the critical interface between the virus and the host cell.¹⁴¹ A crucial step of the entry process mediated by these glycoproteins, is the merging of the viral membrane with the host cell membrane.¹⁴² During the entry step, viral glycoproteins undergo a controlled set of conformational rearrangements, which facilitate the close apposition of the two membranes, and eventually generate a fusion pore with following release of the genetic material inside the host cell.¹⁴³ Now, three different classes of viral glycoproteins specific to each virus are known, which operate through a common mechanism. Trimers of hairpins containing a central α -helical coiled-coil structure are distinctive of class I fusion proteins; trimers of hairpins composed of β structures are typical of class II; a central α -helical trimeric core in the post-fusion trimer like class I fusion proteins is characteristic of class III. However, each fusion domain is composed of two fusion loops localized at the tip of an elongated β -sheet revealing also a striking resemblance with class II. Fusion proteins belonging to class I are the most widely characterized; they possess two heptad repeat domains (HRs): the first one adjacent to the fusion peptide (HR-N) and the second one immediately preceding the transmembrane domain (HR-C).¹⁴⁴ The current model suggests that once fusion is initiated by the binding to cellular receptors, the HR-C and HR-N domains, separated in the pre-hairpin intermediate, fold one on the other (with the HR-N trimer in the center), leading to the formation of a 6-helix bundle (6HB) and ultimately resulting in fusion of the viral and host membranes.¹⁴⁵ Structural and biophysical

analyses suggest that peptide inhibitors can be developed, which binding to their complementary HR region in the pre-hairpin intermediate, prevent HR-N and HR-C from refolding into the stable 6HB structure required for the fusion process.¹⁴⁵ Peptides modelled from either the N or C helical region of several class I fusion proteins have been developed as a promising antiviral strategy and one of them, T20 (enfuvirtide), is in clinical use for HIV-1.^{145 146}

Among the different classes of viruses, *Herpes Simplex Viruse* (HSV) represents one of the major global health problems; over the past 40 years, numerous strategies have been developed to fight the herpetic infection and three classes of drugs are licensed for HSV treatment, all based on the inhibition of viral DNA replication such as acyclovir (ACV), cidofovir, and foscarnet.¹⁴⁷ Although these agents are efficacious against the HSV infection, side effects and limitations are associated with their use. Importantly, the resistance, especially among immunocompromised patients undergoing long-term therapy, represents an important clinical problem.¹⁴⁸ Therefore, it is of utmost importance to identify alternative antiviral systems with different mechanisms of action and different targets.¹⁴⁹ HSV has a multicomponent fusion machinery involving multiple viral glycoproteins and cellular receptors.¹⁵⁰ The glycoproteins gH/gL, gB, and gD can induce fusion of cellular membranes also in the absence of viral infection and are thus all essential for the entry process.¹⁵⁰ In particular, gH/gL and gB comprise the core fusion machinery and cooperate to induce the initial lipid disruption that culminates in fusion. gB and gH are conserved among the *Herpesviridae* family. Structural details of gB suggested that it belongs to a third class of fusion proteins where the fusion peptide is characterized by a bipartite loop domain (19–21), while gH is characteristic of class I and class II fusion proteins and considered an important fusion effector (15, 16, 19, 33). Previously, the gH region comprising amino acids 626–644 has been studied for its ability of inducing lipid mixing of model membranes and inducing 50% of fusion at a low peptide/lipid ratio; furthermore, a mutation in this region induces a loss of activity.¹⁵¹ A detailed deletion study regarding the C- and N-termini of gH, has led to identification of its shorter sequence named gH493-511 (NH₂-AAHLIDALYAEFLGGRVLT-CONH₂), that showed a higher antiviral activity (IC₅₀=160 μM) and a strong ability to inhibit infectivity when present during virus attachment-entry into cells.¹⁵²

Here, to further explore the possibility to enhance the antiviral activity of lead sequences gBh1m and gH493-511, we explored two different delivery strategies:

- i) peptide engineering through cholesterol tagging,
- ii) dendrimer conjugation.

Several peptide-engineering strategies, including optimization through sequence-specific modifications, can be exploited to enhance the potency of peptide inhibitors. A strategy consists in the addition of moieties to native HR derived sequences to increase the antiviral activity without a further need to change the sequence. In particular, the host cell penetration of several viruses requires the presence of lipid rafts, which are formed by cholesterol and sphingolipids. Thus, cholesterol (Chol) tagging has been applied to several enveloped viruses as a tool to achieve a significant increase of the antiviral potency.^{153, 154} Cholesterol tagging of C34, a peptide derived from the HRC domain of HIV-1 gp41, resulted in an inhibitor more potent (25- to 100-fold) than the native sequence and the clinical drug

enfuvirtide (50- to 400-fold).¹⁵⁴ Previous studies have also pointed to the key role played by the addition of a PEG linker between the lipid moiety and the peptide sequence.^{155, 156} PEG proved critical for tissue penetration, apart from being non-toxic, and non-immunogenic.

In addition to peptide-engineering strategies, nanotechnologies provide the foundation for the advancements in antiviral therapies.¹⁵⁷ Several unique features of nanomaterials (such as small-size, high surface-to-volume ratio modifiable surfaces) may contribute to favor antiviral effects, which may include virus inactivation and blocking a virus from entering host cells. Dendrimers, products of an iterative synthesis with discrete monomer building blocks, are platforms capable of securing multiple orthogonally bound functionalities (*e.g.*, dyes, peptides, drugs) within a well-defined and tailored arrangement. Dendrimers are functional nano/macromolecules owing to a well-defined size, tailored structure, and precise number of active termini that dictate their properties and applications.¹⁵⁸ While groundbreaking work on dendrimers was accomplished over 30 years ago, dendrimers^{159, 160} appear to be one of the most attractive synthetic architectures for many disciplines with the most effective applications ranging from transdermal drug delivery,¹⁶¹ gene delivery,¹⁶² magnetic resonance imaging contrast agents,¹⁶³ to dendritic sensors and safe and effective microbicides.^{164, 165} Dendrimers represent one of the most promising drug delivery scaffolds (DDS)¹⁶⁶ for targeted drug delivery.

In this thesis, two different strategies to develop novel antiviral therapies based on peptides have been developed. The first approach is based on the engineering strategy of a sequence derived from the glycoprotein gB, the second on a dendrimer nanosystem functionalized with two different antiviral peptides, one derived from gB and one from gH.

Results and discussion

2.2 Peptide engineering strategy

2.2.1. Design

The first strategy is based on the use of the antiviral sequence gBh1m, previously developed in my group.¹⁶⁷ In particular, the long helical segment of the post-fusion gB protein from HSV-1 contains a heptad repeat sequence, typical of coiled-coil structures.¹⁶⁸ Peptides comprising the N-terminus of this long helical sequence (residues 500 to 523) are more active in inhibition compared to those comprising the C-terminal side (residues 524 to 544), and the N-terminal part of this helix is fully exposed in the prefusion state and can be reached by inhibiting peptides.^{169, 167, 170} Previously, starting from these results, my research group designed a peptide inhibitor gBh1m (residue 503 to 523) with some modifications developed to enhance its ability to adopt a helical structure. In particular, charged glutamic acid and arginine residues were introduced into non-core positions so that the spacing (*i, i+4*) favored the formation of an ion pair in the helical conformation.¹⁶⁷

During my PhD studies, we designed and synthesized a set of peptides derived from gBh1m, adding a lipophilic moiety and a PEG linker to develop a novel antiviral compound based on gBh1m. In particular, we added a cholesterol moiety, which proved to be important for membrane interactions for other viruses and we evaluated the role played by the length

of the PEG linker located between the peptide sequence and the cholesterol moiety. Moreover, the orientation of the peptide inhibitor was evaluated through the conjugation of the PEG-Chol at the N-terminus or at the C-terminus of the peptide. If the N-terminus of the peptide is key for the interaction and thus for the inhibition, it may result that conjugation at the N-terminus is detrimental to inhibitory activity; nonetheless, the presence of the PEG linker may aid in the positioning of the peptide inhibitor and thus determine no effect of the orientation.

2.2.2. Peptide synthesis

The peptides listed in Table 1 were synthesized on a Rink amide resin. Peptides were first acetylated and then cleaved from the resin with an acid solution of TFA in presence of scavengers and precipitated in ice-cold diethyl ether. The peptides were purified by HPLC.

Table 1. Peptide sequences.

Peptide name	Sequence
gBh	Ac-SIEFARLQFTYNHIQRHVNDMLGRVAIAWCELQNHETLWNEARK-CONH ₂
gBh1m	Ac-FARLQFTYNHIQRHVRDMEGR-CONH ₂
gBh1m-Cys-PEG24-Chol	Ac-FARLQFTYNHIQRHVRDMEGRGSGSGC(PEG24-Chol)-CONH ₂
gBh1m-Cys-PEG12-Chol	Ac-FARLQFTYNHIQRHVRDMEGRGSGSGC(PEG12-Chol)-CONH ₂
Chol-PEG24-Cys-gBh1m	Ac-C(PEG4-Chol)GSGSGFARLQFTYNHIQRHVRDMEGR-CONH ₂
Chol-PEG12-Cys-gBh1m	Ac-C(PEG12-Chol)GSGSGFARLQFTYNHIQRHVRDMEGR-CONH ₂

2.2.3. Chemical conjugation

Chemical conjugation of moieties such as Chol and PEG linkers might affect the peptide stability in water solution and induce the formation of nanoparticles; this is certainly implicated in the antiviral activity which is related to a balance between self-aggregation properties in water solution and insertion into the membranes of the target cell and/or of the viral envelope.¹⁷¹ We thus explored the relationship between physicochemical properties and inhibitory efficacy *in vitro*.¹⁷⁰ Synthesis of the cholesterol tagged fusion inhibitors were prepared through conjugation of the cysteine-containing peptides (cysteine located at the N- or C- terminus according to the desired compound) to the bromoacetyl functionalized moieties in presence of DIPEA to obtain: Peptide-PEG12-Chol and Peptide -PEG24-Chol, using syringe pump as strategy for an optimal conjugation and a reduced undesired side reactions. Firstly, we tried to perform the conjugation by mixing directly the cholesterol, the peptide and the base together in a tube but this method, despite the low concentration of the base, led to the formation of the disulfide bridge between the peptides. Instead, mixing the Chol with the base and the subsequent addition of the peptide through the syringe pump has allowed the selective conjugation between the wanted molecules avoiding the undesired oxidation of the peptide cysteines.

2.2.4 Antiviral analysis

The impact of PEG length and position of Chol on *in vitro* antiviral activity was analyzed through a screening of their ability to inhibit plaque formation. The toxic effect was analyzed on cells monolayers which were exposed to a range of peptide concentrations (1, 5, 10, 20, 50, 100, 200 μM) for 24 h, and cell viability was obtained by an MTT assay. Cell cultures without treatment were used as the positive control while cell cultures with 0% DMSO were used as negative control estimating the 50% cytotoxic concentration (CC_{50}).¹⁷² (Figure 1, panel A) All molecules have a rather high CC_{50} , mainly indicating low cytotoxicity at the concentration used for antiviral assays. It was observed a significant toxicity for cells treated with Br-PEG24-Chol moieties (data not shown) compared to viability of control (untreated) cells and that of cells exposed to the peptides. Previously was reported that the peptide gBh1m inhibited HSV infection prior to virus penetration into cells; in particular, in the virus pre-treatment experiment at 100 μM the percentage of inhibition was 100% and at the same concentration in the co-treatment experiment was 50%. The preliminary results (data not shown) obtained for the new compounds at concentrations 50, 100 and 200 μM clearly indicated that the presence of cholesterol and of the PEG linker were able to boost the inhibition activity; we thus performed the experiments at lower concentrations (1, 5, 10, 20 μM). Vero cells were treated with HSV-1 in the presence or absence of each peptide under a range of different conditions are reported. (Figure 1-2). Vero cells were treated with HSV-1 in the presence or absence of each peptide under a range of different conditions, none of the peptides was active in the post-exposure treatment (Figure 1, panel B), in which cells were infected for 45 min and peptides were then added to the cultures. Instead, the co-treatment experiment (Figure 1, panel C) showed clearly that the peptide functionalized with PEG24 at the C-terminus was the most active. In particular, virus pre-incubation resulted to be the best experiment. The cholesterol addition improved significantly the activity of gBh1m with PEG24, producing the best results as estimated by the calculation of the 50% antiviral concentration (IC_{50}) with GraphPad (Figure 2, panel C). A more detailed analysis allowed determining that the analogues with the modifications at the C-terminus were always more effective at blocking entry, indicating that the N-terminus is key for the interaction. In addition, we further analyzed the effect of the PEG linker length and we noticed that while the most active analogue was the one bearing PEG24 and cholesterol at the C-terminus, the results reversed when we compared PEG12 and PEG24 analogues modified at N-terminus, with PEG12 showing the highest activity (Chol-PEG12-Cys-gBh1m show an IC_{50} of 18 μM instead Chol-PEG24-Cys-gBh1m have an IC_{50} of 24 μM). These results clearly indicate that both orientation and length of the linker play a key role.

These data allowed the calculation of the selectivity index defined as the ratio of the CC_{50} to the IC_{50} . The obtained values showed that the highest value was achieved for gBh1m-Cys-PEG24-Chol; thus, the addition of PEG24 at the C-terminus boosts the antiviral activity of gBh1m and increases the selectivity towards the virus compared to the host cells. We also compared the activity of gBh1m-Cys-PEG24-Chol with Cys-PEG24-Chol; the Cys-PEG24-

Chol moiety was not effective, supporting the notion that potency depended on the peptide sequence and not simply on the linker and lipid moiety. (Table 2)

Lipophilicity is likely to be a key factor for antiviral activity because it determines the local concentration of the fusion inhibitors at the membrane level. gBh1m in contrast with the peptides analyzed here, lacks the lipid-binding domain and therefore has a weaker interaction with membranes. The introduction of cholesterol improves the interaction with membranes and determines an increase in antiviral potency, yielding an approximately 10-fold increase in the IC₅₀ relative to gBh1m alone.

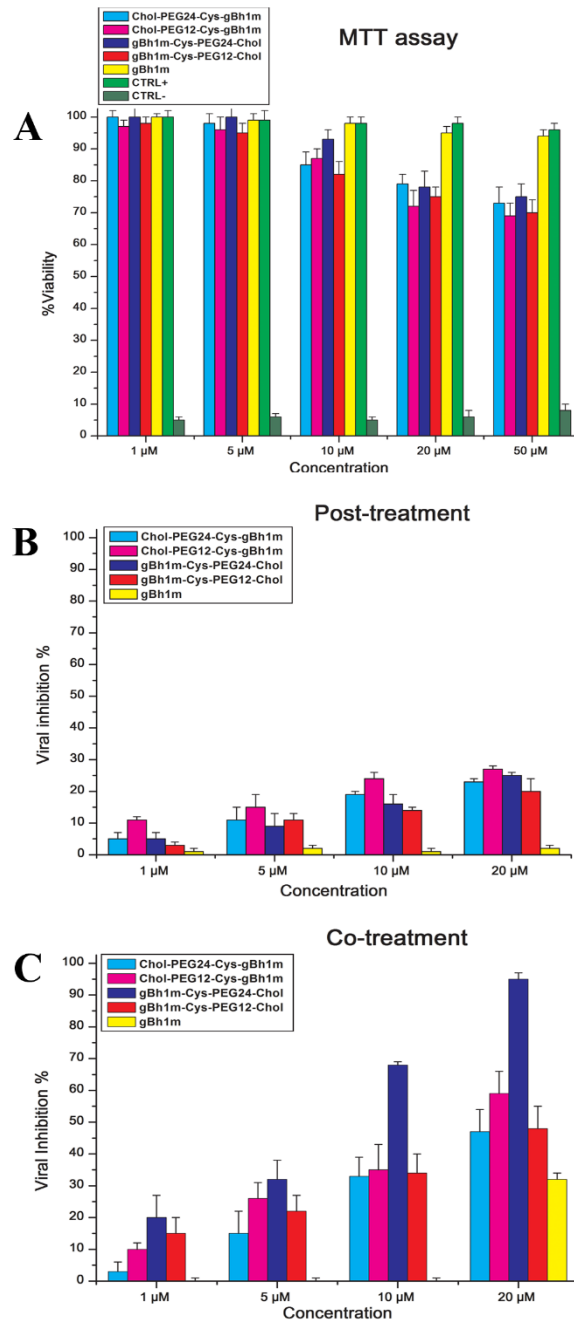


Figure 1. Cell viability measured by the MTT assay. Cell culture without and with 30% DMSO were used as the positive and negative controls, respectively (panel A). Post treatment (panel B) Assay Co-treatment assay (panelC). The data shown represent the average values \pm standard deviation for each experiment performed at least in triplicate; statistical filters were applied (p-value $\leq 0,5$). Figure taken from International Journal of Biological Macromolecules, 2020;162:882-893.

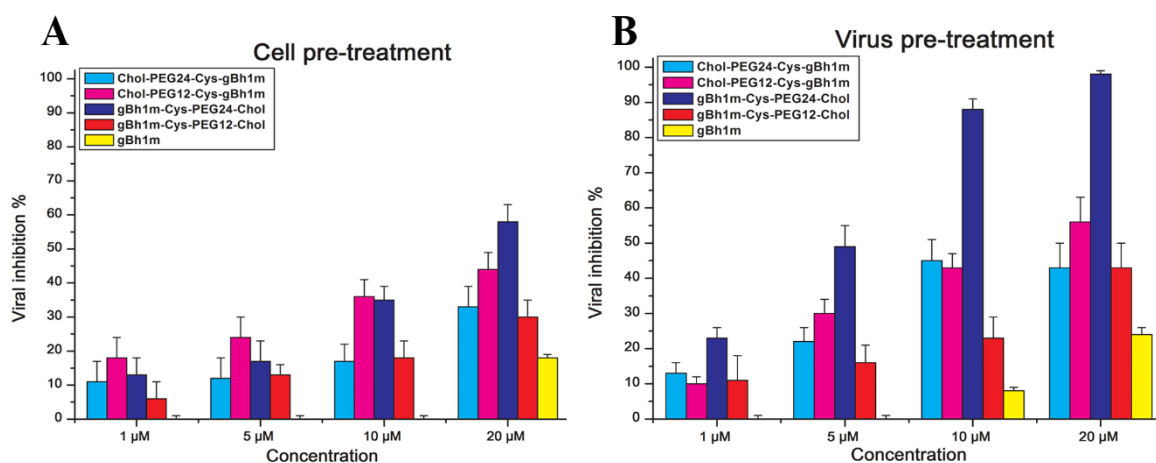


Figure 2. Cell pre-treatment assay (panelA). Virus pre-treatment assay (panel B) The data shown in A and B represent the average values for each experiment performed at least in triplicate \pm standard deviation; statistical filters were applied (p-value $\leq 0,5$). Summary of the data corresponding to the IC₅₀, CC₅₀, selective index (SI), the Critical Aggregation concentration (CAC) and the Generalized polarization (GP) for all the peptides included in this study (panel C). Figure taken from International Journal of Biological Macromolecules, 2020;162:882-893.

Table 2. Summary of the data corresponding to the IC₅₀, CC₅₀, selective index (SI), the Critical Aggregation concentration (CAC) and the Generalized polarization (GP) for all the peptides included in this study (panelC).

Peptide	CC ₅₀ (μ M)	IC ₅₀ (μ M)	SI	CAC(μ M)	GP		
	MTT	Virus pre-treatment	CC ₅₀ / IC ₅₀		No peptide	5 μ M	25 μ M
gBh1m	178 \pm 3	58 \pm 1	3.1	ND	ND	ND	ND
gBh1-Cys-PEG24-Chol	138 \pm 4	6 \pm 1	23.0	21.4 \pm 1.4	0.16	0.14	0.20
gBh1-Cys-PEG12-Chol	105 \pm 3	56 \pm 2	1.9	18.2 \pm 1.8	0.16	0.15	0.17
Chol-PEG24-Cys-gBh1m	150 \pm 3	24 \pm 1	6.2	ND	ND	ND	ND
Chol-PEG12-Cys-gBh1m	180 \pm 3	18 \pm 1	10.0	ND	ND	ND	ND

Abbreviation: ND, not determined.

2.2.5. Structural studies

gBh1m-CysPEG24-Chol and **gBh1m-Cys-PEG12-Chol** were analyzed by a fluorescence assay with the fluorophore Nile red, to evaluate their self-assembling capabilities. Nile red emission signal change in different environments, allows the determination of the CAC at different concentrations of single peptides. Nile red is poorly water soluble and shows a large preference to partition in aggregates with hydrophobic binding sites producing a blue shift and hyperchromic effect. In particular, both peptides were able to aggregate with a CAC value of 18.8 μ M for **gBh1m-Cys-PEG24-Chol** containing the PEG24 linker (Figure 3, panel A) and of 17.5 μ M for **gBh1m-Cys-PEG12-Chol** containing the PEG12 linker (Figure 3, panel B). The CAC are similar, with a slightly higher value for PEG24 compared to

PEG12 indicating that **gBh1m-CysPEG12-Chol** can form more stable nanoassemblies at lower concentrations.

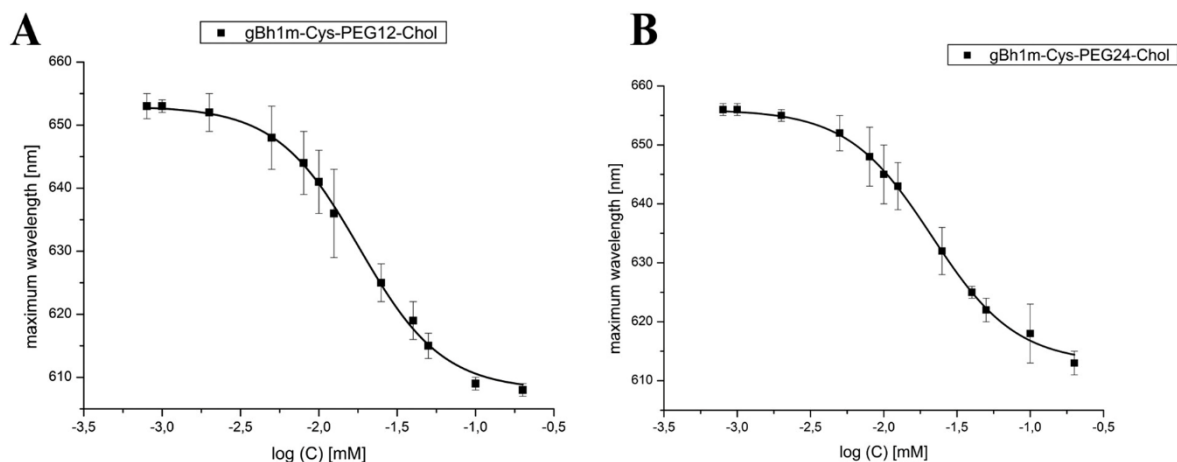


Figure 3. Wavelength corresponding to the maximum fluorescence emission of Nile red was plotted as a function of concentration of: gBh1m-Cys-PEG12-Chol (panel A) and gBh1m-Cys-PEG24-Chol (panel B), to determine their CAC. The measurements were repeated three times. Figure taken from International Journal of Biological Macromolecules, 2020;162:882-893.

2.2.6. Membrane fluidity and DLC analysis

Membrane fluidity before and after the addition of **gBh1m-Cys-PEG24-Chol** and **gBh1m-Cys-PEG12-Chol** was evaluated using the fluorescent probe Laurdan,^{173, 174} in presence of LUVs composed of PC/Chol (2/1) that mimicking the composition of viral and eukaryotic membranes. Laurdan can insert into membranes and distribute equally between lipid phases; when in gel phase membranes, it presents an emission maximum at 440 nm, while when in liquid phase membranes the emission maximum is shifted at 490 nm. The Generalized Polarization (GP) is a parameter used to evaluate the change in the lipid fluidity: a negative value is obtained for liquid phase membranes while a positive value is obtained for gel phase membranes. Before the treatment with peptides, the measured emission spectra of LUVs clearly indicate the presence of ordered phases at 37 and at 25°C. Subsequently, the GP parameter was evaluated to quantify the effect of the peptides on the lipid bilayer. In particular, the fluidity of the membranes at 37°C in the presence of both peptides was slightly modified with a greater effect observed for PEG24. In fact, in the case of PEG24, we observe a slight increase of the GP parameter, indicating a shift towards more ordered membranes. We believe that PEG24 peptides presented a higher ability to insert into the membranes compared to the PEG12 peptides; nonetheless, it is to keep in mind that it remains a formal possibility that these peptides interact with lipids without significantly modifying the fluidity of the membrane. The presence of cholesterol has enhanced the rigidity of the membrane bilayer; thus our results reinforce the importance of the lipid moiety for the interaction and likely indicate that the peptides are able to locate inside the membrane bilayer.

The interaction between peptides and liposomes was further analyzed by DLS to determine whether peptides were able to increase the dimensions of liposomes. We thus determined the hydrodynamic diameter of liposomes before and after the addition of peptides. We

determined the size of the aggregates at two different peptide concentrations: below and above the CAC (5 and 25 μM).

The results obtained are reported in Table 2 and clearly indicate that below the CAC (at 5 μM) the dimension of the liposomes increase slightly while we observe a significant increase of their dimension above the CAC (at 25 μM). In particular, for PEG24 we observe dimensions around 172 nm which do not change with time, while for PEG12, we initially observe a peak around 168 nm ($t = 0$) which then disappears and we detect two peaks one at 691 and the other at 116 nm at 1.5 h; PDI also increased, indicating severe polydispersity and supporting the existence of cluster-type aggregates. This result seems to support the view that PEG12 forms greater aggregates (above the CAC) and after an initial insertion in the LUVs it rapidly favors the formation of clusters; on the contrary we do not observe such behavior for PEG24 peptides which both below and above the CAC is stably inserting into the membranes. (Table 3)

Table 3. Dimensions of LUVs treated with peptides at various times

No peptide	125 \pm 2			
Peptide	t=0 5 μM	t=0 25 μM	t=1.5 h 5 μM	t=1.5 h 25 μM
gBh1m-Cys-PEG24-Chol	138 \pm 6	172 \pm 5	146 \pm 4	149 \pm 3
gBh1m-Cys-PEG12-Chol	139 \pm 4	168 \pm 8	60 \pm 9	691 \pm 20 (76%) 115 \pm 12 (24%)

2.2.7. Binding and surface plasmon resonance analysis

To better understand the mechanism underlying the enhanced antiviral activity, we performed CD experiments to determine any evidence of interaction with gBh. While gBh can adopt a α -helical conformation in water solution, **gBh1m-CysPEG24-Chol** showed a random coil conformation. If two peptides do not interact, no structural change occurs; therefore, the theoretical (the sum of the two spectra of the non-interacting peptides, magenta spectrum) and experimental (the spectrum of the mix of the two peptides, black spectrum) spectra will be identical. On the contrary, if two peptides do interact, a structural change of the components may result; therefore, theoretical and experimental spectra will be different. Figure 4, panel A shows the results of a CD mixing experiment of gBh and **gBh1m-Cys-PEG24-Chol**; a significant difference between the two spectra is evident, strongly suggesting that the two peptides may interact to produce a structural change when mixed in solution. The results of the CD experiments correlate well with the results previously obtained for the interaction between gBh and gBh1m (even though essays were performed in different experimental conditions)

To simulate the location of **gBh1m-Cys-PEG24-Chol** inside the membrane bilayer of the virus/host cell was prepared a liposome containing the peptide (gBh1m/Lip). The method of preparation of this sample implicates that half of the peptide is located on the external surface and half in the aqueous core of the liposome. Thus, we can probe the interaction of the peptide located on the external surface of a liposome with gBh. Also, the peptide in gBh1m/Lip, as **gBh1m-CysPEG24-Chol**, showed a helical conformation in water solution. We further collected the experimental spectrum of the mix and calculated the theoretical

spectrum. Figure 4, panel B shows the results of a CD mixing experiment of gBh and gBh1m/Lip, we observed again a significant difference between the two spectra, strongly suggesting that the two peptides may interact to produce a structural change when mixed in solution. The results of the CD experiments correlate well with the antiviral results obtained. Surface plasmon resonance (SPR) is an optical-based, label-free detection technology for real-time monitoring of binding interactions between two or more molecules. We used SPR to confirm the presence of an interaction between gBh and the peptide **gBh1m-Cys-PEG24-Chol**. We previously reported SPR experiments to probe the interaction between gBh and gBh1m and we clearly obtained that gBh1m initially binds with gBh with a high affinity; this step is further followed by a less stringent step, likely indicating a conformational rearrangement. In this case was designed another experiment to probe the affinity of the two peptides when gBh1m is located on the external surface of a membrane bilayer, thus simulating what happens during the entry of HSV. For this aim, we used the HPA chip, which allows to prepare a monolayer of PC/Chol exposing on its surface the peptide sequence gBh1m (the ligand). To obtain these liposomes with gBh1m on the surface, we inserted **gBh1m-PEG24-Chol** in liposomes preparation exploiting the hydrophobic force. The experimental setting allows only the exposure of gBh1m while the lipids of the monolayer are not accessible to the analyte (gBh) and thus no interaction with the liposome can be envisaged. The sensorgrams revealed that the RU signal intensity increased as a function of the analyte concentration (Figure 5, panel A). The analysis of the shape of each sensorgram reveals important clues concerning the binding kinetics; in particular, the sensorgrams indicate that the ligand binds in a biphasic manner, with an initial association starting as a fast process and then slowing down considerably towards the end of the peptide injection.¹⁷⁵

The dissociation follows a similar pattern, with the signal falling rapidly at the end of injection since the peptide is no longer present and the buffer flow removes a large amount of free or weakly bound peptide, followed by a much slower step. Moreover, the sensorgrams did not return to zero, indicating that the analyte remained significantly bound to the ligand. We employed numerical integration analysis that uses nonlinear analysis to fit an integrated rate equation directly to the sensorgrams.¹⁷⁵ We used several fitting models and we compared them to better understand the mechanism of interaction. When fitting the sensorgrams globally (using different concentrations of the analyte) with the simplest 1:1 Langmuir binding model, a good fit was obtained ($\chi^2 = 2.9$), confirming that this model likely represents an acceptable model for the interaction. A set of peptide sensorgrams with different peptide concentrations was used to estimate the kinetic parameters. The average values for the rate constants obtained from the Langmuir model analysis are listed in Figure 5, panel C along with the affinity constant values (K_A); the data obtained are in agreement with those previously obtained with an affinity constant of the order 10^5 .¹⁶⁷ Then we used the Bivalent Analyte model, which describes the binding of a bivalent analyte to immobilized ligand, where one analyte can bind two ligand molecules. The obtained fit was good as well ($\chi^2 = 2.4$), but the analysis of the kinetic constants obtained showed that the k_{a2} and k_{d2} are too low to support the presence of this second interaction. We also used the Heterogeneous Ligand (parallel reactions) model, which describes an interaction between one analyte and two independent ligands. The obtained fit was very good ($\chi^2 \approx 1$), and the

analysis of the kinetic constants obtained seemed to be significant. (Table 4) Our data support a model (Figure 4, panel B) in which the analyte will bind to a ligand with an affinity of approximately 10^5 and then being close to other analyte molecules, it will be able to bind to at least a second analyte. These findings, demonstrate that several gBh1m molecules can bind to each gBh similarly to what happens in the envelope glycoprotein during the fusion process when the entry involves the formation of a trimer of helices.

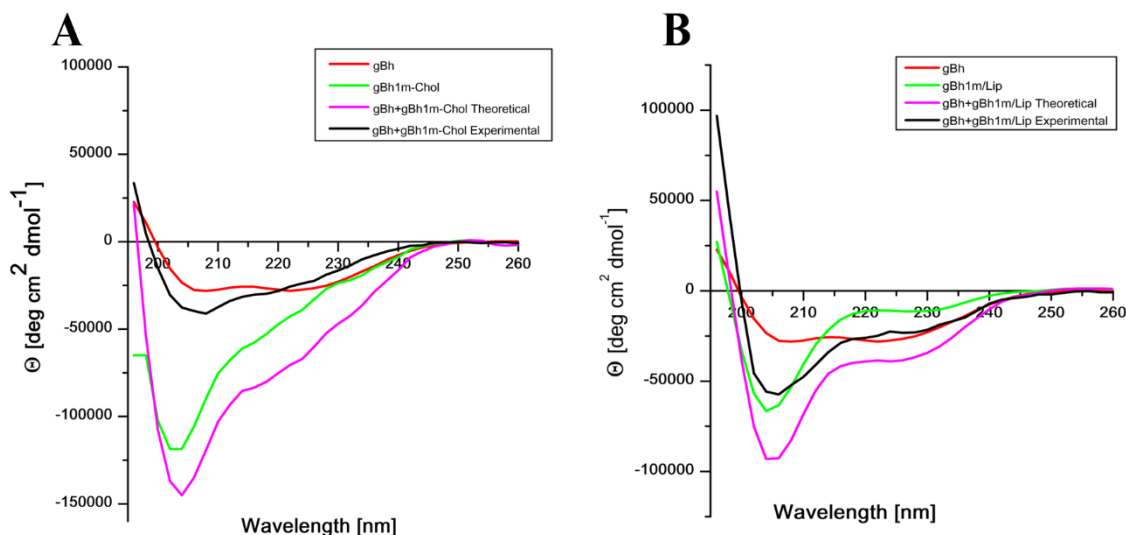


Figure 4. Report the analysis of the interactions between gBh and gBh1m-Chol peptides by Circular Dichroism. Mixing experiments were performed by comparing the spectrum of the two peptides mixed at the desired concentrations (experimental spectrum) and the sum of the spectra of each peptide alone (theoretical spectrum). CD spectra of gBh, gBh1m-PEG24-Chol and their theoretical and experimental spectra in aqueous solution (panel A). CD spectra obtained for gBh1m-PEG24-Chol inserted into liposomes, gBh and their theoretical and experimental spectra (panel B). Figure taken from International Journal of Biological Macromolecules, 2020;162:882-893.

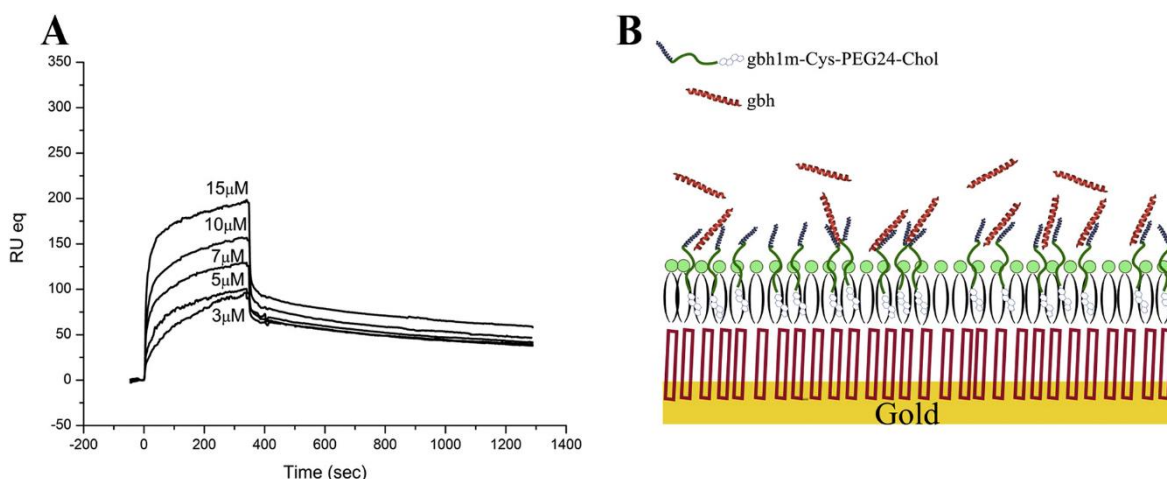


Figure 5. Membrane binding affinity of gBh1m-PEG24-Chol into liposomes and gBh at several concentrations by surface plasmon resonance. Sensorgrams obtained upon injection of 30 μ l of gBh over PC/cholesterol/gBh1m-PEG24-Chol bilayers (HPA chip) (panel A); model of the interaction (panel B). Figure taken from International Journal of Biological Macromolecules, 2020;162:882-893.

Table 4. kinetic parameters of the interaction.

Model	K_{a1}	K_{d1}	K_{a2}	K_{d2}	K_{A1}	K_{A2}	X^2
Langmuir	$(1.37 \pm 0.09)10^3$	$(5.44 \pm 0.02)10^{-4}$	-	-	$2.52 \cdot 10^6$		2.9
Heterogeneous-parallel	$(2.11 \pm 0.04)10^2$	$(1.65 \pm 0.01)10^{-3}$	$(3.67 \pm 0.02)10^3$	$(2.43 \pm 0.13)10^{-8}$	$1.28 \cdot 10^5$	$1.51 \cdot 10^{11}$	0.5
Bivalent analyte	$(7.15 \pm 0.06)10^2$	$(7.22 \pm 0.07)10^{-4}$	$(5.20 \pm 0.35)10^{-4}$	$(1.78 \pm 0.11)10^{-3}$	$9.90 \cdot 10^5$	$2.90 \cdot 10^{-2}$	2.4

2.2.8. Conclusion and future perspectives

The efficacy of peptide inhibitors depends on the strength of the interaction with the target fusion protein (the peptide sequence as demonstrated by CD and SPR), but also on the location of the peptide in proximity to the target fusion protein. Delivering peptides to the correct cellular compartment, which is the membrane where fusion/entry occurs, through the addition of cholesterol moieties enhances their efficacy as antiviral inhibitors. However, correct orientation on the target membrane also plays a key role in efficacy. The C-terminally tagged peptides are highly effective and present higher activity compared to the N-terminally tagged peptides. Moreover, peptides tagged with cholesterol self-assemble into nanoparticles in water solution until they reach the target/viral membranes where they are integrated, enhancing their bio-distribution and half-life while integration into the membrane increases their fusion inhibitory ability. The presence of cholesterol, the type of PEG moiety and the peptide sequence contribute to a balance between self-assembly and disaggregation. The ability of the peptide to move from an aggregate in aqueous solution to a disaggregate structure in the proximity of its target cell is correlated with its ability to locate into the membranes and with its efficacy; moreover, an optimal balance between self-assembly and membrane integration regulates activity. Our results point to the conclusion that the most efficient antiviral peptides are lipid conjugated that self-assemble into looser aggregates and bind extensively to membranes. The presence of cholesterol can target the peptide to the membrane where fusion takes place increasing the local peptide concentration.

Several features are responsible for the *in vitro* potency observed:

- unstable self-aggregation in solution
- capacity to insert into the membrane
- strength of the peptide association with the corresponding domain of the target fusion protein.

It is likely that the cholesterol inhibitors could efficiently bind to both the cellular and viral membranes to exert their antiviral activities. Increasing the PEG linker length between the peptide and the cholesterol moiety led to a more dynamic interaction with model membranes and the presence of PEG24 may increase the exposure of the peptide chain close to the membrane surface. As a result of this higher exposure, it may be easier for the peptide chain to acquire the proper orientation and align with the domain of gB, resulting in higher antiviral activity.

Based on our biophysical and antiviral data we hypothesize that the peptide is able to interact with both the viral and the host cell membranes and may flip between the target host cell and viral membranes as previously reported also for fusion inhibitors.¹⁷⁰ These mechanisms

could also explain why the C-terminally conjugated peptides may be rendered more effective by a long linker, which could optimize alignment with gB or permit activity from both cell and viral surfaces.

Our data confirm previous finding on the applications of this strategy to antiviral compounds showing that peptide membranotropic properties may increase their local concentration at the membrane level and enhance the efficiency of the drug.

Based on these results, we developed dendrimer nanosystems functionalized with two antiviral peptides one derived from gB, namely gBh1m, and another derived from gH, namely gH493-511, to exploit the delivery efficiency of dendrimers to obtain enhanced antiviral activity.

2.3. Dendrimer Strategy

2.3.1. Design

Dendrimer design is based on the Newkome-style dendrimers that are polyamide based, thus mimicking proteins, assuring biocompatibility, and promoting biodegradability. This strategy involves the use of peptides gBh1m and gH493-511 bound to dendrimer to block viral entry at an inhibition concentration of micromolar range. In this study, we bound the peptides to two different dendrimers; that are monofunctional (DendrimerA) and Janus (DendrimerB) dendrimers (Table 5). The gBh1m peptide was coupled from the C-terminus, because a preliminary antiviral analysis performed on the gB peptide linked to the dendrimer from the N-terminus showed that the peptide loses its antiviral activity and confirmed results reported above. Instead, the peptide gH493-511 was bound to dendrimers by its N-terminus.

2.3.2. Peptide Synthesis

Peptide (Table 5) were synthesized on Rink-amide MBHA resin (0.51 mmol/g substitution). Propargyl glycine residue (PrA) was added at the N-terminus to provide a handle for the copper-catalyzed azide/alkyne cycloaddition reaction (CuAAC) with the terminal azides of the monofunctional dendrimer, and, when necessary, a cysteine residue was added at the peptide N terminus to provide thio-lene reaction with alchene groups of Janus bifunctional dendrimer (DendrimerB). Fully synthesized peptides were deprotected from the resin at room temperature and precipitated into ice cold ether. The precipitate was dissolved in water and lyophilized to obtain the crude peptides. Peptides were purified by reverse-phase HPLC as well as checked to exhibit the expected molecular ion on analysis by high-resolution mass spectrometry (HRMS). Pure peptides (higher than 98%) were achieved in good yields (40% for gBh1m peptide and 50% for gH493-511).

2.3.3. Dendrimer functionalization

The peptides were synthesized with a propargyl glycine residue (PrA) at the correct terminus to provide a handle for the copper-catalyzed azide/alkyne cycloaddition reaction (CuAAC) with the terminal azides of DendrimerA. The click functionalization was performed in a water/methanol solution (1:1 v/v) with 2:4 equivalents of $\text{CuSO}_4 \times 5\text{H}_2\text{O}$: sodium ascorbate.

The conjugates were extensively purified through dialysis, HPLC, and ultrafiltration on 30 KDa filters.

Successful peptide conjugation was confirmed using HPLC through the appearance of new peaks at retention times different from the controls that were run at the same conditions, and confirmed by IR spectroscopic analysis demonstrating the disappearance of the azide stretch at 2098 cm^{-1} suggesting that, within the instrumental error range, azides were consumed and converted in triazoles (Figure 6).

DendrimerB was functionalized with Cys-gH via photoinduced thiolene reaction and with gB-h1m via copper-catalyzed azide/alkyne cycloaddition. The thiolene reaction was performed with the Cys-gH peptide in DMF-H₂O in presence of DMPA at 4 °C for 1 h with UV light irradiation. Subsequently, DendrimerB/gH was functionalized with gBh1m as reported. The conjugates were purified through dialysis and analysed by IR spectroscopy (Figure 6 C-D) and potential measurements (Table 6).

Table 5. Peptide sequences and dendrimer used

Compounds	Peptide	Sequence	MW	Charge
gH493-511	PrA-gH493-511	NH ₂ -PrA-AAHLIDALYAEFLGGRVLT-CONH ₂	2124	-1
Cys- gH493-511	Cys-gH493-511	Ac-C-AAHLIDALYAEFLGGRVLT-CONH ₂	2174	-1
gBh1m	gB503-523-PrA	NH ₂ -FARLQFTYNHIQRHVSRDMEGR-PrA-CONH ₂	2769	+2
DendrimerA		Monofunctional dendrimer	3430	
DendrimerB		Bifunctional dendrimer	3043	

Table 6. ζ -Potential measurement of DendrimerB and DendrimerB + gBh1m/gH493-511

	ζ -Potential (mV)	Std. Dev (mV)
DendrimerB	-11.0	± 1.6
DendrimerB+ gBh1m/gH493-511	5.17	± 0.27

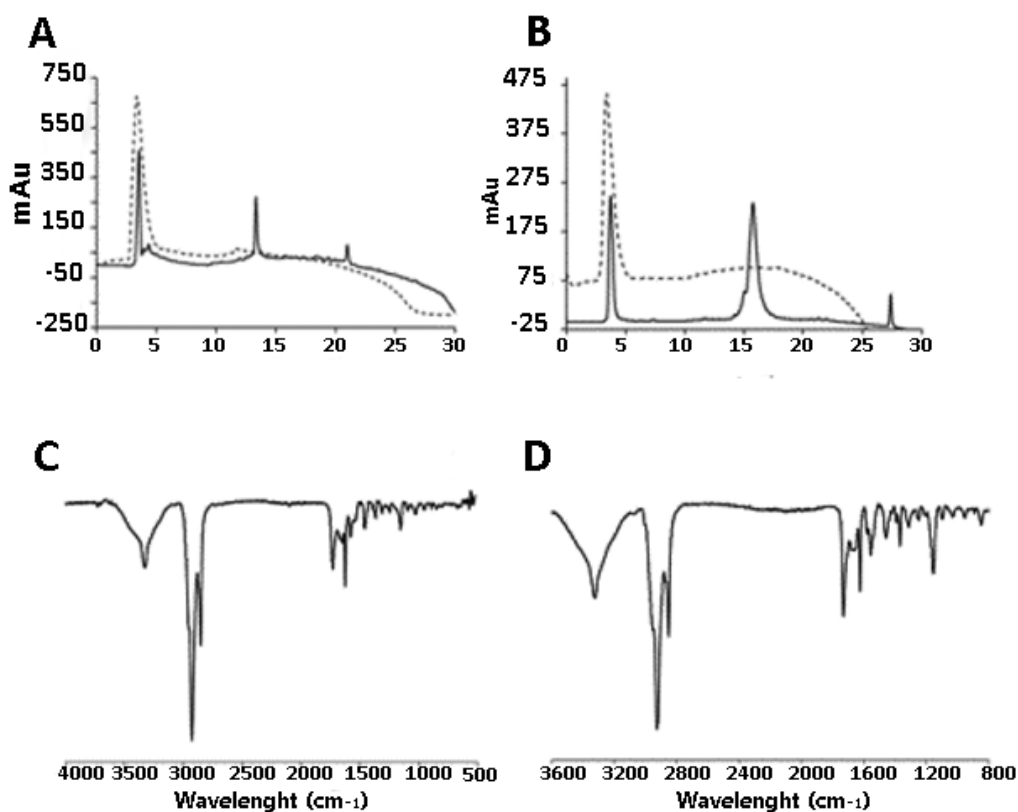


Figure 6. HPLC traces of crude (solid line) and purified (dashed line) peptidodendrimer conjugates, DendrimerA-gH (panel A), DendrimerA-gB (panel B). IR spectroscopic analysis of DendrimerA-gH (panel C) and DendrimerA-gB (panel D). Figure taken from International Journal of Molecular Sciences. 2021;22(12), 6488.

2.3.4. Structural study

The molecular conformation of DendrimerB + gBh1m/ gH493-511 was investigated by far-UV CD spectroscopy. CD spectrum in water indicated a random coil conformation for DendrimerB + gBh1m/ gH493-511 (Figure 7, panel A). Both peptides gH493-511 and gBh1m are random coil in aqueous solution but form an α -helix in membrane-mimetic environments.^{176, 177} CD spectra were obtained in several percentages of trifluoroethanol (TFE), which is widely used to simulate the membrane environment. The spectrum of DendrimerB + gBh1m/ gH493-511 shows that the peptides adopt an α -helix with minima at approximately 208 and 222 nm. (Figure 7, panel A). The obtained spectra suggest that the secondary structure the peptides was not disturbed by attachment to a dendrimer.

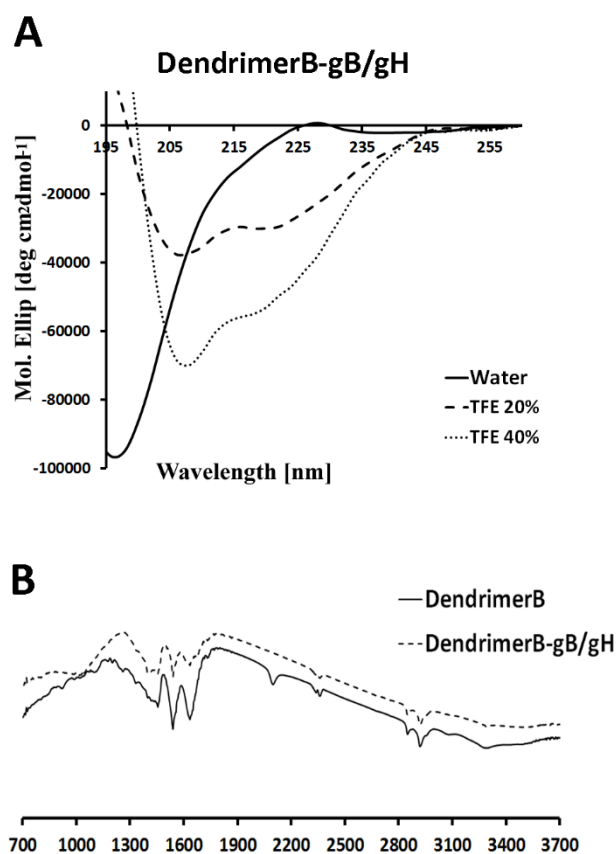


Figure 7. Circular dichroism of DendrimerB + gBh1m/gH493-511 in water with different percentage of TFE (panel A) and IR spectroscopic analysis of DendrimerB and DendrimerB + gBh1m/gH493-511 (panel B). Figure taken from International Journal of Molecular Sciences. 2021;22(12), 6488.

2.3.5. Cytotoxicity studies

Each compound was incubated with monolayers of Vero cell at different concentrations (5.5 nM, 55 nM, 0.28 μ M, 0.55 μ M, 1.1 μ M, 2.8 μ M) for 3, 24 and 48 h, and was determined cell viability by the MTT assay to confirm that synthesized peptide dendrimers do not cause toxic effects on cells. No statistical difference was detected between the viability of control (untreated) cells and that of cells exposed to the peptide dendrimers up to the concentration used in antiviral testing at 3 and 24 h. A small decrease in viability was observed at 48 h. Marginal toxicity was obtained for the dendrimer without the peptides linked to its termini, at concentrations that were considerably higher than those required for antiviral activity.

2.3.6. Antiviral assays

To test whether the peptide dendrimers are able to inhibit HSV-1 *in vitro*, several experiments were performed. A virus yield reduction assay in which the peptide dendrimers of interest were present in the cell culture during and after viral adsorption was initially performed. The degree of HSV-1 replication was determined by titration of harvested viruses and showed a consistent decrease in replication efficiency with more than 60% inhibition at a peptide-dendrimer concentration of 5.5 nM for both DendrimerA-gBh1m and DendrimerB + gBh1m/ gH493-511, while we observed the same percentage of inhibition for

DendrimerA-gH only at 550 nM. Inhibition of HSV-1 replication with the Janus bifunctionalized dendrimer was able to reach 90% already at 55 nM. DendrimerA, without any peptide conjugation, was able to produce an inhibition close to 30% at the highest concentration used (550 nM), suggesting that the dendrimer structure itself grants a certain level of antiviral activity, which is strongly enhanced by the specific peptide sequence coupled to its termini (Figure 8, panel A). To identify the step in the entry process that was being inhibited by our compounds, and thus to understand the mechanism of inhibition, the compounds were tested under different conditions. Our hypothesis was that the Janus dendrimer was able to interfere during the early penetration phase. To exclude the hypothesis of an action inside the cell at a post-entry event, a post-treatment assay was executed by adding the compounds at different concentrations (Figure 8, panel B). No concentrations used in this experiment were able to significantly reduce HSV-1 replication, indicating that both the dendrimer and the peptide dendrimers were ineffective once the viruses had already entered inside the cell, suggesting that our compounds target an early step of the HSV infection cycle (Figure 8). To clarify the mechanism of infection, the virus was incubated with compounds and subsequently added to the cells and the highest inhibition was again achieved for both DendrimerA-gB and DendrimerB + gBh1m/ gH493-511, while we observed a lower percentage of inhibition for DendrimerA- gH493-511 at 550 nM (Figure 9, panel A). The panel B in figure 9 shows that DendrimerA and DendrimerB without peptides had a similar activity. The peptides were analyzed alone, and they do not show activity at the concentration used in the experiments indicating that the functionalization of the dendrimers with peptides gBh1m/ gH493-511 is able to induce a significant enhancement of activity.

The possibility to interfere with an early penetration step was further explored using Vero cells pretreated with the target compounds for 30 min at 37 °C. The panel C in (Figure 9) showed much lower reduction of infectivity, in contrast the dendrimer is retaining its activity. Since the toxicity of the dendrimer is minimal, it was assumed that it may exert an antiviral activity by blocking the cell surface. The lower activity of the peptidodendrimers in this experiment is likely because both peptides are involved in the interaction with the virus, as demonstrated by the high inhibition activity showed in the virus pre-treatment experiment. Since inhibition of HSV penetration is likely the result of a combination obtained by the concerted action of the dendrimer on the cell surface and of the peptides responsible for an interaction with the viral glycoproteins, we performed a co-treatment experiment (Figure 9, panel D). The results obtained from the co-treatment experiment support the key role played by the peptides in regulating the activity of the peptide dendrimer.

The obtained results support the view that, in DendrimerB + gBh1m/ gH493-511, the surface of the dendrimer is covered by the two peptides, thus the activity of the dendrimer may be shielded during the inhibition mechanism in favor of the peptide activities.

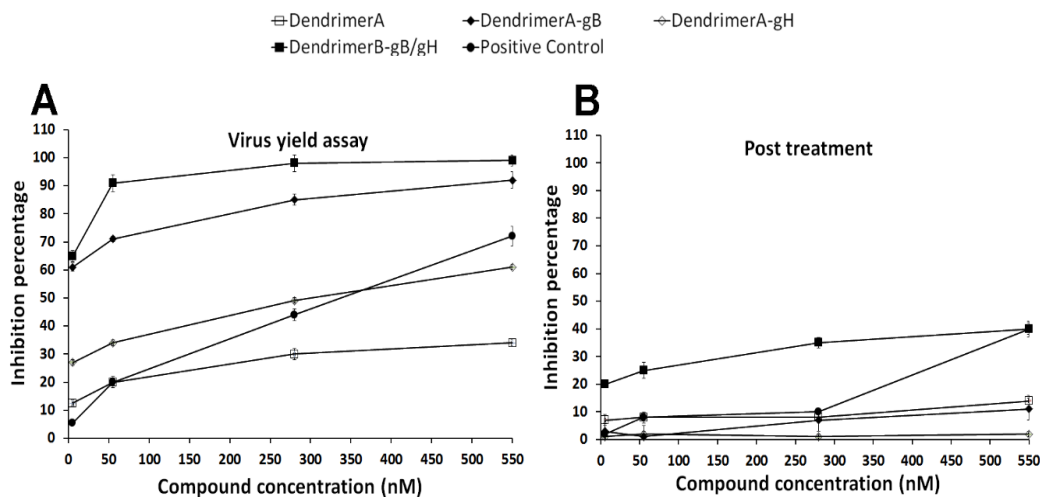


Figure 8. Compounds were present in the cell culture during and after viral adsorption in virus yield assay (panel A); cells were exposed to compounds after virus penetration in post treatment (panel B). The control used in both experiments is acyclovir. Experiments were performed in triplicate, and the percentages of inhibition were calculated with respect to no-compound control experiments. Error bars represent standard deviations. Figure taken from International Journal of Molecular Sciences. 2021;22(12), 6488..

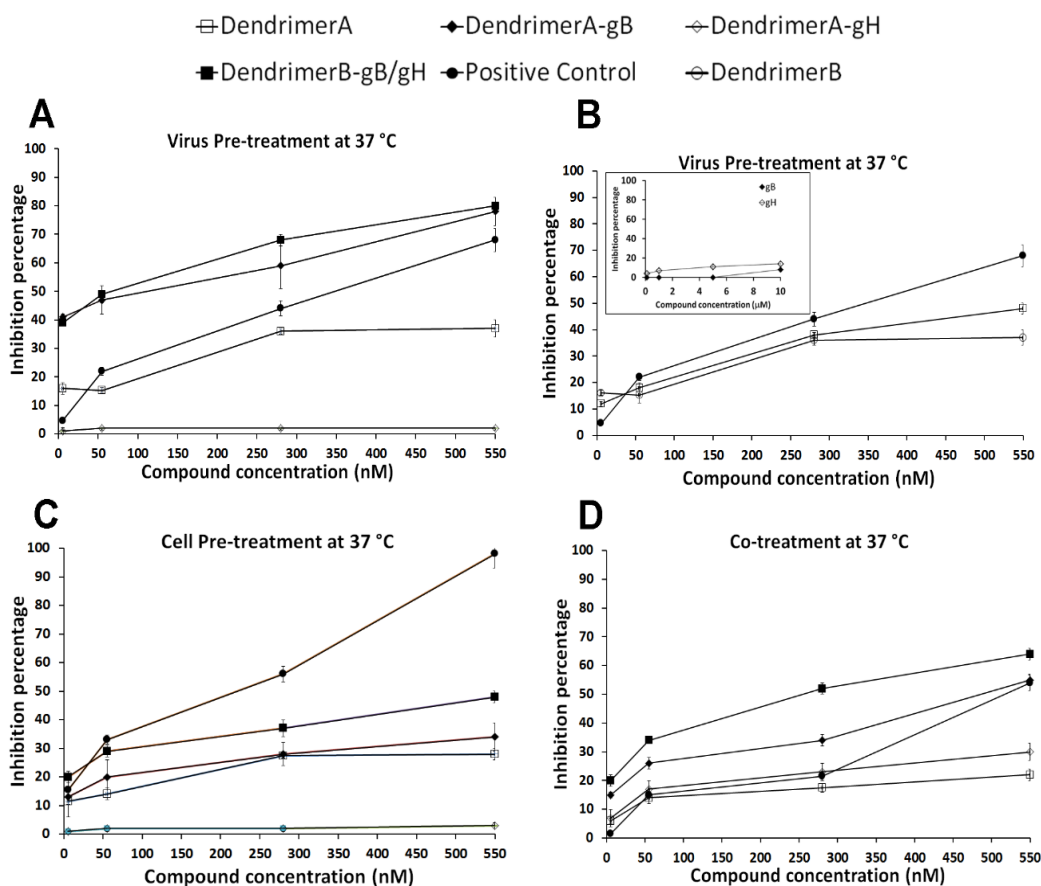


Figure 9. The virus was pre-incubated with compounds for 1 h at 37 °C prior to the addition to the cells in Virus Pre-treatment (panels A and B). Cells were exposed to compounds either prior to infection in Cell Pre-treatment (panel C) or during attachment and entry in co treatment (panel D). The control is melittin in virus pre-treatment and co-treatment and is dextran sulphate in cell pretreatment. Experiments were performed in

triplicate, and the percentages of inhibition were calculated with respect to no-compound control experiments. Error bars represent standard deviations Figure taken from International Journal of Molecular Sciences. 2021;22(12), 6488.

2.3.7. Conclusion and future perspectives

The design of antiviral NVs represents a major challenge in the global fight against viruses. It is possible to improve the inhibition mechanism by engineering new antiviral compounds that lead to multivalent bonds and interactions with the consequent production of irreversible local distortion and loss of infectivity. The use of different peptides with different targeting and inhibition mechanisms on multifunctional dendrimers determines a deformation of the viral particles at much lower concentrations. In this delivery system, the peptides cover the surface of the dendrimer, and the activity of the dendrimer is probably shielded during the inhibition mechanism in favor of peptide activity. Furthermore, the concentration range of peptide activities can be greatly reduced when they are combined on a dendrimeric structure for their enhanced delivery. Selecting peptides with different inhibition mechanisms can increase the activity of the nanocompound, and multiple binding to viral particles is useful for trapping and inactivating the virus. This approach allows the development of a strategy to produce medically relevant drugs to combat many threatening viral infections around the world. The proposed approach is fundamentally broad-spectrum, supporting the potential prevention and treatment of multiple viral infections simply by changing the peptides coupled to the dendrimer, which is a great advantage when unexpected infections occur. Our data further confirm the key role played by nanomaterials to deliver antiviral drugs and vaccines for better therapeutic outcomes, which may represent a general strategy to apply for many infectious diseases.

Chapter 3

Drug delivery systems for antibacterial applications

3.1 Introduction

Antiseptics, silver compounds, surgical drains and arsenicals were used to fight infections, before the introduction of antibiotics; diseases such as pneumonia, meningitis, and bacterial endocarditis had fatal consequences for the patients. After 1940 several classes of antibiotics became available, such as sulfonamides and trimethoprim, penicillins, cephalosporins, chloramphenicol, tetracyclines, colimycins, macrolides, lincosamides, streptogramins, rifamycins, glycopeptides, aminoglycosides, fluoroquinolones, oxazolidinones, glycyglycines, lipoglycopeptides, that are still considered miraculous to treat bacterial infections.^{178, 179} The overuse and misuse of antibiotics has caused a rapid development of bacterial resistance that is responsible of a huge increase of deaths every year worldwide. The mechanisms underlying the resistance are of different nature and are implemented quickly. Pathway regulating multidrug efflux is the first resistance mechanism developed by bacteria. More classes of antibiotics exhibit their activity crossing the outer membrane by diffusing through porin proteins. The permeability reduction of the outer membrane and limitation of antibiotic to entry into the bacterial cell can be achieved by the downregulation of porins or by the replacement of porins with more-selective channels. Another strategy is to target site mutation which reduces affinity for an antibiotic. For example, it may be based on a mutation in the topoisomerase gene such as for fluoroquinolone resistance or may be based on recombination to confer an allele mosaic such as for resistance to lactams. Finally, direct interactions with antibiotics can also be involved. In this case, bacteria produce enzymes that can destroy the antibiotic (for example β -lactamase) by preventing the binding to the target, or by modifying the structure of the antibiotic (for example enzymes that modify the aminoglycosides) which prevents the binding to the target. In both cases resistance is conferred.¹⁷⁸

In addition, bacteria can protect themselves by self-organizing in biofilms, which are hydrated matrices composed of extracellular DNA, proteins, and polysaccharides, in which bacterial cells are embedded where the exchange of genetic material between cells occurs very easily.^{178, 180} In biofilm communities, a slow or incomplete penetration of antibiotic and the transformation of bacterial cells in dormant cells which are less susceptible to antibiotics,¹⁸¹ contribute to antibiotic resistance.

Antimicrobial resistance, which is a natural event widely diffused in the world, represents one of the biggest global health challenges of our time, and it makes the advancement of therapeutic strategies urgent (Figure 1). The development of resistance produces an increased morbidity and mortality due to infectious diseases worldwide. Fighting this trend requires collaborative efforts among research sectors, in fact advances in genomics, system biology and structural biology have provided a lot of information related to events underpinning resistance, since a detailed understanding of resistance mechanisms could be the key to identify novel antibacterial agents, enable countering the resistance threat.

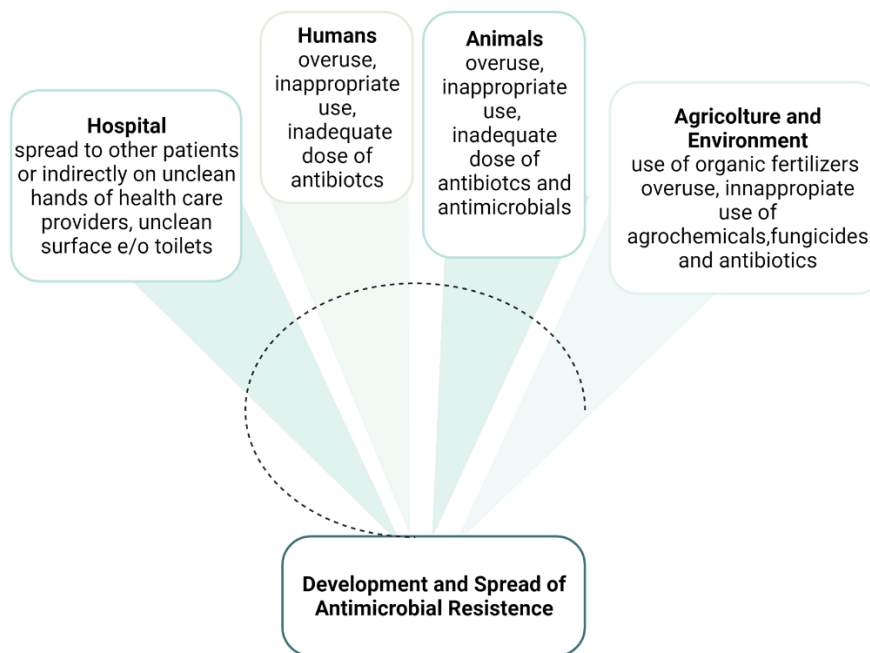


Figure 1. Factors involved in the diffusion of antibiotic resistance: human medicine in the community and in the hospital, animal production, and agriculture and environment.

In this scenario, antimicrobial peptides (AMPs) play a key role as demonstrated by numerous papers on the subject. AMPs are molecules widely present in nature, synthesized by organisms belonging to both the plant and animal kingdoms. They represent the first defense against many pathogens and offer the immune response line. This defense system has been the subject of study since the 1980s with the discovery of cecropins, that are antimicrobial peptides isolated from the silkworm (*Hyalophora cecropia*). After the discovery of these substances, other antimicrobial peptides have been isolated from a large number of organisms and to date more than 1000 of these substances have been isolated from a number of phylogenetically distant organisms, such as mammals, fish, amphibians and insects. These are small molecules, containing 10 to 50 amino acids, with a molecular weight between 1-5 kDa. There are two diverse ways to divide these molecules: peptides with antimicrobial activity (AMPs) that exert direct antimicrobial activity *in vivo*, or host defense peptides (HDP) that more generally exert their activity in context of innate immunity. Some AMPs are produced constitutively, others are synthesized in response to microbial attack. This immediate availability of AMPs plays a key role in the immune system response, making these peptides a highly effective first-line defense in animals. AMPs have a broad spectrum of action against bacteria, fungi¹⁸² and viruses.¹⁸³ Antimicrobial peptides share common characteristics; most have a net positive charge at neutral pH and a tendency to form amphipathic structures in a hydrophobic environment, characteristics that allow peptides to interact with the cell membrane.¹⁸⁴ Thanks to the positive charges AMPs are able to create electrostatic interactions with negatively charged microbial membranes or cell walls,¹⁸⁵ while the hydrophobic residues make the peptides amphiphilic and capable of folding upon membrane contact. The obtained secondary structures (α -helical or β -sheet-based), facilitate

oligomerization and/or translocation through the microbial membrane. The initial electrostatic interaction followed by the insertion of the hydrophobic domains into the lipid bilayer disrupt the membrane, according to several models reported in literature.¹⁸⁶ They usually fold into amphipathic structures when in contact with a membrane and their activity is correlated both to membrane leakage and to interactions with intracellular targets through inhibition of nucleic acid synthesis, protein production, or other enzyme activities as cell-wall synthesis.¹⁸⁷

AMPs derive from pro-peptides and are released in mature form following specific proteolytic cuts made by intracellular proteases. Most precursors contain a signal sequence for the endoplasmic reticulum; an anionic pro sequence, of variable length, with the activity of neutralizing the positive charges of the peptide making it inactive.¹⁸⁸ AMPs could be divided into distinct categories based on their origin, size, conformational structure, amino acid sequence, biological activity and mechanism of action. There are some AMPs containing cysteines that form one (bactenecine, brevinine, esculentine) or more disulfide bridges and adopt an antiparallel β -sheet structure (defensins, tachiplesins).^{189, 190} Other AMPs contain a high percentage of specific amino acid which are often amino acid residues such as proline (such as proline-rich peptides originally isolated from insects), tryptophan and arginine (such indolicidin and tritrypticin), histidine (such as human salivary histatin) and lack secondary structure. Linear AMPs including magainin, cecropin, pexiganan, temporins, indolicidin and melittin are usually unstructured in aqueous solution but can adopt an amphipathic α -helical structure when interacting with biological membranes or membrane-mimicking environments. Among AMPs, indolicidin is an antimicrobial peptide composed by 13-residues isolated from cytoplasmic granules of bovine neutrophils, which exhibits activity against Gram-positive and Gram-negative bacteria as well as fungi.¹⁹¹ Indolicidin is rich in proline and tryptophan residues and has been previously used against severe acne and skin infections caused by methicillin resistant *Staphylococcus aureus*.¹⁹²

Another strategy to combat pathologies previously treated with conventional antibiotics is represented by antibacterial nanosystems. Among metal nanoparticles (NPs), silver nanoparticles (AgNPs) are considered potential candidates thanks to their broad spectrum antibacterial /antiviral properties and their cost-effective synthetic procedures.^{193, 194}

Today the mechanism of action of AgNPs has been elucidated and it is widely accepted that they are able to physically interact with the cell surface of bacteria. Many studies have reported that AgNPs can damage cell membranes leading to structural changes, which render bacteria more permeable.^{195, 196} This activity is strongly dependent on the size.^{197, 198} In fact, the bactericidal activity of AgNPs of smaller dimensions (<30 nm) was found to be optimal against *Staphylococcus aureus* and *Klebsiella pneumoniae*.¹⁹⁹ The interaction with the membranes is based on electrostatic forces that develop when nanoparticles with a positive zeta potential encounter bacteria with a negative surface charge that promote a closer attraction and interaction between the two entities and possibly the penetration in bacterial membranes; this parameter can be modulated according to the size. The AgNPs are able to damage membranes and induce the release of reactive oxygen species (ROS), forming free radicals to bactericidal action.¹⁹⁷ Moreover, silver ions or small AgNPs can enter in the microbial cells causing the damage of its intracellular structures inducing a ribosomes

denaturation, blocking the replication system in bacterial cell.²⁰⁰⁻²⁰² The anti bactericidal effect and the active AgNP concentrations are bacterial class dependent.²⁰³

Despite the numerous conflicts in the literature regarding the effects of antibacterial AgNPs, their action is likely to be the result of a combined effect of several characteristics, which provides a broad spectrum of antibacterial activity and decreases the likelihood of developing resistance.²⁰⁴ The use of AgNPs in combination with antibiotic drugs can be an alternative for more difficult treatments.²⁰⁵ Enhancement of the antibacterial effect was observed for amoxicillin in the presence of AgNPs against *P. aeruginosa* and penicillin demonstrated a 3-fold increase of efficiency against *Streptococcus mutans*. Vancomycin, showed 3.8-fold increase of activity against *Enterobacter aerogenes* and was reported to have the highest overall synergistic activity in combination with AgNPs compared to all other antibiotics.

One of the research topics of my PhD is related to the functionalization of AgNPs with AMPs with the main scope of obtaining a synergic activity between the delivery NP (possessing its own antibacterial activity) and the peptide. Thus, we developed AgNPs coated with indolicidin, which have a good antibacterial activity also at low doses of indolicidin attached to nanoparticles, lower than those used with indolicidin or NPs alone.²⁰⁶

Moreover, the rapid production, use and marketing of AgNPs have determined an inevitable release of metal ions into the environment. AgNPs could accumulate in the environment into different level organisms and there could be trophic transfer to food webs, which consequently induces a negative effect on human health.²⁰⁷ It is important to perform ecotoxicological studies that would enable a mechanistic analysis of absorption, distribution, metabolism and excretion (ADME) to verify the effective antimicrobial activity of nanoparticle but also the low toxicity to the environment and for humans. During my PhD, I also evaluated the ecotoxicity of AgNPs coated with indolicidin.

3.2 Results and discussion

3.2.1 Peptide synthesis

Indolicidin was synthesized using standard solid-phase-9-fluorenylmethoxycarbonyl (Fmoc) method on a Rink amide p-methylbenzhydrylamine (MBHA) resin with a good yield in purified peptide (55%).

3.2.2 AgNPs preparation and indolicidin functionalization

AgNPs were prepared via an *in-situ* approach by applying redox reactions. The indolicidin was used to coat AgNPs; in particular, indolicidin was used as a capping agent, hydrazine was added as a reducing agent to donate electrons to allow Ag ions to complete their outer valence shell and be converted into Ag nanoparticles. The functional groups of the AMP indolicidin possess high affinity to transition elements and are useful to anchor peptide chains on the particle surface. This passive facilitation mechanism also allows us to avoid the Ag cluster aggregation. In principle, the generated Ag atoms formed by redox reactions tend to coalesce and grow into larger clusters. Nonetheless, by adding the indolicidin molecules, this coalescent process is inhibited, and the peptide acts not only as a cluster stabilizer but also contributes to control the size and size distribution of the generated AgNPs. UV-Vis spectrometer was used to confirm the formation of AgNPs in colloidal

solution already reported in a previous work.²⁰⁶ Briefly, the UV-vis spectra in (Figure 2) shows very broad band of aggregated AgNPs prepared in absence of indolicidin, nevertheless, in presence of indolicidin a narrow band appeared at 365 nm. These observations stated above could be attributed to the reduction process of silver ions to silver atom using hydrazine followed by anchoring between AgNPs at the cluster surface, while the amino acids of the oligopeptide protects the cluster from fusion with the next silver molecule to facilitate unique surface chemistry. This is contributed to the collective properties of the formed Ag nanoparticles. On the other hand, different amounts of the reducing agent were added which indicates no preferences in the wavelength 365 nm but significant increase in the intensity.

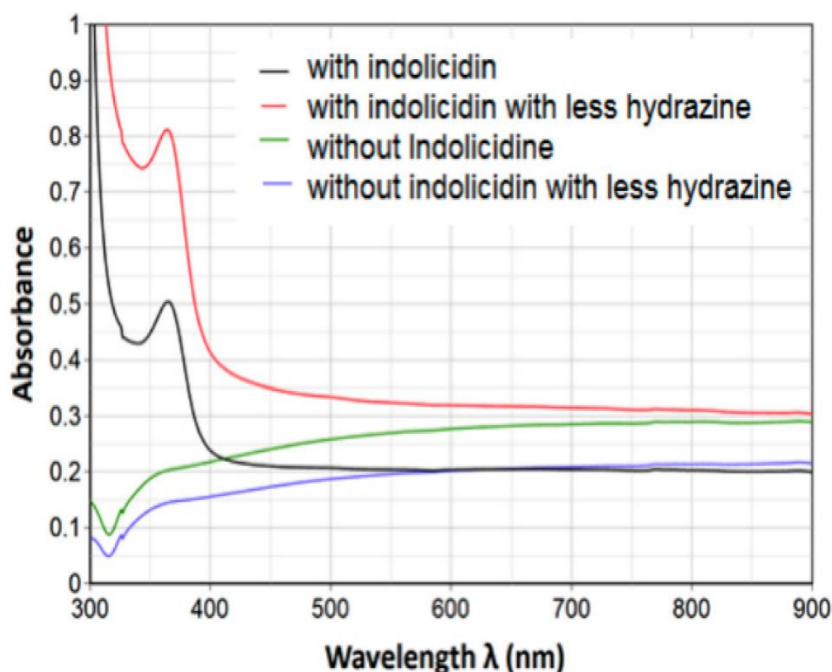


Figure 2. UV-Vis spectra of silver colloids prepared using 150 μL and 10 μL $\text{N}_2\text{H}_4\cdot\text{H}_2\text{O}$ in the presence of indolicidin. UV-Vis spectra of silver colloids prepared using 150 μL and 10 μL $\text{N}_2\text{H}_4\cdot\text{H}_2\text{O}$ without indolicidin indicated in light blue. Figure taken from International Journal of Nanomedicine, 2020;15:8097-8108.

3.2.3 Toxicity Tests on *Daphnia Magna*

D. magna is one of the freshwater test species most sensitive to silver, the experiments were performed both with short-term and long-term endpoints. To evaluate the toxicity of AgNPs and IndAgNPs towards *D. magna*, dose-response curves under 24 and 48 h exposure were obtained, during the exposure period the mortality in the control groups was less than 5% for all tests, indicating that there was no significant effect on *D. magna* mortality. Immobility was observed at the highest concentrations used, with a 48-h LC50 of 1.8 and 2.9 $\mu\text{g/L}$ for AgNPs and IndAgNPs respectively, suggesting a higher toxicity of AgNPs to *Daphnia* mortality than AgNPs coated with indolicidin. For indolicidin alone no toxicity was found at all concentrations tested (Figure 3). While after exposing *Daphnia* to increasing concentrations of NPs, we observed a dose-response increase of silver accumulation in different body locations. Comparing the swimming of *Daphnia* with the control groups, *Daphnia* exhibited a normal swimming, while in the samples with AgNPs

and IndAgNPs, it showed three different kind of swimming BOT (bottom), SUR (surface), ERR (erratic).

Daphnids exposed to AgNPs, showed a high percentage of normal swimming only at 0.5×10^{-3} concentration tested while IndAgNPs showed the result at both concentrations $0.5 \times 10^{-3} \mu\text{g/L}$ – $16 \times 10^{-3} \mu\text{g/L}$ (Table 1). The toxicity of AgNPs, IndAgNPs and indolicidin changed in the chronic experiment with *D. magna* where a sublethal doses of $1 \mu\text{g/L}$ for 21 days was used. Beginning from day 13, the survival for AgNPs and IndAgNPs was 80% and remained constant until day 19. After day 19, the survival decreased to 70% until the end of the test for AgNPs exposure, as shown in (Figure 4, panelA). *Daphnia* exposed to sublethal dose of AgNPs, IndAgNPs and indolicidin showed a significant delay of reproduction times compared to controls as shown in (Figure 4, palenB). In fact, the first brood was observed after 16 days in the group of *D. magna* exposed to AgNPs and after 14 days in the group exposed to IndAgNPs. *Daphnia* treated with the peptide indolicidin alone reproduced significantly earlier, so that the first brood was detected at day 10. The number of offspring and the average number of neonates differed between control *Daphnia* not exposed and those exposed to sublethal concentration of AgNPs and IndAgNPs. When we compared silver bioaccumulation at the end of exposure, we noticed that daphnids exposed to AgNPs and IndAgNPs showed amounts of nanoparticles in the digestive tract, droplets usually surrounding the intestine and clogging of the carapace. No sign of impaired feeding and no effects on growth were observed.

Table 1. Percentage of Normal and Abnormal *D. magna* During Swimming 48 h Exposure to Different Concentration of AgNPs, AgNPs Coated with Indolicidin and Indolicidin

Sample	Conc.($\mu\text{g/L}$)	Normal %	Abnormal%	Bottom%	Surface%	%Erratic
Indolicidin	0.5×10^{-3}	86.6	13.4	13.4	0	0
	1×10^{-3}	60	40	20	0	20
	2×10^{-3}	0	100	80	6.6	13.4
	4×10^{-3}	0	100	80	6.6	13.4
	8×10^{-3}	0	100	80	6.6	13.4
	16×10^{-3}	0	100	90	0	10
AgNPs	0.5×10^{-3}	86.6	13.4	13.4	0	0
	1×10^{-3}	0	100	44.4	11.2	33.4
	2×10^{-3}	0	100	57.3	14.2	28.5
	4×10^{-3}	0	100	80	0	20
	8×10^{-3}	-	-	-	-	-
	16×10^{-3}	-	-	-	-	-
IndAgNPs	0.5×10^{-3}	86.6	13.4	13.4	0	0
	1×10^{-3}	66.6	33.4	20	0	13.4
	2×10^{-3}	0	100	80	0	20
	4×10^{-3}	0	100	100	0	0
	8×10^{-3}	0	100	100	0	0
	16×10^{-3}	-	-	-	-	-

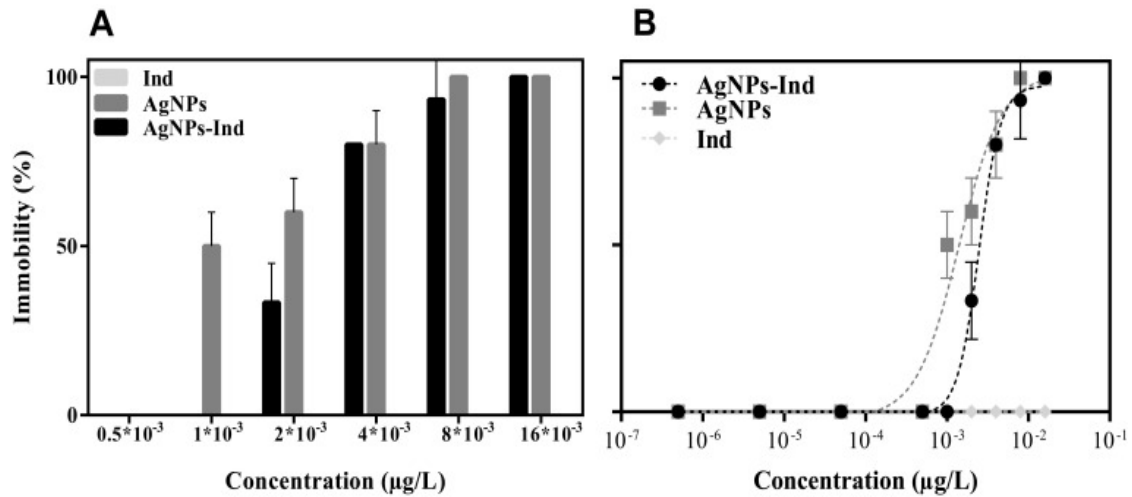


Figure 3. Immobilization comparison of *D. magna* exposed to different concentrations of indolicidin, AgNPs and AgNPs with indolicidin after 48h (panel A) and fitted curves by log10 in 48 h (panel B). Figure taken from International Journal of Nanomedicine, 2020;15:8097-8108.

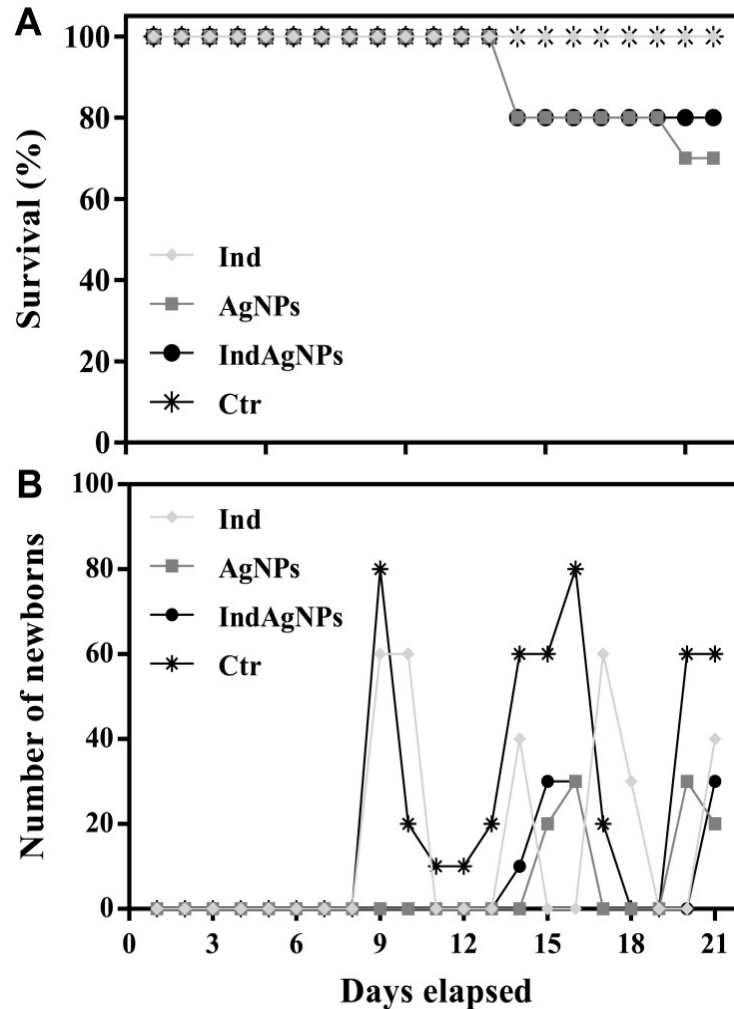


Figure 4. Cumulative percentage survival for each of the tested substances subjected to a chronic test for 21 days (panel A) Cumulative live offspring produced per female for each of the tested substances after 21 days of exposure (panel B). Figure taken from International Journal of Nanomedicine, 2020;15:8097-8108..

3.2.4 Toxicity Tests on *R. subcapitata*

Microalgae *R. subcapitata* has an important role in the aquatic system and are a member of food chains and respond quickly to environmental changes thanks a short generation time. We tested the growth inhibition at 72 h. AgNPs exposure, caused a dose-response increase in growth inhibition, reaching 78% at the concentration of 5 $\mu\text{g/L}$, which was considered toxic. The same trend was observed for IndAgNPs even if the percentages were lower compared to pristine AgNPs. Indolicidin showed a growth inhibition of 25% at the concentration of 16.10⁻³ $\mu\text{g/L}$. The EC₅₀ and EC₂₀ with 95% CI were 2.9 and 0.3; 0.95 and 0.2 not determined and 1.7, respectively for IndAgNPs, AgNPs, indolicidin (Table 2). These results confirm that after 72 h exposure, it is sufficient only 0.3 $\mu\text{g/L}$ of AgNPS to inhibit 50% of the population growth (Figure 5). This result may have important ecological consequences if we consider that *R. subcapitata* was grown under ideal conditions without the stressors that are likely found in nature together with other components with synergistic effects.

Table 2. Nominal Concentration Values on *D. magna* of EC₅₀ and EC₂₀ of AgNPs and AgNPs, coated with Indolicidin, with their 95% CI, r-Square Value (R²) and Degrees of Freedom (df)

		EC ₅₀ (CI)	EC ₂₀ (CI)	R ²	df
Indolicidin		ND	ND	ND	ND
D. magna	AgNPs	1.8 (1.7-1.9)	0.9 (0.8-1.1)	0.99	25
	InAgNPs	2.9 (2.7-3.1)	1.9 (1.8-2.1)	0.98	25
R. subcapitata	Indolicidin	ND	1.7 (1.08-2.6)	0.99	6
	AgNPs	0.95 (0.4-2.1)	0.2 (0.07-0.43)	0.89	6
	IndAgNPs	2.9 (1.8-4.7)	0.3 (0.16-0.44)	0.97	6

Abbreviation: ND, not determined.

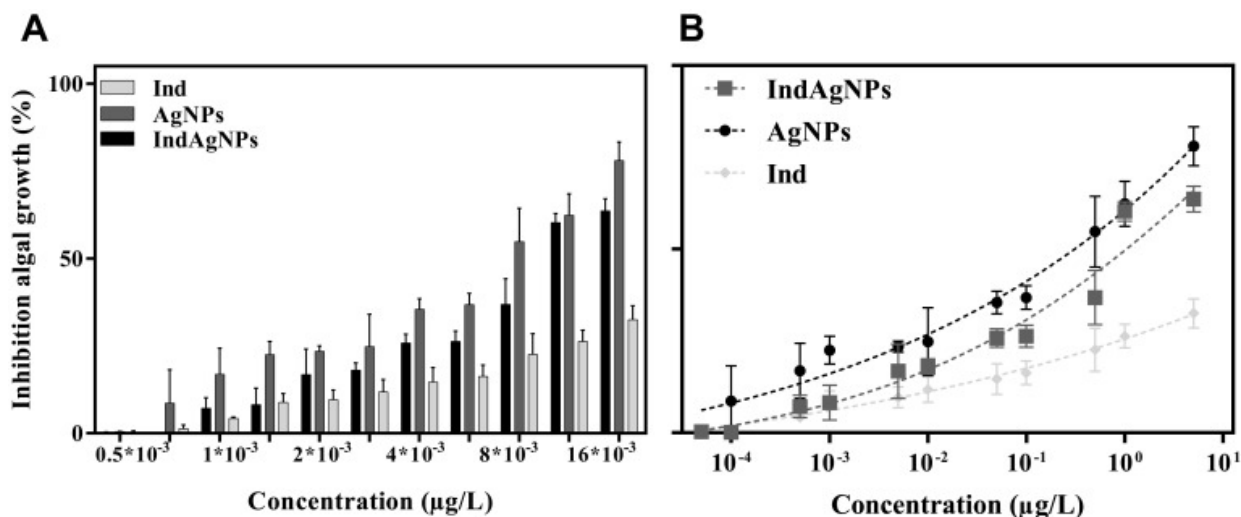


Figure 5. Growth inhibition of the microalgae *R. subcapitata* after 72 h exposure to AG, IndAg, Ind. Column representation to easily compare values (panel A), row representation to show the inhibition increase as a function of concentration (panel B). Figure taken from International Journal of Nanomedicine, 2020;15:8097-8108.

3.2.5 Effect of nanoparticles on seed germination

Seed germinations were used to determine the phytotoxic effects of nanoparticles, when growing, plants absorb large amounts of essential and nonessential elements, which at certain concentration may be toxic and can be transferred along the food chain to consumers. *L. sativum*, *C. sativus*, *L. sativa* are considered important models to test phytotoxicity. Various concentrations ranging from 1 $\mu\text{g/L}$ to 5 $\mu\text{g/L}$ were analyzed for the effects on seedling growth. Exposure of *L. sativum*, to different doses of AgNPs, IndAgNPs, indolicidin showed a low inhibition of germination with IG between 51, 29 and 76.5%. Furthermore, the exposition of *C. sativus* showed a low inhibition at the highest concentration tested for all substances. Only *L. sativa* showed differences of inhibition. Indolicidin caused a low inhibition showing an IG of 47.8% and 65.5%, while for both AgNPs and IndAgNPs showed a marked inhibition of growth with value IG lower than 40% (Figure 6, panel A–C). We reported a bioaccumulation of NPs only for *L. sativa* exposed to AgNPs and an abnormal growth of roots in all three bioindicators exposed to AgNPs pared to negative control but also in samples exposed to AgNPs with indolicidin (not shown). It is that the seed germination increase may be due to water uptake by seeds as previously reported. This activated water uptake process could be responsible for the significantly faster germination rates and higher biomass production for the plants that were exposed to small sized nanoparticles even if molecular mechanisms that induce water uptake inside plant seeds are not clear and require further investigation.

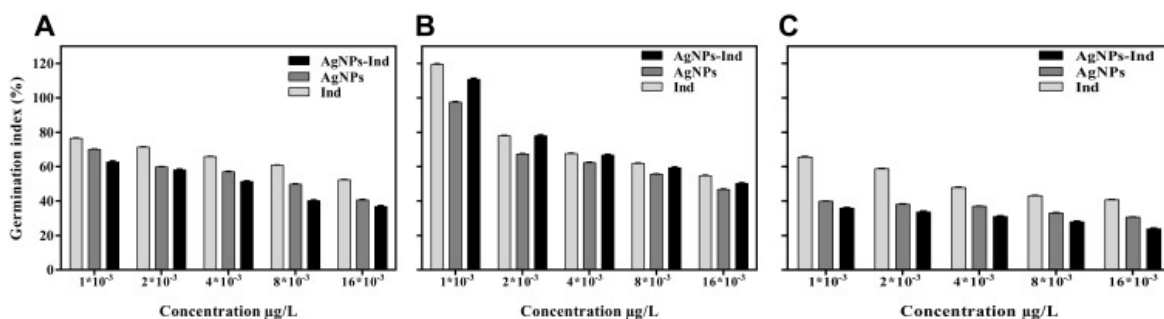


Figure 6. Effect of 72 h-seed germination to different concentration of AgNPs, AgNPs-Ind, Ind for *L. sativum* (panel A), *C. sativus* (panel B), *L. sativa* (panel C). Figure taken from International Journal of Nanomedicine, 2020;15:8097-8108.

3.3 Conclusion and future perspectives

The use of NVs that possess also antimicrobial activity is particularly interesting. Here, we decided to use AgNPs that are widely exploited for their antibacterial and antiviral properties. Unfortunately, the use of metal NPs is hampered by their toxicity essentially correlated to the release of ions. Our strategy was to coat the NV with an AMP already known for its activity.

To contrast the toxicity of AgNPs in environment the nanoparticles composed of AgNPs and indolicidine were analyzed on aquatic species. The EC_{50} values obtained for AgNPs, IndAgNPs and indolicidin indicate that the most sensitive organism to AgNPs was crustacean *D. magna* followed by *R. subcapitata* and plant seeds. This order of sensitivity

agrees with the literature. AgNPs produce acute toxicity on *D. magna* at a concentration of 1.6 $\mu\text{g/L}$; nonetheless, only *daphnids* exposed to the highest concentrations showed brown color in their gut lines, indicating that AgNPs were ingested. In the chronic toxicity tests with a sublethal concentration of 1 $\mu\text{g/L}$, *daphnids* showed a reduced reproduction and offspring delay while lower mortality was found for AgNPs functionalized with indolicidin. The comparison of the results obtained for the chronic and acute toxicity against *daphnids* did not produce significant variation in the EC_{10} , as far as it concerns the reproductive rate, the probability of survival to maturation and doses; it is likely that the amount of dissolved silver decreased in the presence of food algae.

The exposition of seeds to AgNPs, IndAgNPs, and indolicidin had a clear phytotoxic effect for AgNPs on *L. sativa* and was dependent upon the concentration of AgNPs. The low seed germination rate and low root elongation associated with AgNPs are likely related to metal ions released from the nanoparticle tested.

IndAgNPs were utilized to maintain the stability of AgNPs and reduce Ag^+ release thanks to the type of coating. Our NPs were prepared in presence of hydrazine which both helps the stabilization and likely reduces the Ag^+ release; the addition of the peptide coating further reduces toxicity of metal ions and may represent a valuable strategy for the development of novel antimicrobial drugs with lower toxicity to the environment. The use of NPs has significant advantages in research and medical applications, but at the same time it is required the acquisition of toxicity data to ensure the biosafety. The major finding of our research, based on the data of the three indicator species, is that AgNPs coated with an AMP such as indolicidin are less toxic for the environment compared to naked AgNPs. The highlight of this chapter is not only to support the synergy of AMP and AgNPs but also underline the advantages of drug delivery over traditional systems.

Chapter 4

Experimental Studies

4.1 Chemistry

4.1.1 Materials.

Fmoc-protected amino acid derivatives, coupling reagents, and rink amide *p*-methylbenzhydrylamine (MBHA) resin; Fmoc-L-Lys (Mtt)-OH and nonadecanoic acid (C19) were purchased from Iris Biotech GmbH (Germany). Anhydrous solvents [*N,N*-dimethylformamide (DMF) and dichloromethane (DCM)]. Doxo-EMCH, matrix metalloproteinase-9 (MMP9) and dialysis tubing benzoylated, Nile Red and Thioflavin T were purchased from Sigma-Aldrich (Italy). Piperidine, and trifluoroacetic acid (TFA) were purchased from Iris-Biotech GMBH. Silver nitrate (AgNO₃), and trisodium citrate were obtained from Sigma-Aldrich (Saint-Quentin-Fallavier, France). Ultrapure water was produced using a Barnstead EASYpure RoDi system (Thermo Fisher Scientific, France). All chemicals and reagents were of analytical grade and used as received. L-phosphatidylcholine (Egg) and cholesterol were purchased from Avanti Polar Lipids, Inc. (United States): Cholesterol tagging reagents were given by A. Pessi and M. Porotto. Dendrons 1 and 6 were synthesized as previously reported from starting materials purchased from Frontier Scientific. 3-Azidopropylamine was synthesized as previously reported. Dialysis membranes (SpectraPor 6) were purchased from Spectrum Labs

4.1.2 Peptide Synthesis and Purification.

The peptides were synthesized on a Rink amide resin which was purchased from Iris Biotech GmbH (Germany). The Fmoc protecting amino acid group was removed with a solution of piperidine (30% v/v in DMF) for 10 min for 2 cycles. All the couplings were conducted in the presence of an activator for carboxyl group and a base. In brief, the first coupling was performed in presence of 4 eq Fmoc-protected amino acid, 4 eq DIC and 4 eq oxymapure while the second coupling in presence of 4 eq amino acid, 4 eq HATU and 8 eq DIPEA. After acetylation of then-terminus (acetic anhydride/pyridine/NMP 4.7/4/91.3 vol), the crude peptides were cleaved with an acid solution of TFA in presence of scavengers and precipitated in ice-cold diethyl ether. The peptides were purified using a Phenomenex Jupiter 4 μ m Proteo 90 Å, 250 \times 21.20 mm column with a linear gradient of solvent B (0.1% TFA in acetonitrile) in solvent A (0.1% TFA in water) from 10 to 70% in 20 min with UV detection at 210 nm. The peptides were checked by analysis using high-resolution mass spectrometry (HRMS). For each pure peptide, very good yields of approximately 50% were obtained.

4.1.3 Synthesis of the cholesterol derivatives

The pure peptides were conjugated with the cholesterol-PEG moiety via chemoselective reaction between the bromoacetyl derivate of cholesterol and the cysteine group present either at the C or N terminus of the peptide. The cholesterol-PEG moiety was dissolved in

THF and added to peptides dissolved in DMSO, by a syringe pump in presence of DIPEA. The equivalents used are: peptide/cholesterol-PEG/DIPEA in ratio 1/1/2 mol/mol/mol and the reaction was conducted at room temperature overnight. The obtained compounds were purified by HPLC with a linear gradient of solvent B in A from 30 to 70% in 20 min

4.1.4 Synthesis of Monofunctional Dendrimer and the Bifunctional Dendrimer (Janus)

Synthesis of the monofunctional dendrimer scaffold has been reported previously.²⁰⁸

Briefly, the starting dendron 1 was functionalized at the amino termini with succinic anhydride to achieve the hemisuccinate dendron 2. The two dendrons are convergently coupled using HATU and Hünig's base to afford the symmetrical dendrimer 3. After deprotection of the tert-butyl esters, the carboxylic acid groups of dendrimer 4 were subsequently coupled with azidopropylamine to obtain the final monofunctional dendrimer 5, called DendrimerA. The synthesis of the Janus-type dendrimer has been reported previously.²⁰⁹ Briefly, the amino ester dendron 6 was protected at the amine terminus with a 9 fluorenylmethylcarbamate (Fmoc), after which the ester termini were deprotected. Coupling of 3-azidopropylamine and subsequent deprotection of the Fmoc afforded the aminononaazide dendron 9. This was coupled to the hemisuccinate dendron 2 using HATU in the presence of Hünig's base and deprotected using formic acid to yield the Janus bifunctional dendrimer 11. Dendrimer 11 was purified using preparative HPLC using a water/acetonitrile gradient. The eluted product was monomodal, indicative of its monodispersity. ¹H NMR spectroscopic analysis revealed full functionalization, as evidenced by the relative integration of the core protons to the azidopropyl methylene units. The final coupling of dendrimer 11 with allylamine in the presence of HATU and Hünig's base afforded the target bifunctional dendrimer 12 with functionalized dendrimer faces (DendrimerB). DendrimerB was purified using dialysis (1000 MWCO) against methanol, and characterized using ¹H and ¹³C NMR spectroscopy, as well as MALDI-TOF spectroscopy.

4.1.5 Functionalization of Monofunctional Dendrimer.

The dendrimer (1 equivalent) functionalization with PrA-peptide (gH and gB) (36 equivalents of each peptide) was performed in a water/methanol solution (1:1 v/v, about 1 mL) by using 2:4 equivalents (to the azide moiety) of CuSO₄·5 H₂O: sodium ascorbate. The reactions were left stirring for 1 h at 40 °C and for 2 days at room temperature. The resulting functionalized dendrimers were dialyzed against water/EDTA with 1000 MWCO membranes overnight, followed by purification by reverse-phase HPLC using a C4 column with water (0.1% TFA) and acetonitrile (Acn) (0.1% TFA) with a flow rate of 5 mL/min. Solvent gradients of 30 to 95% Acn over 20 min for Dendrimer-gH493-511 (DendrimerA-gH) and from 5 to 90% Acn over 20 min for Dendrimer-gB503-523 (DendrimerA-gB) were used. After HPLC purification, the peptidodendrimers were passed three times through a 30 KDa (MWCO) ultrafiltration membrane using water:MeOH:DMSO 50/45/5. The functionalization yields were confirmed by UV analysis ($\epsilon_{gH} = 1189 \text{ m}^{-1} \text{ cm}^{-1}$ at $\lambda = 280 \text{ nm}$); ($\epsilon_{gB} = 1090 \text{ m}^{-1} \text{ cm}^{-1}$ at $\lambda = 280 \text{ nm}$) and compared to the ratio of peptide initially used for the reaction (36 mol peptide per mol dendrimer). From the UV analysis, the peptide functionalization yields were 50% of the equivalents added.

4.1.6 Functionalization of DendrimerB.

The Janus bifunctional dendrimer was functionalized with gB via copper-catalyzed azide/alkyne cycloaddition and with Cys-gH via photoinduced thiol-ene reaction. In particular, dendrimer (1 eq), Cys-gH (1.5 eq) and DMPA (0.2 eq) in a 4:1 mixture of DMF:H₂O were irradiated with UV light (Spectroline model ENF-240C/FE) while stirring for one hour at 4 °C. After this reaction, gB was coupled to the dendrimer via copper-catalyzed azide/alkyne cycloaddition reaction using the same condition as described above. The Janus bifunctional dendrimer was purified using dialysis (1000 MWCO) against water and characterized using IR spectroscopy.

4.1.7 Synthesis of the cholesterol derivatives

The pure peptides were conjugated with the cholesterol-PEG moiety via chemoselective reaction between the bromoacetyl derivative of cholesterol and the cysteine group present either at the C or N terminus of the peptide. The cholesterol-PEG moiety was dissolved in THF and added to peptides dissolved in DMSO, by a syringe pump in presence of DIPEA. The equivalents used are: peptide/cholesterol-PEG/DIPEA in ratio 1/1/2 mol/mol/mol and the reaction was conducted at room temperature overnight. The obtained compounds were purified by HPLC with a linear gradient of solvent B in A from 30 to 70% in 20 min.

4.1.8 Liposome preparation

Large unilamellar vesicles (LUVs) and small unilamellar vesicles (SUVs) consisting of PC/Chol (2/1 ratio in moles) were prepared in PBS, pH 7.4. Lipids were first dissolved and mixed in an organic solvent to ensure a homogeneous mixture; the solvent is then removed by evaporation with a stream of nitrogen to produce a lipid layer and water was added (total lipid concentration was 0.1 mM). The lipid solution is frozen and the mixture is lyophilized overnight. LUVs were prepared using the extrusion method as previously reported. For fluorescence experiments, buffer was added to dry lipid films and vortexed for 1 h; then the hydrated samples were loaded into an automatic extruder previously assembled in all its parts (Lipex Thermobarr), including the interposition of support filters and a polycarbonate filter with pores of the size of 0.1 μm to obtain LUVs. SUVs were prepared by sonication of LUVs.

4.1.9 Synthesis and characterization of superparamagnetic iron oxide nanoparticles.

SPIONs were synthesized as aqueous ferrofluids by a coprecipitation of ferric and ferrous chlorides in alkaline medium. Briefly, magnetite nanoparticles were precipitated by adding ammonia solution (30 mL, 35%) to an aqueous mixture of Fe³⁺ (0.032 mol FeCl₃, 350 mL H₂O) and Fe²⁺ (0.016 mol, FeCl₂ 20 mL HCl 1.5 M) salts. To stabilize the chemical composition of SPIONs (magnetite/maghemite ratio), after the co-precipitation step, the SPIONs were additionally oxidized using ferric nitrate, thus increasing the surface layer of maghemite. Finally, the SPIONs were peptized in nitric acid and re-suspended in a determined volume of water. The next step consisted in coating the SPIONs with polysiloxane layer (Sil. SPIONs). For that, 2.20 mL (12.4 mmol) of APS (3-aminopropyltrimethoxysilane) in 10 mL of methanol were added to a mixture of 20 mL (8.8 mmol of iron) of SPIONs and 10 mL of methanol. The mixture was stirred at room temperature for 12 h. To the resulting solution, 20 mL of glycerol was added and methanol then water was removed with a rotary evaporator. After evaporation, the solution was dehydrated in vacuum at 100 °C for 2 h. The treated nanoparticles were washed three times with 40 mL of water/acetone mixture (30/70 v/v). Following the addition of 40 mL of water,

peptization was performed by slowly decreasing pH to 3 with 1M nitric acid under vigorous stirring^{210, 211}. The SPIONs were characterized by dynamic light scattering techniques, while determining their average hydrodynamic diameter (D_H) and surface charge (ζ -potential), using Zetasizer Nano-ZS (Malvern Instruments, Worcestershire, UK). All the measurements were performed in triplicate.

4.1.10 Preparation of Silver Colloids Using Hydrazine

150 μ L hydrazine monohydrate ($N_2H_4 \cdot H_2O$, Sigma Aldrich) were added to 1 mL $AgNO_3$ solution (1 mM). Deionized water was added to the solution up to 2 mL, mixed for one minute and allowed to settle at room temperature for four hours. To prepare silver colloids in the presence of indolicidin, 150 μ L $N_2H_4 \cdot H_2O$ were added to 1 mL $AgNO_3$ solution (1 mM). The solution was filled up to 2 mL with the peptide solution (indolicidin in deionized water=560 μ g/mL), mixed and allowed to settle at room temperature. The nominal concentrations of the obtained solutions were 0.5 mM of AgNPs alone and 0.5 mM of AgNPs+238 μ g/mL of indolicidin for the complex. We reported the concentrations for all the sequent experiments as a function of the concentration of the peptide indolicidin. When we used AgNPs without the peptide, we used the same amount of NPs contained in the relative solution with indolicidin (for simplicity of parisons we indicate it with the concentration value of indolicidin).

4.1.11 Preparation of silver plasmonic nanoparticles.

Aqueous colloids of citrate-coated AgNPs were obtained by heat-mediated reducing of silver in the presence of an excess of trisodium citrate, according to a standard protocol described by Lee and Meisel²⁴⁷. Briefly 90mg of silver nitrate was dissolved in 500ml of pure water and heated until boiling. Then, 10ml of trisodium citrate (1% m/V) was added droplet by droplet under constant agitation and the solution was kept boiling for 1 hour. Silver colloid formation leads to the appearance of a characteristic green-brown color. To protect the suspension from light, an aluminium paper was put around the glass vial.

4.2 Conformational analysis

4.2.1 Critical Aggregation Concentration (CAC) Determination. CACs of self-assembling peptides were determined by a fluorescence assay with Nile red (NR), a solvatochromic fluorescent probe. NR is poorly water-soluble while displaying a large preference to partition in aggregates that present hydrophobic binding sites and producing a blue shift and hyperchromic effect, which was measured. A methanolic NR solution was prepared at 500 nM. All the samples were freeze-dried and hydrated with the proper volume of NR solution to obtain the desired dye concentrations for the CAC determination by spectrofluorometry (see the Experimental Section). Before fluorescence measurement, all the solutions were left to equilibrate for 1 h. Emission spectra for each solution were measured by a Cary Eclipse Varian spectrometer. The NR emission spectra (exc wavelength 550 nm, emission wavelength range 570 to 700 nm) were measured at least in triplicate for each solution. The data were analyzed by plotting the maximum emission fluorescence corresponding wavelength (y) as a function of peptide concentration (x) and fitting with the sigmoidal Boltzmann equation:

$$y = \frac{A_1 - A_2}{1 + e^{-(x - x_0) / \Delta x}} + A_2$$

4.2.2 Circular Dichroism (CD) Analysis.

CD spectra were recorded from 195 nm to 260 nm in a Jasco J-810 spectropolarimeter using a 0.1 cm or a 1 cm quartz cell at room temperature under a constant flow of nitrogen gas. Other experimental settings were: scan speed of 5 nm/min, sensitivity of 50 mdeg, time constant of 16 s, bandwidth of 1 nm. Each spectrum was obtained through averaging three scans; spectra were recorded and corrected for the blank. The signal was converted to mean molar ellipticity (Θ), $\Theta = \text{obsd}/lc$, where obsd is the ellipticity measured in millidegrees, l is the path length of the cell in cm, and c is the peptide concentration in mol/L.

4.2.3 Membrane fluidity LUVs containing Laurdan were prepared to determine membrane fluidity.²¹² Lipid films containing Laurdan were hydrated and used for the experiments. The peptide was added to LUVs at 5 and 25 μM concentrations and the fluorescence spectra were recorded at time 0, and 1.5 h using a 1 cm path length quartz cell. Spectra were corrected for the baseline signal. Laurdan emission spectra were recorded from 400 to 550 nm with λ_{ex} 365 nm in the absence or presence of peptides in PBS (pH 7.4). Laurdan emission shifts from 440 nm in the ordered phase, to 490 nm in the disordered phase. The excitation generalized polarization (GP) was calculated as $\text{GP} = (I_{440} - I_{490}) / (I_{440} + I_{490})$ where I_{440} and I_{490} are the fluorescence intensities at the maximum emission wavelength in the ordered (λ_{em} 440 nm) and disordered (λ_{em} 490 nm) phases.²¹³

4.2.4 Surface plasmon resonance SPR experiments were carried out with a BIAcore 3000 analytical system (Biacore, Uppsala, Sweden) using an HPA sensor chip. The HPA sensor chip contains hydrophobic alkanethiol chains, which allow to create a lipid heteromonolayer.¹⁷⁴ We prepared PC/Chol (2/ 1 mol/mol) SUVs containing the peptide gBh1m-Cys-PEG24-Chol; after SUV immobilization we obtained a monolayer exposing on its surface the peptide sequence at the total peptide concentration used for the preparation of SUVs (25 μM). The experimental protocol was previously reported.¹⁶⁸ All solutions were freshly prepared, degassed, and filtered through 0.22 μm pores; the running buffer used was PBS (pH 7.4); the regeneration buffer was 40 mM N-octyl β -D-glucopyranoside; moreover, the operating temperature was 25°C. The HPA chip was installed, and the alkanethiol surface was cleaned by an injection of the nonionic detergent N-octyl β -D-glucopyranoside (25 μL , 40 mM) at a flow rate of 5 $\mu\text{L}/\text{min}$. SUVs (80 μL , 0.5 mM) containing the peptide were applied to the chip surface at a flow rate of 2 $\mu\text{L}/\text{min}$. We used NaOH 10 mM (25 μL) increasing the flow rate to 50 $\mu\text{L}/\text{min}$ to remove any multilamellar structures from the lipid surface which resulted in a stable baseline corresponding to the lipid monolayer linked to the chip and exposing the peptide sequence on their surface; considering the dimension of the chip and the concentration of lipids and peptide molecules, the surface of the cell is completely covered with lipids and peptide which bearing a PEG24 moiety is flexibly covering the surface of the lipid monolayer. The negative control BSA was injected (25 μL , 0.1 mg/ μL in PBS) to confirm complete coverage of the nonspecific binding sites. Peptide solutions of gBh (30 μL at a flow rate of 5 $\mu\text{L}/\text{min}$) were injected onto the lipid surface. PBS alone then replaced the peptide solution for 15 min to allow peptide dissociation. SPR detects changes in the reflective index of the surface layer of peptides and lipids in contact with the sensor chip. A sensorgram is obtained by plotting the SPR angle against time; the change in the angle is then translated to response units. Analysis of the peptide–lipid binding event was performed from a series of sensorgrams collected at different gBh concentrations

(3, 5, 7, 10, 15 μM). These data were analyzed by BIA evaluation software for curve fitting using numerical integration analysis¹⁷⁵ and for complete kinetic analyses. Several curve fitting algorithms were used to understand the mechanism of interaction. The sensograms obtained were fitted globally by simultaneous fitting. The corresponding differential rate equations for this reaction model are represented where RU1 and RU2 are the response units for the first and second steps, respectively, CA is the peptide concentration, RU_{max} is the maximum peptide binding capacity (or equilibrium binding response), and k_a , k_d are the association and dissociation rate constants. Kinetic data were assessed by using χ^2 values, plots of the residuals from the model fitting and the significance of each parameter assessed by standard deviations. The quality of the fit to a specific parameter was considered significant if the standard deviation was $\leq 10\%$. Except where specifically indicated, all parameter values were significant to the fit.

4.2.5 NMR spectroscopy

The reaction between P4 peptide and Doxo-EMCH was followed by NMR spectroscopy in 1D [¹H] NMR spectra were recorded on a Varian Unity Inova 600 MHz spectrometer equipped with a cold probe. Spectra were acquired at 298 K on samples at roughly 200 μM concentration and volumes equal to 500 μL in either DMSO (Dimethyl-Sulfoxide-d₆, 99.9% D, Sigma-Aldrich, Milan, Italy) and in D₂O (Deuterium Oxide 99.9% D, Sigma-Aldrich, Milan 20-21). 2D [¹H, ¹H] TOCSY (Total Correlation Spectroscopy) experiments were recorded with mixing times equal to 70 ms with a number of scans ranging from 16 to 64 scans, 128-256 FIDs in t₁, 1024 or 2048 data points in t₂. NMR spectra were processed with VNMRJ 1.1D (Varian by Agilent Technologies, Italy); 2D TOCSY spectra were analysed with the software NEASY32 enclosed in CARRA

4.2.6 IR Spectroscopy. The samples were analyzed by FT-IR spectroscopy. The FT-IR spectra were recorded on a UV-Vis spectrophotometer (Jasco, Easton, MD, USA). The characteristic peaks of IR transmission spectra were recorded at a resolution of 4 cm^{-1} over a wavenumber region of 400–4000 cm^{-1} .

4.2.7 ζ -Potential Measurement. The ζ -potential of DendrimerB and DendrimerB-gB/gH solutions were measured using Zetasizer Nano-ZS (Malvern Instruments, Worcestershire, UK). All measurements were performed at 25 °C in water, at pH 7 in triplicate.

4.2.8 Characterization by UV-VIS. UV-Vis spectra of the resulting nanoparticle solutions were recorded at room temperature using a Lambda 25 UV-Vis spectrophotometer (Perkin Elmer). The monochromator slit width was 10 nm.

4.2.9 SERS spectra acquisition. SERS spectra measurements were carried out using a LabRAM confocal microspectrometer (Horiba Jobin-Yvon, France) using 690 nm diode laser source. For SERS, the Ag NPs were aggregated by addition of 50% of PBS buffer pH 7.4 and mixed with 10% volume of the sample. SERS spectra (region from 300 to 1750 cm^{-1}) were recorded using a 5 μL droplet placed under a 10 \times microscope objective of the microspectrometer. Spectra presented in the figures are averages of at least three independent measurements. Both experiment control and following data treatment were performed using the LABSPEC software package.

4.3 Biology

4.3.1 Cell culture

Triple MDA-MB-231 (ECACC, Salisbury, U.K.) and SK-BR-3 cells (Euromedex, Souffelweyersheim, France) were cultured at 37°C in an atmosphere containing 5% CO₂. The culture medium was made of DMEM supplemented with 10% fetal bovine serum, 1% non-essential amino acid (Hyclone Laboratories, Logan, Utah) and 1% penicillin/streptomycin (Gibco®, Life Technologies, Paisley UK). The cell harvesting was made with trypsin/EDTA (0.05%) (Gibco®, Life Technologies, Paisley UK) at 80% of confluence.

4.3.2 Cytotoxicity Assay.

Vero cells were exposed to increasing concentrations of peptides, and the number of viable cells was determined using the 3-(4,5-dimethylthiazol-2-yl)-2,5-diphenyltetrazolium bromide (MTT) assay. It is based on the reduction of the yellowish MTT to the insoluble and dark blue formazan by viable and metabolically active cells.¹⁷² Vero cells were sub-cultured in 96-well plates at a seeding density of 2×10^4 cells/well and treated with peptides at the increasing concentrations of 1, 5, 10, 20, 50, 100 and 200 μ M for 24 h. The medium was then gently aspirated, MTT solution (5 mg/mL) was added to each well, and the cells were incubated for further 3 h at 37°C. The medium with MTT solution was removed, and the formazan crystals were dissolved with dimethyl sulfoxide (DMSO). The absorption values at 570 nm were measured using a TECAN infinite 200 microplate reader (lifesciences.tecan.com). The viability of Vero cells in each well was presented as a percentage of control cells. All experiments were performed in triplicate and the average with standard deviation was reported. Cell culture without and with 30% DMSO were used as the positive and negative controls, respectively.

4.3.3 Antiviral Assays.

Antiviral experiments were executed at different concentrations for all compounds. All experiments were done in triplicate. The infectivity inhibition percentage was calculated by fixing as 0% inhibition, the number of plaques obtained in negative controls (only virus). To determine the effect of functionalized dendrimers on inhibition of HSV infectivity, cell monolayers were treated in different ways.

- Virus yield reduction assay: confluent Vero cell monolayers (12-well plates) were washed with phosphate-buffered saline (PBS) and infected with HSV-1 at multiplicity of infection (MOI) of 1 for 1 h at 37°C. Then, virus inocula were mixed with the antiviral compounds at the concentrations indicated above. Infected cells were washed with PBS, covered with fresh culture medium, and incubated for 48 h; then, they were scraped into culture medium and disrupted by sonication.
- Post-treatment assay: 5×10^5 Vero cells (12-well plates) were incubated firstly with virus (MOI 0.01) for 45 min at 37°C and then the compounds were added to the cells followed by an additional incubation period of 30 min at 37°C.
- Co-treatment.
- Co-exposure experiment: 5×10^5 cells were incubated with peptides and with the viral inoculum at MOI of 0.01 for 45 min at 37°C.
- Cell pretreatment.
- In cell pre-exposure experiment, 5×10^5 Vero cells were incubated with compounds

for 30 min at 37°C and subsequently infected with HSV-1 at MOI of 0.01 for 45 min at 37°C.

- Virus pre-treatment: in virus pre-exposure assay, HSV-1 at MOI of 0.1 was incubated with compounds for 45 min at 37°C, and then the mixture was titrated on Vero cell monolayers.

For all treatments, non-penetrated viruses were inactivated by citrate buffer at pH 3.0 after 45 min incubation with cells at 37°C. The cells were then incubated for 24 h at 37°C in DMEM supplemented with carboxymethyl cellulose (CMC) 5%. The total virus yield in each well was titrated by plaque assay. Plaques were stained with X-gal and microscopically counted. The mean plaque counts for each concentration were reported as a percentage of the mean plaque count compared to the control virus. The number of plaques was plotted as a function of concentration; concentrations producing 50% reductions in plaque formation were determined as the IC₅₀.

4.3.4 Test organisms and culture conditions for ecotoxicological studies.

D. magna daphnids were cultured in our laboratory in M4 medium⁴⁹ at a constant temperature of 20°C and a photoperiod of 16 h light and 8 h dark. Culture medium was changed twice a week and daphnids were fed with a suspension of green algae. *R. subcapitata* algae was maintained in our laboratory, in 500 mL culture flasks with 200 mL of medium (ISO 982 2012) prepared by adding macro and micronutrient solutions to Milli-Q water. The pH of medium was 7.5. Algal cultures were grown under continuous illumination equipped by white fluorescent lamps at 25°C on an orbital shaker at 100 rpm. Cultures were maintained in exponential growth phase subcultivating a small amount of old culture in a fresh sterile medium every seven days. The plant species assayed were: *L. sativum*, *C. sativus* and *L. sativa*. The seeds were sterilized in 10% Na hypochlorite solution for 20 min to avoid fungal growth and washed with distilled water many times.

4.3.5 Daphnia Acute Toxicity Test.

It was carried out according to OECD guideline 202. Every test was done four times with four control groups. Briefly, 30 neonates aged <24 h were divided into four groups and exposed to different concentrations of AgNPs, IndAgNPs, indolicidin with a range 0.0005 µg/L to 0.016 µg/L. All tests were performed in a water bath system with a constant temperature (20±2°C) and 16 h light/8 h dark cycles and animals were not fed during the experiments. After 48 h exposure, neonates that were unable to swim within 15 seconds were considered to be immobilized after gentle agitation. GraphPad Prism program was used to create dose-response curves with a nonlinear regression model and calculate the median effect concentration EC₅₀ and EC₂₀ values, as well as their confidence intervals (95%). After 24 and 48 h of exposure, the immobilization and mortality of the *D. magna* were estimated using a light microscope (Leica EZ4HD, 10×/20) and any visible uptake and adsorption of nanoparticles by *D. magna* were photographed with a digital camera. Furthermore, the live Daphnia were classified in four groups according to their swimming type: normal swimming (NOR), erratic swimming (ERR), at the bottom (BOT), at the surface (SUR).

4.3.6 Daphnia Chronic Test. The chronic toxicity test was performed according to the standard protocol OECD Guideline 202. Neonates aged <24 h were exposed to a sublethal concentration of AgNPs, IndAgNPs and indolicidin (1 µg/L) for a period of 21 days. The exposure conditions were the same as those used in the routine cultures. Neonates were fed

every two days and media and nanoparticle solution were changed simultaneously. Survival, offspring and newly born neonates were observed and monitored every day. At the end of the exposure, surviving parents and newborns were collected and photographed. To determine significant differences in the survival organisms like total number of neonates, total number of clutches, age at first reproduction at the end of the experiment, we used a oneway ANOVA.

4.3.7 Algae Growth Inhibition.

Test The growth inhibition test of *R. subcapitata* was assessed following the method of OECD 201.52 We used exponentially growing algal cultures that were exposed to various concentrations of the test substances under controlled conditions. Briefly, with an initial concentration of 5×10^4 cells/mL was incubated in each well containing serial dilutions (starting from the concentration of 10 $\mu\text{g/L}$ with arithmetic progression of 1:2) of AgNPs and IndAgNPs and indolicidin on MBL medium. For each sample, eight concentrations in a geometric series were tested in the concentration range previously settled in a preliminary test. All assays were replicated three times. Plates were incubated in a light-temperature controlled chamber at 25°C for 72 h with a photoperiod of 16 h:8 h light-dark. Samples from each well were read in a spectrophotometer at 670 nm after 72 h. Cell growth inhibition was the endpoint measured after 72 h in a Bürker cell counting chamber and calculated by dividing the difference of the number of control and sample cells to the number of control cells. The specific growth rate of *R. subcapitata* in each replicate culture was calculated from the logarithmic increase in cell density in the intervals from 0 to 72 h using the following

$$\text{equation: } \mu = \frac{1nN_n - 1nN_0}{t_n - t_0}$$

where N_0 is the cell concentration at $t=0$, N_n the final cell concentration after 72 h of exposure, t_0 the time of start measurement, and t_n the time of last measurement (hours from start). The inhibition of the cell growth, expressed as percentage, at sample (% I) was calculated as the difference between the rate growth of the control and the rate growth, Values are expressed as the mean \pm SD of the replicates ($p \leq 0.05$). EC_{50} and EC_{20} were calculated using GraphPad Prism program and Excel macro REGTOX.

4.3.8 Phytotoxicity Test.

Phytotoxicity assays were conducted following the OECD 208 method. Seeds were sown in 90 mm diameter petri dishes that contained one sheet of Whatman No. 1 filter paper as support and 3 mL of test solutions. Ten seeds, in three replicates, were sown per container. The seeds were incubated in a growth chamber at 25°C for 72 h. After this period, the germination index (GI) was calculated by multiplying the germinated seed number (G) and length of roots (L). The toxic effect was expressed as percentage germination index (GI%) with respect to the control and calculated as follows: $GI\% = (IG_c - IG_s) / IG_c * 100$, where G_s and IG_c are the germination indices calculated for samples and control, respectively.

5. List of abbreviations

6HB_6 Helices

AgNPs_Silver Nanoparticles

AMP_Antimicrobial peptide

ATP_Adenosine Triphosphate

AZA_Azelaic Acid

BBB_Blood–Brain Barrier

BOT_Bottom

BSA_Bovine Serum Albumin

C19_Nonadecanoic Acid

CAC_Critical Aggregation Concentration

CC50_Cytotoxic Concentration

CD_Circular Dichroism Spectroscopy

Chol_Cholesterol

CMC_Carboxymethyl Cellulose

CPPs_Cell-penetrating peptides

CSI_Confocal Spectral Imaging

CuAAC_Copper-catalyzed azide/alkyne cycloaddition reaction

D2O_Deuterium Oxide

DCM_Dichloromethane

DIC_Diisopropylcarbodiimide

DIPEA_Diisopropylethylamine

DLS_Dynamic Light Scattering

DMEM_Dulbecco's modified Eagle's medium

DMF_N,N-dimethylformamide

DMPA_DimethylolPropionic Acid;Bis(hydroxymethyl) propionic acid

DMSO_Dimethyl Sulfoxide

DOX_Doxorubicin

EDT_Ethane-1,2-dithiol,
ER_Estrogen Receptors
ERR_Erratic swimming
Fmoc_9-fluorenylmethylcarbamate
G5Ds_Fifth-generation polyester-based dendrimers
gB_glycoprotein B
gD_glycoprotein D
gH_glycoprotein H
gL_glycoprotein L
GP_Generalized Polarization
HATU_(1-[Bis(dimethylamino)methylene]-1H-1,2,3-triazolo[4,5-b] pyridinium 3-oxide hexafluorophosphate, Hexafluorophosphate Azabenzotriazole Tetramethyl Uronium)
HCV_Hepatitis C Virus
HDP_Host Defense Peptides
Her2_Epidermal growth factor receptor
HIV-1_Herpes simplex virus type I
HOBt_Hydroxybenzotriazole (HOBt)
HPLC_High Performance Liquid Chromatography,
HPV_Papilloma Virus
HRMS_High-Resolution Mass Spectrometry
HRs_Heptad Repeat domains
HRV_Rhinovirus
HSV_Herpes Simplex Virus
IC50_Inhibitory Concentration
LUVs_Large Unilamellar Vesicles
MAbs_Monoclonal Antibodies
MBHA_Rink Amide p-methylbenzhydrylamine
MDR_Multidrug Resistance
MMP2/9_Metalloproteinases 2/9

MTT_3-(4,5-dimethylthiazol-2-yl)-2,5-diphenyltetrazolium bromide) tetrazolium reduction assay

MWCO_Membranes overnight

NFCL-Doxo_Nanofiber whit Doxo

NIR_Near Infrared

NMP_N-metil-2-pirrolidone. metilpirrolidone.

NMR_Nuclear Magnetic Resonance spectroscopy

NOR_Normal swimming

Novel drug delivery vehicles_Nanovectors

NPs_Nanoparticles

NR_Nile Red

P1_Peptide 1

P2_Peptide 2

P3_Peptide 3

P4_Peptide 4

P5_Peptide 5

PBS_Phosphate Buffered Saline

PC/Chol_L-phosphatidylcholine/Cholesterol

PDI_Polydispersity Index

PEG_Polyethylene Glycol

PLA_Biodegradable polymers

PLGA_Poly Lactic-co-Glycolic Acid

PP_Penetration Peptide

PPPs_Photo- and pH-responsive Peptides

PR_Progesterone

PrA_Propargyl glycine residue

PyBOP_Benzotriazol-1-yl-oxytris(pyrrolidino)phosphonium hexafluorohosphate

RES_Reticuloendothelial System

RP-HPLC_Preparative Liquid Chromatography

RSV_Respiratory Syncytial Virus

RT_Retention Times

SAL_ Salinomycin

SARSC_Severe Acute Respiratory Syndrome Coronavirus

Sil. SPIONs_Silanizade SPIONs

SPIONs_Superparamagnetic iron oxide nanoparticles

SPR_Surface Plasmon Resonance

SUR_Surface

SUVs_Small Unilamellar Vesicles

TEM_Transmission Electron Microscope

TFA_Trifluoroacetic Acid

TFE_Trifluoroethanol

THF_Tetrahydrofuran

ThT_Thioflavin T

TNBC_Triple negative breast cancer

TP_Targeting Peptide

VACV_Vaccinia Virus

6. References

- [1] Markman, J. L., Rekechenetskiy, A., Holler, E., and Ljubimova, J. Y. (2013) Nanomedicine therapeutic approaches to overcome cancer drug resistance, *Advanced drug delivery reviews* 65, 1866-1879.
- [2] Toita, R., Murata, M., Abe, K., Narahara, S., Piao, J. S., Kang, J. H., Ohuchida, K., and Hashizume, M. (2013) Biological evaluation of protein nanocapsules containing doxorubicin, *Int J Nanomedicine* 8, 1989-1999.
- [3] Chandrakala, V., Aruna, V., and Angajala, G. A.-O. (2022) Review on metal nanoparticles as nanocarriers: current challenges and perspectives in drug delivery systems, *Emergent materials*, 1–23. .
- [4] Ahmad, F., Salem-Bekhit, M. M., Khan, F., Alshehri, S., Khan, A., Ghoneim, M. M., Wu, H.-F., Taha, E. I., and Elbagory, I. (2022) Unique Properties of Surface-Functionalized Nanoparticles for Bio-Application: Functionalization Mechanisms and Importance in Application, *Nanomaterials* 12.
- [5] Bulbake, U., Doppalapudi, S., Kommineni, N., and Khan, W. (2017) Liposomal Formulations in Clinical Use: An Updated Review, *Pharmaceutics* 9, 12.
- [6] Ma, P., and Mumper, R. J. (2013) Paclitaxel Nano-Delivery Systems: A Comprehensive Review, *J Nanomed Nanotechnol* 4, 1000164-1000164.
- [7] Jahangirian, H., Lemraski, E. G., Webster, T. J., Rafiee-Moghaddam, R., and Abdollahi, Y. (2017) A review of drug delivery systems based on nanotechnology and green chemistry: green nanomedicine, *International journal of nanomedicine*, 12, 2957–2978.
- [8] Yun, Y. H., Lee, B. K., and Park, K. (2015) Controlled Drug Delivery: Historical perspective for the next generation, *Journal of controlled release : official journal of the Controlled Release Society*, 219, 2–7.
- [9] Garbayo E, P.-G. S., Rodríguez-Nogales C, Saludas L, Estella-Hermoso de Mendoza A, Blanco-Prieto MJ. (2020) Nanomedicine and drug delivery systems in cancer and regenerative medicine. , *Wiley Interdiscip Rev Nanomed Nanobiotechnol*. 12(5):e1637.
- [10] Yetisgin, A. A., Cetinel, S., Zuvin, M., Kosar, A., and Kutlu, O. (2020) Therapeutic Nanoparticles and Their Targeted Delivery Applications, *Molecules* 25.
- [11] Li, Z., Tan, S., Li, S., Shen, Q., and Wang, K. (2017) Cancer drug delivery in the nano era: An overview and perspectives (Review), *Oncol Rep* 38, 611-624.
- [12] Wang, J., Ni, Q., Wang, Y., Zhang, Y., He, H., Gao, D., Ma, X., and Liang, X. J. (2021) Nanoscale drug delivery systems for controllable drug behaviors by multi-stage barrier penetration, *J Control Release* 331, 282-295.
- [13] Kim, S. M., Faix, P. H., and Schnitzer, J. E. (2017) Overcoming key biological barriers to cancer drug delivery and efficacy, *Journal of controlled release : official journal of the Controlled Release Society*, 267, 15–30.
- [14] Jin, F., Liu, D., Yu, H., Qi, J., You, Y., Xu, X., Kang, X., Wang, X., Lu, K., Ying, X., You, J. A.-O., Du, Y. A.-O., and Ji, J. (2019) Sialic Acid-Functionalized PEG-PLGA Microspheres Loading Mitochondrial-Targeting-Modified Curcumin for Acute Lung Injury Therapy, *Molecular pharmaceutics*, 16(1), 71–85.
- [15] Dolman, M. E., Harmsen S Fau - Storm, G., Storm G Fau - Hennink, W. E., Hennink We Fau - Kok, R. J., and Kok, R. J. (2010) Drug targeting to the kidney: Advances in the active targeting of therapeutics to proximal tubular cells, *Advanced drug delivery reviews*, 62(14), 1344–1357.
- [16] Liu, D., Shu, G., Jin, F., Qi, J., Xu, X., Du, Y., Yu, H., Wang, J., Sun, M., You, Y., Zhu, M., Chen, M., Zhu, L., Shen, Q., Ying, X., Lou, X., Jiang, S., and Du, Y. (2020) ROS-responsive chitosan-SS31 prodrug for AKI therapy via rapid distribution in the kidney and long-term retention

- in the renal tubule. LID - 10.1126/sciadv.abb7422 [doi] LID - eabb7422, *Science advances*, 6(41), eabb7422.
- [17] Barenholz, Y. (2012) Doxil®--the first FDA-approved nano-drug: lessons learned, *Journal of controlled release : official journal of the Controlled Release Society*, 160(2), 117–134.
- [18] Xiao, G., and Gan, L. S. (2013) Receptor-mediated endocytosis and brain delivery of therapeutic biologics, *International journal of cell biology*, 2013, 703545.
- [19] Patel, M. M., and Patel, B. M. (2017) Crossing the Blood-Brain Barrier: Recent Advances in Drug Delivery to the Brain, *CNS drugs*, 31(2), 109–133. .
- [20] Mason, E. A., and Kronstadt, B. (1967) Graham's laws of diffusion and effusion, *Journal of Chemical Education* 44, 740.
- [21] Chillistone, S., and Hardman, J. G. (2017) Factors affecting drug absorption and distribution, *Anaesthesia & Intensive Care Medicine* 18, 335-339.
- [22] Tyrrell, H. J. V. (1964) The origin and present status of Fick's diffusion law, *Journal of chemical education* 41, 397.
- [23] Parrott, N., Lukacova, V., Fraczkiewicz, G., and Bolger, M. B. (2009) Predicting pharmacokinetics of drugs using physiologically based modeling—application to food effects, *The AAPS journal* 11, 45-53.
- [24] Sten-Knudsen, O. (1978) Passive transport processes, In *Concepts and Models*, pp 5-113, Springer.
- [25] Seddon, A. M., Casey, D., Law, R. V., Gee, A., Templer, R. H., and Ces, O. (2009) Drug interactions with lipid membranes, *Chemical Society Reviews* 38, 2509-2519.
- [26] Kramer, E. M., and Myers, D. R. (2013) Osmosis is not driven by water dilution, *Trends in plant science* 18, 195-197.
- [27] Sharma, N., Agarwal, G., Rana, A. C., Bhat, Z. A., and Kumar, D. (2011) A review: transdermal drug delivery system: a tool for novel drug delivery system, *International journal of drug development and research* 3, 0-0.
- [28] Elkhodiry, M. A., Momah, C. C., Suwaidi, S. R., Gadalla, D., Martins, A. M., Vitor, R. F., and Husseini, G. A. (2016) Synergistic nanomedicine: passive, active, and ultrasound-triggered drug delivery in cancer treatment, *Journal of nanoscience and nanotechnology* 16, 1-18.
- [29] Mogoşanu, G. D., Grumezescu, A. M., Bejenaru, L. E., and Bejenaru, C. (2016) Natural and synthetic polymers for drug delivery and targeting, In *Nanobiomaterials in drug delivery*, pp 229-284, Elsevier.
- [30] Gonçalves, C., Pereira, P., and Gama, M. (2010) Self-assembled hydrogel nanoparticles for drug delivery applications, *Materials* 3, 1420-1460.
- [31] Torres-Martínez, A., Bedrina, B., Falomir, E. A.-O., Marín, M. J., Angulo-Pachón, C. A., Galindo, F. A.-O., and Miravet, J. A.-O. (2021) Non-Polymeric Nanogels as Versatile Nanocarriers: Intracellular Transport of the Photosensitizers Rose Bengal and Hypericin for Photodynamic Therapy, *ACS applied bio materials* 4(4), 3658–3669.
- [32] Chouikrat, R., Seve A Fau - Vanderesse, R., Vanderesse R Fau - Benachour, H., Benachour H Fau - Barberi-Heyob, M., Barberi-Heyob M Fau - Richeter, S., Richeter S Fau - Raehm, L., Raehm L Fau - Durand, J. O., Durand Jo Fau - Verelst, M., Verelst M Fau - Frochot, C., and Frochot, C. (2012) Non polymeric nanoparticles for photodynamic therapy applications: recent developments, *Current medicinal chemistry* 19(6), 781–792.
- [33] Balaure, P. C., Gudovan, D., and Gudovan, I. A. (2018) Smart Triggered Release in Controlled Drug Delivery, *Current drug targets* 19(4), 318–327.
- [34] Bej R Fau - Ghosh, S., and Ghosh, S. A.-O. (2019) Glutathione Triggered Cascade Degradation of an Amphiphilic Poly(disulfide)-Drug Conjugate and Targeted Release, *Bioconjugate chemistry*, 30(1), 101–110.
- [35] Franco, M. S., Gomes, E. R., Roque, M. C., and Oliveira, M. C. (2012) Triggered Drug Release From Liposomes: Exploiting the Outer and Inner Tumor Environment, *Frontiers in oncology*, 11, 623760.

- [36] Kumar, P. A.-O., Huo, P. A.-O., and Liu, B. (2019) Formulation Strategies for Folate-Targeted Liposomes and Their Biomedical Applications. LID - 10.3390/pharmaceutics11080381 [doi] LID - 381, *Their Biomedical Applications. Pharmaceutics*, 11(8), 381.
- [37] Almeida, B. A.-O., Nag, O. A.-O., Rogers, K. E., and Delehanty, J. A.-O. (2020) Recent Progress in Bioconjugation Strategies for Liposome-Mediated Drug Delivery. , *Molecules* , 25(23), 5672.
- [38] Zhang, Y., Wang J Fau - Bai, X., Bai X Fau - Jiang, T., Jiang T Fau - Zhang, Q., Zhang Q Fau - Wang, S., and Wang, S. (2012) Mesoporous silica nanoparticles for increasing the oral bioavailability and permeation of poorly water soluble drugs, *Molecular pharmaceutics*, 9(3),.
- [39] Sherje, A. P., Jadhav, M., Dravyakar, B. R., and Kadam, D. (2018) Dendrimers: A versatile nanocarrier for drug delivery and targeting, *International journal of pharmaceutics*, 548(1), 707–720.
- [40] Falanga, A., Del Genio, V., and Galdiero, S. (2021) Peptides and Dendrimers: How to Combat Viral and Bacterial Infections, *Pharmaceutics* 13.
- [41] Galbiati, A., Tabolacci, C., Morozzo Della Rocca, B., Mattioli, P., Beninati, S., Paradossi, G., and Desideri, A. (2011) Targeting tumor cells through chitosan-folate modified microcapsules loaded with camptothecin, *Bioconjugate Chemistry* 22, 1066-1072.
- [42] Peers, S., Montembault, A., and Ladavière, C. (2022) Chitosan hydrogels incorporating colloids for sustained drug delivery, *Carbohydrate Polymers* 275, 118689.
- [43] Rosiere, R., Van Woensel, M., Gelbcke, M., Mathieu, V., Hecq, J., Mathivet, T., Vermeersch, M., Van Antwerpen, P., Amighi, K., and Wauthoz, N. (2018) New folate-grafted chitosan derivative to improve delivery of paclitaxel-loaded solid lipid nanoparticles for lung tumor therapy by inhalation, *Molecular pharmaceutics* 15, 899-910.
- [44] Makadia, H. K., and Siegel, S. J. (2011) Poly Lactic-co-Glycolic Acid (PLGA) as Biodegradable Controlled Drug Delivery Carrier, *Polymers (Basel)* 3, 1377-1397.
- [45] Danhier, F., Ansorena E Fau - Silva, J. M., Silva Jm Fau - Coco, R., Coco R Fau - Le Breton, A., Le Breton A Fau - Pr eat, V., and Pr eat, V. (2012) PLGA-based nanoparticles: an overview of biomedical applications, *Journal of controlled release : official journal of the Controlled Release Society*, 161(2), 505–522.
- [46] Sainlos, M., and Imperiali, B. (2007) Tools for investigating peptide–protein interactions: peptide incorporation of environment-sensitive fluorophores via on-resin derivatization, *Nature Protocols* 2, 3201-3209.
- [47] Sch onauer, R., Kaiser, A., Holze, C., Babilon, S., K obberling, J., Riedl, B., and Beck-Sickinger, A. G. (2015) Fluorescently labeled adrenomedullin allows real-time monitoring of adrenomedullin receptor trafficking in living cells, *Journal of Peptide Science* 21, 905-912.
- [48] Zhang, L., and Bulaj, G. (2012) Converting peptides into drug leads by lipidation, *Current medicinal chemistry* 19, 1602-1618.
- [49] Kurtzhals, P., Havelund, S., Jonassen, I., Kiehr, B., Larsen, U. D., Ribel, U., and Markussen, J. (1995) Albumin binding of insulins acylated with fatty acids: characterization of the ligand-protein interaction and correlation between binding affinity and timing of the insulin effect in vivo, *Biochemical Journal* 312, 725-731.
- [50] Chatterjee, J., Rechenmacher F Fau - Kessler, H., and Kessler, H. (2013) N-methylation of peptides and proteins: an important element for modulating biological functions, *Angewandte Chemie (International ed. in English)*, 52(1), 254–269.
- [51] Weinstock, M. T., Francis Jn Fau - Redman, J. S., Redman Js Fau - Kay, M. S., and Kay, M. S. (2012) Protease-resistant peptide design-empowering nature's fragile warriors against HIV, *Biopolymers*, 98(5), 431–442.
- [52] Ovadia, O., Greenberg S Fau - Laufer, B., Laufer B Fau - Gilon, C., Gilon C Fau - Hoffman, A., Hoffman A Fau - Kessler, H., and Kessler, H. (2010) Improvement of drug-like properties of peptides: the somatostatin paradigm, . *Expert opinion on drug discovery*, 5(7), 655–671.

- [53] Glas, A., Bier D Fau - Hahne, G., Hahne G Fau - Rademacher, C., Rademacher C Fau - Ottmann, C., Ottmann C Fau - Grossmann, T. N., and Grossmann, T. N. (2014) Constrained peptides with target-adapted cross-links as inhibitors of a pathogenic protein-protein interaction, *Angewandte Chemie (International ed. in English)*, 53(9), 2489–2493.
- [54] Cheloha, R. W., Maeda, A., Dean, T., Gardella, T. J., and Gellman, S. H. (2014) Backbone modification of a polypeptide drug alters duration of action in vivo, *Nature biotechnology*, 32(7), 653–655.
- [55] L, D. (2015) - Strategic approaches to optimizing peptide ADME properties, *AAPS J.* 17, 134–143.
- [56] Tugyi, R., Uray K Fau - Iván, D., Iván D Fau - Fellingner, E., Fellingner E Fau - Perkins, A., Perkins A Fau - Hudecz, F., and Hudecz, F. (2005) Partial D-amino acid substitution: Improved enzymatic stability and preserved Ab recognition of a MUC2 epitope peptide, *Proceedings of the National Academy of Sciences of the United States of America*, 102(2), 413–418.
- [57] Tian, Y., and Zhou, S. A.-O. (2021) Advances in cell penetrating peptides and their functionalization of polymeric nanoplateforms for drug delivery, *Wiley Interdiscip Rev Nanomed Nanobiotechnol* 13, e1668.
- [58] Cavaco, M. A.-O., Andreu, D. A.-O., and Castanho, M. A.-O. (2021) The Challenge of Peptide Proteolytic Stability Studies: Scarce Data, Difficult Readability, and the Need for Harmonization, *Angewandte Chemie (International ed. in English)* 60, 1686–1688.
- [59] Lundberg, P., and Langel, U. (2003) A brief introduction to cell-penetrating peptides, *Journal of molecular recognition : JMR*, 16(5), 227–233.
- [60] Fonseca, S. B., Pereira Mp Fau - Kelley, S. O., and Kelley, S. O. (2009) Recent advances in the use of cell-penetrating peptides for medical and biological applications, *Advanced drug delivery reviews*, 61(11), 953–964.
- [61] Singh, T. A.-O., Murthy, A. A.-O., Yang, H. A.-O., and Im, J. A.-O. (2018) Versatility of cell-penetrating peptides for intracellular delivery of siRNA, *Drug delivery*, 25(1), 1996–2006.
- [62] Frankel, A. D., and Pabo, C. O. (1988) Cellular uptake of the tat protein from human immunodeficiency virus, *Cell*, 55(6), 1189–1193.
- [63] Taylor, B. N., Mehta Rr Fau - Yamada, T., Yamada T Fau - Lekmine, F., Lekmine F Fau - Christov, K., Christov K Fau - Chakrabarty, A. M., Chakrabarty Am Fau - Green, A., Green A Fau - Bratescu, L., Bratescu L Fau - Shilkaitis, A., Shilkaitis A Fau - Beattie, C. W., Beattie Cw Fau - Das Gupta, T. K., and Das Gupta, T. K. (2009) Noncationic peptides obtained from azurin preferentially enter cancer cells, *Cancer research*, 69(2), 537–546.
- [64] Derossi, D., Joliot Ah Fau - Chassaing, G., Chassaing G Fau - Prochiantz, A., and Prochiantz, A. (1994) The third helix of the Antennapedia homeodomain translocates through biological membranes, *The Journal of biological chemistry*, 269(14), 10444–10450.
- [65] Futaki, S., Suzuki T Fau - Ohashi, W., Ohashi W Fau - Yagami, T., Yagami T Fau - Tanaka, S., Tanaka S Fau - Ueda, K., Ueda K Fau - Sugiura, Y., and Sugiura, Y. (2001) Arginine-rich peptides. An abundant source of membrane-permeable peptides having potential as carriers for intracellular protein delivery, *The Journal of biological chemistry*, 276(8), 5836–5840.
- [66] Alizadeh, S., Irani, S., Bolhassani, A., and Sadat, S. M. (2020) HR9: An Important Cell Penetrating Peptide for Delivery of HCV NS3 DNA into HEK-293T Cells, *Avicenna journal of medical biotechnology*, 12(1), 44–51.
- [67] Lönn, P., and Dowdy, S. F. (2015) Cationic PTD/PPP-mediated macromolecular delivery: charging into the cell, *Expert opinion on drug delivery*, 12(10), 1627–1636.
- [68] Pooga, M., Hällbrink M Fau - Zorko, M., Zorko M Fau - Langel, U., and Langel, U. (1998) Cell penetration by transportan, *FASEB journal : official publication of the Federation of American Societies for Experimental Biology*, 12(1), 67–77.
- [69] Elmquist, A., Lindgren M Fau - Bartfai, T., Bartfai, T. F. A. U. L. U., and Langel, U. (2001) VE-cadherin-derived cell-penetrating peptide, pVEC, with carrier functions, *Experimental cell research*, 269(2), 237–244.

- [70] Oehlke, J., Scheller A Fau - Wiesner, B., Wiesner B Fau - Krause, E., Krause E Fau - Beyermann, M., Beyermann M Fau - Klauschenz, E., Klauschenz E Fau - Melzig, M., Melzig M Fau - Bienert, M., and Bienert, M. (1998) Cellular uptake of an alpha-helical amphipathic model peptide with the potential to deliver polar compounds into the cell interior non-endocytically, *Biochimica et biophysica acta*, 1414(1-2), 127–139.
- [71] Morris, M. C., Depollier J Fau - Mery, J., Mery J Fau - Heitz, F., Heitz F Fau - Divita, G., and Divita, G. (2001) A peptide carrier for the delivery of biologically active proteins into mammalian cells, *Nature biotechnology*, 19(12), 1173–1176.
- [72] Crombez, L., Aldrian-Herrada G Fau - Konate, K., Konate K Fau - Nguyen, Q. N., Nguyen Qn Fau - McMaster, G. K., McMaster Gk Fau - Brasseur, R., Brasseur R Fau - Heitz, F., Heitz F Fau - Divita, G., and Divita, G. (2009) A new potent secondary amphipathic cell-penetrating peptide for siRNA delivery into mammalian cells, *Molecular therapy : the journal of the American Society of Gene Therapy*, 17(1), 95–103.
- [73] Shahbazi, S., and Bolhassani, A. (2018) Comparison of six cell penetrating peptides with different properties for in vitro and in vivo delivery of HPV16 E7 antigen in therapeutic vaccines, *International immunopharmacology*, 62, 170–180. .
- [74] Carnevale, K. A.-O., Muroski, M. E., Vakil, P. N., Foley, M. E., Laufersky, G., Kenworthy, R., Zorio, D. A.-O., Morgan, T. J., Jr., Levenson, C. W., and Strouse, G. A.-O. X. (2018) Selective Uptake Into Drug Resistant Mammalian Cancer by Cell Penetrating Peptide-Mediated Delivery, *Bioconjugate chemistry*, 29(10), 3273–3284.
- [75] Galdiero, S., Vitiello M Fau - Falanga, A., Falanga A Fau - Cantisani, M., Cantisani M Fau - Incoronato, N., Incoronato N Fau - Galdiero, M., and Galdiero, M. (2012) Intracellular delivery: exploiting viral membranotropic peptides, *Current drug metabolism*, 13(1), 93–104.
- [76] Galdiero, S., Falanga, A., Morelli, G., and Galdiero, M. (2015) gH625: a milestone in understanding the many roles of membranotropic peptides, *Biochimica et biophysica acta*, 1848(1 Pt A), 16–25.
- [77] Milletti, F. (2012) Cell-penetrating peptides: classes, origin, and current landscape, *Drug discovery today*, 17(15-16), 850–860.
- [78] Rhee, M., and Davis, P. (2006) Mechanism of uptake of C105Y, a novel cell-penetrating peptide, *The Journal of biological chemistry*, 281(2), 1233–1240.
- [79] Gomez, J. A., Gama V Fau - Yoshida, T., Yoshida T Fau - Sun, W., Sun W Fau - Hayes, P., Hayes P Fau - Leskov, K., Leskov K Fau - Boothman, D., Boothman D Fau - Matsuyama, S., and Matsuyama, S. (2007) Bax-inhibiting peptides derived from Ku70 and cell-penetrating pentapeptides, *Biochemical Society transactions*, 35(Pt 4), 797–801.
- [80] Gao, C., Mao S Fau - Ditzel, H. J., Ditzel HJ Fau - Farnaes, L., Farnaes L Fau - Wirsching, P., Wirsching P Fau - Lerner, R. A., Lerner Ra Fau - Janda, K. D., and Janda, K. D. (2002) A cell-penetrating peptide from a novel pVII-pIX phage-displayed random peptide library, *Bioorganic & medicinal chemistry*, 10(12), 4057–4065.
- [81] Pei, D. A.-O., and Buyanova, M. (2019) Overcoming Endosomal Entrapment in Drug Delivery, *Bioconjugate chemistry*, 30(2), 273–283.
- [82] Ruseska, I., and Zimmer, A. A.-O. X. (2020) Internalization mechanisms of cell-penetrating peptides, *Beilstein journal of nanotechnology*, 11, 101–123.
- [83] Richard, J. P., Melikov K Fau - Vives, E., Vives E Fau - Ramos, C., Ramos C Fau - Verbeure, B., Verbeure B Fau - Gait, M. J., Gait Mj Fau - Chernomordik, L. V., Chernomordik Lv Fau - Lebleu, B., and Lebleu, B. (2003) Cell-penetrating peptides. A reevaluation of the mechanism of cellular uptake, *The Journal of biological chemistry*, 278(1), 585–590.
- [84] Lundberg, M., Wikström S Fau - Johansson, M., and Johansson, M. (2003) Cell surface adherence and endocytosis of protein transduction domains, *Molecular therapy : the journal of the American Society of Gene Therapy*, 8(1), 143–150.

- [85] Futaki, S. (2002) Arginine-rich peptides: potential for intracellular delivery of macromolecules and the mystery of the translocation mechanisms, *International journal of pharmaceuticals*, 245(1-2), 1–7.
- [86] Pooga, M., Soomets U Fau - Hällbrink, M., Hällbrink M Fau - Valkna, A., Valkna A Fau - Saar, K., Saar K Fau - Rezaei, K., Rezaei K Fau - Kahl, U., Kahl U Fau - Hao, J. X., Hao Jx Fau - Xu, X. J., Xu Xj Fau - Wiesenfeld-Hallin, Z., Wiesenfeld-Hallin Z Fau - Hökfelt, T., Hökfelt T Fau - Bartfai, T., Bartfai T Fau - Langel, U., and Langel, U. (1998) Cell penetrating PNA constructs regulate galanin receptor levels and modify pain transmission in vivo, *Nature biotechnology*, 16(9), 857–861.
- [87] Morris, M. C., Vidal P Fau - Chaloin, L., Chaloin L Fau - Heitz, F., Heitz F Fau - Divita, G., and Divita, G. (1997) A new peptide vector for efficient delivery of oligonucleotides into mammalian cells, *Nucleic acids research*, 25(14), 2730–2736.
- [88] Jones, S. W., Christison R Fau - Bundell, K., Bundell K Fau - Voyce, C. J., Voyce Cj Fau - Brockbank, S. M. V., Brockbank Sm Fau - Newham, P., Newham P Fau - Lindsay, M. A., and Lindsay, M. A. (2005) Characterisation of cell-penetrating peptide-mediated peptide delivery, *European journal of medicinal chemistry*, 130, 336–345.
- [89] Nakase, I., Tadokoro A Fau - Kawabata, N., Kawabata N Fau - Takeuchi, T., Takeuchi T Fau - Katoh, H., Katoh H Fau - Hiramoto, K., Hiramoto K Fau - Negishi, M., Negishi M Fau - Nomizu, M., Nomizu M Fau - Sugiura, Y., Sugiura Y Fau - Futaki, S., and Futaki, S. (2007) Interaction of arginine-rich peptides with membrane-associated proteoglycans is crucial for induction of actin organization and macropinocytosis, *Biochemistry*, 46(2), 492–501.
- [90] Fittipaldi, A., Ferrari A Fau - Zoppé, M., Zoppé M Fau - Arcangeli, C., Arcangeli C Fau - Pellegrini, V., Pellegrini V Fau - Beltram, F., Beltram F Fau - Giacca, M., and Giacca, M. (2003) Cell membrane lipid rafts mediate caveolar endocytosis of HIV-1 Tat fusion proteins, *The Journal of biological chemistry*, 278(36), 34141–34149.
- [91] Nakase, I., Niwa M Fau - Takeuchi, T., Takeuchi T Fau - Sonomura, K., Sonomura K Fau - Kawabata, N., Kawabata N Fau - Koike, Y., Koike Y Fau - Takehashi, M., Takehashi M Fau - Tanaka, S., Tanaka S Fau - Ueda, K., Ueda K Fau - Simpson, J. C., Simpson Jc Fau - Jones, A. T., Jones At Fau - Sugiura, Y., Sugiura Y Fau - Futaki, S., and Futaki, S. (2004) Cellular uptake of arginine-rich peptides: roles for macropinocytosis and actin rearrangement, *Molecular therapy : the journal of the American Society of Gene Therapy*, 10(6), 1011–1022.
- [92] Vandembroucke, R. E., De Smedt Sc Fau - Demeester, J., Demeester J Fau - Sanders, N. N., and Sanders, N. N. (2007) Cellular entry pathway and gene transfer capacity of TAT-modified lipoplexes, *Biochimica et biophysica acta*, 1768(3), 571–579.
- [93] Fischer, R., Köhler K Fau - Fotin-Mleczek, M., Fotin-Mleczek M Fau - Brock, R., and Brock, R. (2004) A stepwise dissection of the intracellular fate of cationic cell-penetrating peptides, *The Journal of biological chemistry*, 279(13), 12625–12635.
- [94] Galdiero, S., Vitiello M Fau - Falanga, A., Falanga A Fau - Cantisani, M., Cantisani M Fau - Incoronato, N., Incoronato N Fau - Galdiero, M., and Galdiero, M. (2012) Intracellular delivery: exploiting viral membranotropic peptides, *Current drug metabolism*, 13(1), 93–104.
- [95] Larsson, P., and Kasson, P. M. (2013) Lipid tail protrusion in simulations predicts fusogenic activity of influenza fusion peptide mutants and conformational models, *PLoS computational biology*, 9(3), e1002950.
- [96] Kozlov, M. M., McMahon Ht Fau - Chernomordik, L. V., and Chernomordik, L. V. (2010) Protein-driven membrane stresses in fusion and fission, *Trends in biochemical sciences*, 35(12), 699–706.
- [97] Falanga, A., Cantisani M Fau - Pedone, C., Pedone C Fau - Galdiero, S., and Galdiero, S. (2009) Membrane fusion and fission: enveloped viruses, *Protein and peptide letters*, 16(7), 751–759.

- [98] Van Meter, M. E. M., and Kim, E. S. (2010) Bevacizumab: current updates in treatment, *Current opinion in oncology* 22, 586-591.
- [99] Modjtahedi, H., Ali, S., and Essapen, S. (2012) Therapeutic application of monoclonal antibodies in cancer: advances and challenges, *British medical bulletin* 104, 41-59.
- [100] Shadidi, M., and Sioud, M. (2003) Selective targeting of cancer cells using synthetic peptides, *Drug Resistance Updates* 6, 363-371.
- [101] Gottesman, M. M. (2002) Mechanisms of cancer drug resistance, *Annual review of medicine* 53, 615-627.
- [102] Lingasamy, P., Tobi, A., Kurm, K., Kopanchuk, S., Sudakov, A., Salumäe, M., Rätsep, T., Asser, T., Bjerkvig, R., and Teesalu, T. (2020) Tumor-penetrating peptide for systemic targeting of Tenascin-C, *Scientific reports* 10, 1-13.
- [103] Moore, S. J., Hayden Gephart, M. G., Bergen, J. M., Su, Y. S., Rayburn, H., Scott, M. P., and Cochran, J. R. (2013) Engineered knottin peptide enables noninvasive optical imaging of intracranial medulloblastoma, *Proceedings of the National Academy of Sciences of the United States of America* 110, 14598-14603.
- [104] Cox, N., Kintzing, J. R., Smith, M., Grant, G. A., and Cochran, J. R. (2016) Integrin-Targeting Knottin Peptide-Drug Conjugates Are Potent Inhibitors of Tumor Cell Proliferation, *Angewandte Chemie (International ed. in English)* 55, 9894-9897.
- [105] Li, Z., Zhao R Fau - Wu, X., Wu X Fau - Sun, Y., Sun Y Fau - Yao, M., Yao M Fau - Li, J., Li J Fau - Xu, Y., Xu Y Fau - Gu, J., and Gu, J. (2005) Identification and characterization of a novel peptide ligand of epidermal growth factor receptor for targeted delivery of therapeutics, *FASEB journal : official publication of the Federation of American Societies for Experimental Biology*, 19(14), 1978-1985.
- [106] Ying, M., Shen, Q., Liu, Y., Yan, Z., Wei, X., Zhan, C., Gao, J., Xie, C., Yao, B., and Lu, W. (2016) Stabilized Heptapeptide A7R for Enhanced Multifunctional Liposome-Based Tumor-Targeted Drug Delivery, *ACS applied materials & interfaces*, 8(21), 13232-13241.
- [107] Ying, M., Shen, Q., Zhan, C., Wei, X., Gao, J., Xie, C., Yao, B., and Lu, W. (2016) A stabilized peptide ligand for multifunctional glioma targeted drug delivery, *Journal of controlled release : official journal of the Controlled Release Society*, 243, 86-98.
- [108] Oller-Salvia, B., Sánchez-Navarro, M., Giralte, E., and Teixidó, M. (2016) Blood-brain barrier shuttle peptides: an emerging paradigm for brain delivery, *Chemical Society reviews*, 45(17), 4690-4707.
- [109] Wu, J., Williams, G. R., Niu, S., Gao, F., Tang, R., and Zhu, L. A.-O. (2019) A Multifunctional Biodegradable Nanocomposite for Cancer Theranostics, *Advanced science (Weinheim, Baden-Wurttemberg, Germany)*, 6(14), 1802001.
- [110] Juang, V., Chang, C. H., Wang, C. S., Wang, H. E., and Lo, Y. L. (2019) pH-Responsive PEG-Shedding and Targeting Peptide-Modified Nanoparticles for Dual-Delivery of Irinotecan and microRNA to Enhance Tumor-Specific Therapy, *Small (Weinheim an der Bergstrasse, Germany)* 15, e1903296.
- [111] Han, H., Hou, Y., Chen, X., Zhang, P., Kang, M., Jin, Q., Ji, J., and Gao, M. (2020) Metformin-Induced Stromal Depletion to Enhance the Penetration of Gemcitabine-Loaded Magnetic Nanoparticles for Pancreatic Cancer Targeted Therapy, *J Am Chem Soc* 142, 4944-4954.
- [112] Harada, H., Hiraoka, M., and Kizaka-Kondoh, S. (2002) Antitumor effect of TAT-oxygen-dependent degradation-caspase-3 fusion protein specifically stabilized and activated in hypoxic tumor cells, *Cancer research* 62, 2013-2018.
- [113] Jiang, T., Olson, E. S., Nguyen, Q. T., Roy, M., Jennings, P. A., and Tsien, R. Y. (2004) Tumor imaging by means of proteolytic activation of cell-penetrating peptides, *Proceedings of the National Academy of Sciences of the United States of America* 101, 17867-17872.
- [114] Wang, S., Zhang, S., Liu, J., Liu, Z., Su, L., Wang, H., and Chang, J. (2014) pH- and Reduction-Responsive Polymeric Lipid Vesicles for Enhanced Tumor Cellular Internalization and Triggered Drug Release, *ACS applied materials & interfaces* 6, 10706-10713.

- [115] Shi, Y., Zhu, M. L., Wu, Q., Huang, Y., Xu, X. L., and Chen, W. (2021) The Potential of Drug Delivery Nanosystems for Sepsis Treatment, *Journal of inflammation research* 14, 7065-7077.
- [116] Kumar, S., Tripathy, S., Jyoti, A., and Singh, S. G. (2019) Recent advances in biosensors for diagnosis and detection of sepsis: A comprehensive review, *Biosensors & bioelectronics* 124-125, 205-215.
- [117] Zhang, C. Y., Gao, J., and Wang, Z. (2018) Bioresponsive Nanoparticles Targeted to Infectious Microenvironments for Sepsis Management, *Advanced materials (Deerfield Beach, Fla.)* 30, e1803618.
- [118] Hou, X., Zhang, X., Zhao, W., Zeng, C., Deng, B., McComb, D. W., Du, S., Zhang, C., Li, W., and Dong, Y. (2020) Vitamin lipid nanoparticles enable adoptive macrophage transfer for the treatment of multidrug-resistant bacterial sepsis, *Nature nanotechnology* 15, 41-46.
- [119] Fan, X., Fan, J., Wang, X., Wu, P., and Wu, G. (2015) S-thanatin functionalized liposome potentially targeting on *Klebsiella pneumoniae* and its application in sepsis mouse model, *Frontiers in pharmacology* 6, 249.
- [120] Alfei, S., and Schito, A. M. (2020) From Nanobiotechnology, Positively Charged Biomimetic Dendrimers as Novel Antibacterial Agents: A Review, *Nanomaterials (Basel, Switzerland)* 10.
- [121] Wrońska, N., Majoral, J. P., Appelhans, D., Bryszewska, M., and Lisowska, K. (2019) Synergistic Effects of Anionic/Cationic Dendrimers and Levofloxacin on Antibacterial Activities, *Molecules* 24.
- [122] Cheng, Y., Qu, H., Ma, M., Xu, Z., Xu, P., Fang, Y., and Xu, T. (2007) Polyamidoamine (PAMAM) dendrimers as biocompatible carriers of quinolone antimicrobials: an in vitro study, *European journal of medicinal chemistry* 42, 1032-1038.
- [123] Gholami, M., Mohammadi, R., Arzanlou, M., Akbari Dourbash, F., Kouhsari, E., Majidi, G., Mohseni, S. M., and Nazari, S. (2017) In vitro antibacterial activity of poly (amidoamine)-G7 dendrimer, *BMC infectious diseases* 17, 395.
- [124] Tam, J. P., Lu, Y. A., and Yang, J. L. (2002) Antimicrobial dendrimeric peptides, *European journal of biochemistry* 269, 923-932.
- [125] Pires, J., Siriwardena, T. N., Stach, M., Tinguely, R., Kasraian, S., Luzzaro, F., Leib, S. L., Darbre, T., Reymond, J. L., and Endimiani, A. (2015) In Vitro Activity of the Novel Antimicrobial Peptide Dendrimer G3KL against Multidrug-Resistant *Acinetobacter baumannii* and *Pseudomonas aeruginosa*, *Antimicrobial agents and chemotherapy* 59, 7915-7918.
- [126] Ben Jeddou, F., Falconnet, L., Luscher, A., Siriwardena, T., Reymond, J. L., van Delden, C., and Köhler, T. (2020) Adaptive and Mutational Responses to Peptide Dendrimer Antimicrobials in *Pseudomonas aeruginosa*, *Antimicrobial agents and chemotherapy* 64.
- [127] Nag, M., Lahiri, D., Sarkar, T., Ghosh, S., Dey, A., Edinur, H. A., Pati, S., and Ray, R. R. (2021) Microbial Fabrication of Nanomaterial and Its Role in Disintegration of Exopolymeric Matrices of Biofilm, *Frontiers in chemistry* 9, 690590.
- [128] de Alteriis, E., Maione, A., Falanga, A., Bellavita, R., Galdiero, S., Albarano, L., Salvatore, M. M., Galdiero, E., and Guida, M. (2022) Activity of Free and Liposome-Encapsulated Essential Oil from *Lavandula angustifolia* against Persister-Derived Biofilm of *Candida auris*, *Antibiotics* 11.
- [129] Fulaz, S., Vitale, S., Quinn, L., and Casey, E. (2019) Nanoparticle-Biofilm Interactions: The Role of the EPS Matrix, *Trends in microbiology* 27, 915-926.
- [130] Shkodenko, L., Kassirov, I., and Koshel, E. (2020) Metal Oxide Nanoparticles Against Bacterial Biofilms: Perspectives and Limitations, *Microorganisms* 8.
- [131] Ikuma, K., Decho, A. W., and Lau, B. L. (2015) When nanoparticles meet biofilms-interactions guiding the environmental fate and accumulation of nanoparticles, *Frontiers in microbiology* 6, 591.

- [132] Gómez-Núñez, M. F., Castillo-López, M., Sevilla-Castillo, F., Roque-Reyes, O. J., Romero-Lechuga, F., Medina-Santos, D. I., Martínez-Daniel, R., and Peón, A. N. (2020) Nanoparticle-Based Devices in the Control of Antibiotic Resistant Bacteria, *Frontiers in microbiology* 11, 563821.
- [133] Fernandez, J., Martin-Serrano, Á., Gómez-Casanova, N., Falanga, A., Galdiero, S., Javier de la Mata, F., Heredero-Bermejo, I., and Ortega, P. (2021) Effect of the Combination of Levofloxacin with Cationic Carbosilane Dendron and Peptide in the Prevention and Treatment of Staphylococcus aureus Biofilms, *Polymers* 13.
- [134] Cantisani, M., Leone, M., Mignogna, E., Kampanaraki, K., Falanga, A., Morelli, G., Galdiero, M., and Galdiero, S. (2013) Structure-activity relations of myxinidin, an antibacterial peptide derived from the epidermal mucus of hagfish, *Antimicrobial agents and chemotherapy* 57, 5665-5673.
- [135] Cantisani, M., Finamore, E., Mignogna, E., Falanga, A., Nicoletti, G. F., Pedone, C., Morelli, G., Leone, M., Galdiero, M., and Galdiero, S. (2014) Structural insights into and activity analysis of the antimicrobial peptide myxinidin, *Antimicrobial agents and chemotherapy* 58, 5280-5290.
- [136] Lombardi, L., Stellato, M. I., Oliva, R., Falanga, A., Galdiero, M., Petraccone, L., D'Errico, G., De Santis, A., Galdiero, S., and Del Vecchio, P. (2017) Antimicrobial peptides at work: interaction of myxinidin and its mutant WMR with lipid bilayers mimicking the P. aeruginosa and E. coli membranes, *Scientific reports* 7, 44425.
- [137] Quader, S., and Kataoka, K. (2017) Nanomaterial-Enabled Cancer Therapy, *Molecular Therapy* 25, 1501-1513.
- [138] Wang, J., and Cui, H. (2016) Nanostructure-Based Theranostic Systems, *Theranostics*, 6(9), 1274–1276.
- [139] Zhao, M., Ding, X. F., Shen, J. Y., Zhang, X. P., Ding, X. W., and Xu, B. (2017) Use of liposomal doxorubicin for adjuvant chemotherapy of breast cancer in clinical practice, *Journal of Zhejiang University. Science. B*, 18(1), 15–26.
- [140] Hassan, S., Prakash, G., Ozturk, A., Saghadzadeh, S., Sohail, M. F., Seo, J., Dockmeci, M., Zhang, Y. S., and Khademhosseini, A. (2017) Evolution and Clinical Translation of Drug Delivery Nanomaterials, *Nano today*, 15, 91–106.
- [141] Baloch, S., Baloch, M. A., Zheng, T., and Pei, X. (2020) The Coronavirus Disease 2019 (COVID-19) Pandemic, *The Tohoku journal of experimental medicine*, 250(4), 271–278.
- [142] Kim, E. A.-O., Lim, E. K., Park, G., Park, C., Lim, J. W., Lee, H., Na, W., Yeom, M., Kim, J., Song, D., and Haam, S. A.-O. (2021) Advanced Nanomaterials for Preparedness Against (Re-)Emerging Viral Diseases, *Advanced Nanomaterials for Preparedness Against (Re-)Emerging Viral Diseases. Advanced materials (Deerfield Beach, Fla.)*, 33(47), e2005927.
- [143] Cheng, W., Yang, C., Ding, X., Engler, A. C., Hedrick, J. L., and Yang, Y. Y. (2015) Broad-Spectrum Antimicrobial/Antifouling Soft Material Coatings Using Poly(ethylenimine) as a Tailorable Scaffold, *Biomacromolecules*, 16(7), 1967–1977.
- [144] Lienkamp, K., and Tew, G. N. (2009) Synthetic mimics of antimicrobial peptides--a versatile ring-opening metathesis polymerization based platform for the synthesis of selective antibacterial and cell-penetrating polymers, *Chemistry (Weinheim an der Bergstrasse, Germany)*, 15(44), 11784–11800.
- [145] Fiore, G. L., Rowan S. J., Fau - Weder, C., and Weder, C. (2013) Optically healable polymers, *Chemical Society reviews*, 42(17), 7278–7288.
- [146] Korzhikov, V. A., Gusevskaya, K. V., Litvinchuk, E. N., Vlach, E. G., and Tennikova, T. B. (2013) Enzyme-mediated ring-opening polymerization of pentadecalactone to obtain biodegradable polymer for fabrication of scaffolds for bone tissue engineering, *International Journal of Polymer Science* 2013.
- [147] Arvin, A., Campadelli-Fiume, G., Mocarski, E., Moore, P. S., Roizman, B., Whitley, R., and Yamanishi, K. (2007) Human herpesviruses: biology, therapy, and immunoprophylaxis, *Human Herpesviruses: Biology, Therapy, and Immunoprophylaxis*.

- [148] Englund, J. A., Zimmerman Me Fau - Swierkosz, E. M., Swierkosz Em Fau - Goodman, J. L., Goodman JI Fau - Scholl, D. R., Scholl Dr Fau - Balfour, H. H., Jr., and Balfour, H. H., Jr. (1990) Herpes simplex virus resistant to acyclovir. A study in a tertiary care center, *Annals of internal medicine*, 112(6), 416–422.
- [149] Clementi, N., Criscuolo, E., Cappelletti, F., Burioni, R., Clementi, M., and Mancini, N. (2016) Novel therapeutic investigational strategies to treat severe and disseminated HSV infections suggested by a deeper understanding of in vitro virus entry processes, *Drug discovery today*, *Drug discovery today*, 21(4), 682–691..
- [150] Goto, K., Okuzu, Y., So, K., Kuroda, Y., and Matsuda, S. (2016) Clinical and radiographic evaluation of cemented socket fixation concomitant to acetabular bone grafting fixed with absorbable hydroxyapatite-poly-l-lactide composite screws, *Journal of orthopaedic science : official journal of the Japanese Orthopaedic Association*, 21(1), 57–62.
- [151] Bai, Y., Xing, H., Vincil, G. A., Lee, J., Henderson, E. J., Lu, Y., Lemcoff, N. G., and Zimmerman, S. C. (2014) Practical synthesis of water-soluble organic nanoparticles with a single reactive group and a functional carrier scaffold, *Chemical Science* 5, 2862-2868.
- [152] Galdiero, S., Falanga A Fau - Vitiello, M., Vitiello M Fau - D'Isanto, M., D'Isanto M Fau - Cantisani, M., Cantisani M Fau - Kampanaraki, A., Kampanaraki A Fau - Benedetti, E., Benedetti E Fau - Browne, H., Browne H Fau - Galdiero, M., and Galdiero, M. (2008) Peptides containing membrane-interacting motifs inhibit herpes simplex virus type 1 infectivity, *Peptides*, 29(9), 1461–1471.
- [153] Liu, Q., Chen, S., Chen, J., and Du, J. (2015) An asymmetrical polymer vesicle strategy for significantly improving T 1 MRI sensitivity and cancer-targeted drug delivery, *Macromolecules* 48, 739-749.
- [154] Qian, J., Yong, X., Xu, W., and Jin, X. (2013) Preparation and characterization of bimodal porous poly (γ -benzyl-L-glutamate) scaffolds for bone tissue engineering, *Materials Science and Engineering: C* 33, 4587-4593.
- [155] Borchmann, D. E., Carberry, T. P., and Weck, M. (2014) “Bio”-Macromolecules: Polymer-Protein Conjugates as Emerging Scaffolds for Therapeutics, *Macromolecular rapid communications* 35, 27-43.
- [156] Gauthier, M. A., and Klok, H.-A. (2008) Peptide/protein–polymer conjugates: synthetic strategies and design concepts, *Chemical Communications*, 2591-2611.
- [157] Kim, E., Lim, E. K., Park, G., Park, C., Lim, J. W., Lee, H., Na, W., Yeom, M., Kim, J., and Song, D. (2021) Advanced Nanomaterials for Preparedness Against (Re-) Emerging Viral Diseases, *Advanced Materials* 33, 2005927.
- [158] Issberner, J., Moors, R., and Vögtle, F. (1995) Dendrimers: From generations and functional groups to functions, *Angewandte Chemie International Edition in English* 33, 2413-2420.
- [159] Tomalia, D. A., Baker, H., Dewald, J., Hall, M., Kallos, G., Martin, S., Roeck, J., Ryder, J., and Smith, P. (1985) A new class of polymers: starburst-dendritic macromolecules, *Polymer journal* 17, 117-132.
- [160] Hawker, C. J., and Frechet, J. M. J. (1990) Preparation of polymers with controlled molecular architecture. A new convergent approach to dendritic macromolecules, *Journal of the American Chemical Society* 112, 7638-7647.
- [161] Yiyun, C., Na, M., Tongwen, X., Rongqiang, F., Xueyuan, W., Xiaomin, W., and Longping, W. (2007) Transdermal delivery of nonsteroidal anti-inflammatory drugs mediated by polyamidoamine (PAMAM) dendrimers, *Journal of pharmaceutical sciences* 96, 595-602.
- [162] Fu, H. L., Cheng, S. X., Zhang, X. Z., and Zhuo, R. X. (2008) Dendrimer/DNA complexes encapsulated functional biodegradable polymer for substrate-mediated gene delivery, *The Journal of Gene Medicine: A cross-disciplinary journal for research on the science of gene transfer and its clinical applications* 10, 1334-1342.
- [163] Patel, H. N., and Patel, P. M. (2013) Dendrimer applications—A review, *Int J Pharm Bio Sci* 4, 454-463.

- [164] Ardestani, M. S., Fordoei, A. S., Abdoli, A., Ahangari Cohan, R., Bahramali, G., Sadat, S. M., Siadat, S. D., Moloudian, H., Nassiri Koopaei, N., and Bolhasani, A. (2015) Nanosilver based anionic linear globular dendrimer with a special significant antiretroviral activity, *Journal of Materials Science: Materials in Medicine* 26, 1-8.
- [165] Worley, B. V., Schilly, K. M., and Schoenfisch, M. H. (2015) Anti-biofilm efficacy of dual-action nitric oxide-releasing alkyl chain modified poly (amidoamine) dendrimers, *Molecular pharmaceutics* 12, 1573-1583.
- [166] Astruc, D., Boisselier, E., and Ornelas, C. (2010) Dendrimers designed for functions: from physical, photophysical, and supramolecular properties to applications in sensing, catalysis, molecular electronics, photonics, and nanomedicine, *Chemical reviews* 110, 1857-1959.
- [167] Cantisani, M., Falanga A Fau - Incoronato, N., Incoronato N Fau - Russo, L., Russo L Fau - De Simone, A., De Simone A Fau - Morelli, G., Morelli G Fau - Berisio, R., Berisio R Fau - Galdiero, M., Galdiero M Fau - Galdiero, S., and Galdiero, S. (2013) Conformational modifications of gB from herpes simplex virus type 1 analyzed by synthetic peptides, *Journal of medicinal chemistry*, 56(21), 8366–8376.
- [168] Galdiero, S., Falanga A Fau - Vitiello, G., Vitiello G Fau - Vitiello, M., Vitiello M Fau - Pedone, C., Pedone C Fau - D'Errico, G., D'Errico G Fau - Galdiero, M., and Galdiero, M. (2010) Role of membranotropic sequences from herpes simplex virus type I glycoproteins B and H in the fusion process, *Biochimica et biophysica acta*, 1798(3), 579–591.
- [169] Galdiero, S., Vitiello, M., D'Isanto, M., Falanga, A., Collins, C., Raieta, K., Pedone, C., Browne, H., and Galdiero, M. (2006) Analysis of synthetic peptides from heptad-repeat domains of herpes simplex virus type 1 glycoproteins H and B, *The Journal of general virology*, 87(Pt 5), 1085–1097.
- [170] Mathieu, C., Augusto, M. T., Niewiesk, S., Horvat, B., Palermo, L. M., Sanna, G., Madeddu, S., Huey, D., Castanho, M. A., Porotto, M., Santos, N. C., and Moscona, A. (2017) Broad spectrum antiviral activity for paramyxoviruses is modulated by biophysical properties of fusion inhibitory peptides, *Scientific reports*, 7, 43610.
- [171] Shi, Y., Lin, R., Cui, H., and Azevedo, H. S. (2018) Multifunctional Self-Assembling Peptide-Based Nanostructures for Targeted Intracellular Delivery: Design, Physicochemical Characterization, and Biological Assessment, *Methods in molecular biology*, 1758, 11–26.
- [172] Fotakis, G., and Timbrell, J. A. (2006) In vitro cytotoxicity assays: comparison of LDH, neutral red, MTT and protein assay in hepatoma cell lines following exposure to cadmium chloride, *Toxicology letters*, 160(2), 171–177.
- [173] Hope, M. J., Bally Mb Fau - Webb, G., Webb G Fau - Cullis, P. R., and Cullis, P. R. (1985) Production of large unilamellar vesicles by a rapid extrusion procedure: characterization of size distribution, trapped volume and ability to maintain a membrane potential, *Biochimica et biophysica acta*, 812(1), 55–65.
- [174] Kalb, E., Frey S Fau - Tamm, L. K., and Tamm, L. K. (1992) Formation of supported planar bilayers by fusion of vesicles to supported phospholipid monolayers, *Biochimica et biophysica acta*, 1103(2), 307–316.
- [175] Morton, T. A., Myszka Dg Fau - Chaiken, I. M., and Chaiken, I. M. (1995) Interpreting complex binding kinetics from optical biosensors: a comparison of analysis by linearization, the integrated rate equation, and numerical integration, *Analytical biochemistry*, 227(1), 176–185.
- [176] Galdiero, S., Falanga A Fau - Vitiello, M., Vitiello M Fau - Raiola, L., Raiola L Fau - Fattorusso, R., Fattorusso R Fau - Browne, H., Browne H Fau - Pedone, C., Pedone C Fau - Isernia, C., Isernia C Fau - Galdiero, M., and Galdiero, M. (2008) Analysis of a membrane interacting region of herpes simplex virus type 1 glycoprotein H, *The Journal of biological chemistry*, 283(44), 29993–30009.
- [177] Kumar P Fau - Nagarajan, A., Nagarajan A Fau - Uchil, P. D., and Uchil, P. D. (2018) Analysis of Cell Viability by the MTT Assay. , *Cold Spring Harbor protocols*, 2018(6),10.1101.

- [178] Zinner, S. H. (2007) Antibiotic use: present and future, *MICROBIOLOGICA-BOLOGNA*- 30, 321.
- [179] Alexander, J. W. (2009) History of the medical use of silver, *Surgical infections* 10, 289-292.
- [180] Hadadi-Fishani, M., Khaledi, A., and Fatemi-Nasab, Z. S. (2020) Correlation between biofilm formation and antibiotic resistance in *Pseudomonas aeruginosa*: a meta-analysis, *Le infezioni in medicina*, 28(1), 47–54.
- [181] Song, X., Liu, P., Liu, X., Wang, Y., Wei, H., Zhang, J., Yu, L., Yan, X., and He, Z. (2021) Dealing with MDR bacteria and biofilm in the post-antibiotic era: Application of antimicrobial peptides-based nano-formulation, *Materials science & engineering. C, Materials for biological applications*, 128, 112318.
- [182] Lai, Y., and Gallo, R. L. (2009) AMPed up immunity: how antimicrobial peptides have multiple roles in immune defense, *Trends in immunology*, 30(3), 131–141.
- [183] Tomasinsig, L., Skerlavaj B Fau - Papo, N., Papo N Fau - Giabbai, B., Giabbai B Fau - Shai, Y., Shai Y Fau - Zanetti, M., and Zanetti, M. (2006) Mechanistic and functional studies of the interaction of a proline-rich antimicrobial peptide with mammalian cells, *The Journal of biological chemistry*, 281(1), 383–391.
- [184] Rinaldi, A. C. (2002) Antimicrobial peptides from amphibian skin: an expanding scenario, *Current opinion in chemical biology*, 6(6), 799–804.
- [185] Bechinger, B., and Gorr, S. U. (2017) Antimicrobial Peptides: Mechanisms of Action and Resistance, *Journal of dental research*, 96(3), 254–260.
- [186] Gao, L., and Fang, W. (2009) Effects of induced tension and electrostatic interactions on the mechanisms of antimicrobial peptide translocation across lipid bilayer, *Soft Matter* 5, 3312-3318.
- [187] Last, N. B., Schlamadinger, D. E., and Miranker, A. D. (2013) A common landscape for membrane-active peptides, *Protein Science* 22, 870-882.
- [188] Ageitos, J. M., Sánchez-Pérez, A., Calo-Mata, P., and Villa, T. G. (2017) Antimicrobial peptides (AMPs): Ancient compounds that represent novel weapons in the fight against bacteria, *Biochemical pharmacology* 133, 117-138.
- [189] Scudiero, O., Nigro, E., Cantisani, M., Colavita, I., Leone, M., Mercurio, F. A., Galdiero, M., Pessi, A., Daniele, A., Salvatore, F., and Galdiero, S. (2015) Design and activity of a cyclic mini- β -defensin analog: a novel antimicrobial tool, *International journal of nanomedicine*, 10, 6523–6539.
- [190] Scudiero, O., Brancaccio, M., Mennitti, C., Laneri, S., Lombardo, B., De Biasi, M. G., De Gregorio, E., Pagliuca, C., Colicchio, R., Salvatore, P., and Pero, R. (2020) Human Defensins: A Novel Approach in the Fight against Skin Colonizing *Staphylococcus aureus*. , *Antibiotics*, 9(4), 198.
- [191] Mahlapuu, M., Håkansson, J., Ringstad, L., and Björn, C. (2016) Antimicrobial peptides: an emerging category of therapeutic agents, *Frontiers in cellular and infection microbiology* 6, 194.
- [192] Franci, G., Falanga, A., Galdiero, S., Palomba, L., Rai, M., Morelli, G., and Galdiero, M. (2015) Silver nanoparticles as potential antibacterial agents, *Molecules* 20, 8856-8874.
- [193] Dos Santos, C. A., Seckler, M. M., Ingle, A. P., Gupta, I., Galdiero, S., Galdiero, M., Gade, A., and Rai, M. (2014) Silver nanoparticles: therapeutical uses, toxicity, and safety issues, *Journal of pharmaceutical sciences*, *Journal of pharmaceutical sciences*, 103(7), 1931–1944.
- [194] Rai, M. K., Deshmukh Sd Fau - Ingle, A. P., Ingle Ap Fau - Gade, A. K., and Gade, A. K. (2012) Silver nanoparticles: the powerful nanoweapon against multidrug-resistant bacteria, *Journal of applied microbiology*, 112(5), 841–852.
- [195] Dimitrov, D. S. (2004) Virus entry: molecular mechanisms and biomedical applications, *Microbiology*, 2(2), 109–122.

- [196] Collins, K. B., Patterson Bk Fau - Naus, G. J., Naus Gj Fau - Landers, D. V., Landers Dv Fau - Gupta, P., and Gupta, P. (2000) Development of an in vitro organ culture model to study transmission of HIV-1 in the female genital tract, *Nature medicine*, 6(4), 475–479.
- [197] Papp, I., Sieben C Fau - Ludwig, K., Ludwig K Fau - Roskamp, M., Roskamp M Fau - Böttcher, C., Böttcher C Fau - Schlecht, S., Schlecht S Fau - Herrmann, A., Herrmann A Fau - Haag, R., and Haag, R. (2010) Inhibition of influenza virus infection by multivalent sialic-acid-functionalized gold nanoparticles, *Small (Weinheim an der Bergstrasse, Germany)*, 6(24), 2900–2906.
- [198] Speshock, J. L., Murdock Rc Fau - Braydich-Stolle, L. K., Braydich-Stolle Lk Fau - Schrand, A. M., Schrand Am Fau - Hussain, S. M., and Hussain, S. M. (2010) Interaction of silver nanoparticles with Tacaribe virus, *Interaction of silver nanoparticles with Tacaribe virus. Journal of nanobiotechnology*, 8, 19.
- [199] Doms, R. W., and Moore, J. P. (2000) HIV-1 membrane fusion: targets of opportunity, *The Journal of cell biology*, 151(2), F9–F14.
- [200] Schabes-Retchkiman, P. S., Canizal, G., Herrera-Becerra, R., Zorrilla, C., Liu, H. B., and Ascencio, J. A. (2006) Biosynthesis and characterization of Ti/Ni bimetallic nanoparticles, *Optical materials* 29, 95-99.
- [201] Shukla, D., and Spear, P. G. (2001) Herpesviruses and heparan sulfate: an intimate relationship in aid of viral entry, *The Journal of clinical investigation*, 108(4), 503–510.
- [202] Turner, A., Bruun B Fau - Minson, T., Minson T Fau - Browne, H., and Browne, H. (1998) Glycoproteins gB, gD, and gHgL of herpes simplex virus type 1 are necessary and sufficient to mediate membrane fusion in a Cos cell transfection system, *Journal of virology*, 72(1), 873–875.
- [203] Wei, D., Sun W Fau - Qian, W., Qian W Fau - Ye, Y., Ye Y Fau - Ma, X., and Ma, X. (2009) The synthesis of chitosan-based silver nanoparticles and their antibacterial activity, *Carbohydrate research*, 344(17), 2375–2382.
- [204] Spear, P. G. (2004) Herpes simplex virus: receptors and ligands for cell entry, *Cellular microbiology*, 6(5), 401–410.
- [205] Heldwein, E. E., Lou H Fau - Bender, F. C., Bender Fc Fau - Cohen, G. H., Cohen Gh Fau - Eisenberg, R. J., Eisenberg Rj Fau - Harrison, S. C., and Harrison, S. C. (2006) Crystal structure of glycoprotein B from herpes simplex virus 1, *Science*, 313(5784), 217–220.
- [206] Zannella, C., Shinde, S., Vitiello, M., Falanga, A., Galdiero, E., Fahmi, A., Santella, B., Nucci, L., Gasparro, R., Galdiero, M., Boccellino, M., Franci, G., and Di Domenico, M. (2020) Antibacterial Activity of Indolicidin-Coated Silver Nanoparticles in Oral Disease, *Applied Sciences*, 10(5), 1837.
- [207] Wu, J. A.-O., Bosker, T., Vijver, M. G., and Peijnenburg, W. (2021) Trophic Transfer and Toxicity of (Mixtures of) Ag and TiO₂ Nanoparticles in the Lettuce-Terrestrial Snail Food Chain, *Environmental science & technology*, 55(24), 16563–16572.
- [208] Carberry, T. P., Tarallo R Fau - Falanga, A., Falanga A Fau - Finamore, E., Finamore E Fau - Galdiero, M., Galdiero M Fau - Weck, M., Weck M Fau - Galdiero, S., and Galdiero, S. (2012) Dendrimer functionalization with a membrane-interacting domain of herpes simplex virus type 1: towards intracellular delivery, *Chemistry*, 18(43), 13678–13685.
- [209] Kaufman, E. A., Tarallo, R., Elacqua, E., Carberry, T. P., and Weck, M. (2017) Synthesis of Well-Defined Bifunctional Newkome-Type Dendrimers, *Macromolecules* 50, 4897-4905.
- [210] Abdelrahman, M., Douziech Eyrolles, L., Alkarib, S. Y., Hervé-Aubert, K., Ben Djemaa, S., Marchais, H., Chourpa, I., and David, S. (2017) siRNA delivery system based on magnetic nanovectors: Characterization and stability evaluation, *Eur J Pharm Sci* 106, 287-293.
- [211] Hervé, K., Douziech-Eyrolles, L., Munnier, E., Cohen-Jonathan, S., Soucé, M., Marchais, H., Limelette, P., Warmont, F., Saboungi, M. L., Dubois, P., and Chourpa, I. (2008) The development of stable aqueous suspensions of PEGylated SPIONs for biomedical applications, *Nanotechnology* 19, 465608.

- [212] Falanga, A., Valiante, S., Galdiero, E., Franci, G. A.-O., Scudiero, O., Morelli, G., and Galdiero, S. A.-O. (2017) Dimerization in tailoring uptake efficacy of the HSV-1 derived membranotropic peptide gH625, *Scientific reports*, 7(1), 9434.
- [213] Amaro, M., Reina, F., Hof, M., Eggeling, C., and Sezgin, E. (2017) Laurdan and Di-4-ANEPPDHQ probe different properties of the membrane, *Journal of physics D: Applied physics*, 50(13), 134004.



Valentina DEL GENIO

**PEPTIDE-BASED DYNAMIC
 NANOVECTORS FOR ANTICANCER
 AND ANTIMICROBIAL DRUGS.**

Sommaire

La recherche biomédicale consacre un effort considérable pour développer de nouveaux nanovecteurs pour une délivrance contrôlée de médicaments, afin d'augmenter leur efficacité thérapeutique et parvenir à une médecine personnalisée. Cette thèse de doctorat porte sur le développement de nanovecteurs à base de peptides pouvant être utilisés dans diverses situations, notamment pour délivrer des médicaments anticancéreux ou des médicaments antimicrobiens. L'introduction présente le concept de nanotechnologie, une science qui stimule d'importantes innovations dans les traitements médicaux et sanitaires. Grâce au contrôle des matériaux à l'échelle nanométrique, il est possible de produire des nanovecteurs capables de protéger les médicaments de la dégradation, de moduler leur pharmacocinétique, d'améliorer leur pénétration intracellulaire et la distribution intracellulaire tout en réduisant les effets secondaires indésirables. L'introduction décrit des stratégies de délivrance de médicaments visant à améliorer la spécificité des approches thérapeutiques actuelles, notamment par l'utilisation de peptides. Ensuite, deux sections principales sont consacrées respectivement aux nanovecteurs anticancéreux et antimicrobiens. La section 1 est axée sur la conception, la synthèse et la caractérisation d'une nouvelle génération de nanovecteurs anticancéreux auto-assemblés basés sur des peptides et conçus pour la libération de médicaments en réponse aux stimuli. L'auto-assemblage des peptides est régi par des interactions non covalentes qui peuvent être modulées en faisant varier les séquences d'acides aminés et en manipulant les paramètres environnementaux. Décorés en leur surface avec un peptide gH625 pénétrant dans les cellules, les nanovecteurs ont montré et amélioré l'absorption dans les cellules cancéreuses. Les nanoparticules d'oxyde de fer superparamagnétique (SPION) ont également été incluses dans la formulation, afin de (i) favoriser l'accumulation dans les tissus cibles à l'aide d'un champ magnétique externe et (ii) suivre leur biodistribution par IRM. La section 2 décrit l'utilisation de peptides pour le développement d'outils d'administration de médicaments utiles pour les applications antimicrobiennes. En particulier, nous avons obtenu plusieurs analogues d'un peptide antiviral développé dans notre laboratoire contre le virus Herpes Simplex Virus de type 1. Les analogues peptidiques obtenus ont été caractérisés par la présence d'un fragment PEG-Cholestérol qui favorise l'interaction avec la bicouche membranaire de la cellule cible et améliore l'activité anti-microbienne. Ces résultats ont ensuite été exploités pour développer un nanovecteur basé sur l'utilisation d'un dendrimère Janus fonctionnalisé avec deux séquences antivirales différentes. Enfin, nous avons également conçu des nanovecteurs constitués de nanoparticules d'argent qui combinent l'action des ions d'argent et d'un peptide antimicrobien indolicidine et démontrent une activité antibactérienne accrue et une cyto- et endo-toxicité plus faible.

Summary

Biomedical research devotes a huge effort to develop novel nanovectors for sustainable and controlled delivery of drugs, to augment their therapeutic effectiveness and to achieve personalized medicine. This PhD thesis is focused on the development of peptide-based nanovectors that can be used in various situations, namely to deliver anticancer drugs or antimicrobial drugs. The introduction presents the concept of nanotechnology, a science that stimulates important innovations in the medical and healthcare treatments. Through the control of materials at the nanoscale level, it is possible to produce nanovectors able to protect drugs from degradation, to modulate pharmacokinetics, to enhance intracellular penetration and intracellular distribution while reducing undesired secondary effects. The introduction describes drug delivery strategies aimed at improving the specificity of current therapeutic approaches, in particular through the use of peptides. Then there are two main sections devoted respectively to the anti-cancer and anti-microbial nanovectors. Section 1 is focused on the design, synthesis and characterization of new generation of self-assembling nanovectors based on peptides and designed for stimuli-responsive release of drugs. Peptide self-assembly is governed by noncovalent interactions that can be modulated by varying the amino acid sequences and manipulating the environmental parameters. Decorated on their surface with a cell-penetrating peptide gH625, the nanovectors shown and enhanced uptake in cancer cells. The superparamagnetic iron oxide nanoparticles (SPION) were additionally included in the formulation, to (i) favour accumulation in target tissues with help of external magnetic field and (ii) follow their biodistribution by MRI. Section 2 describes the use of peptides for the development of drug delivery tools useful for antimicrobial applications. In particular, we obtained several analogues of an antiviral peptide developed in our laboratory against *Herpes Simplex Virus type 1*. The obtained peptide analogues were characterized by the presence of a PEG-Cholesterol moiety which favours the interaction with the membrane bilayer of the target cell and enhances the anti-microbial activity. These results were further exploited to develop a carrier based on the use of a Janus dendrimer functionalized with two different antiviral sequences. Finally, we also designed nanovectors made of silver nanoparticles which combine the action of both silver ions and of an antimicrobial peptide indolicidin and demonstrate an enhanced antibacterial activity and a lower cyto- and endo-toxicity.

Stefanie Jelodier
 I. CHOURPA

K. Hervé-Aubert